Diplomarbeit
Theoretisch

Investigation and evaluation of different Combined Heat and Power configurations

Konstantinos Vergos

DA 400
2014/10

- Diese Seite in der gedruckten Version entfernen; nur für die PDF-Version
- Remove this page in the print-out; This page is for the pdf-version only

Lehrstuhl für Energiesysteme

Betreuer der Arbeit:	Dominik Meinel Technische Universität München Lehrstuhl für Energiesysteme Boltzmannstr. 15 85748 Garching b. München
Ausgegeben:	07.04.2014
Abgegeben:	06.10.2014

Eidesstattliche Erklärung

Hiermit versichere ich, die vorliegende Arbeit selbständig und ohne Hilfe Dritter angefertigt zu haben. Gedanken und Zitate, die ich aus fremden Quellen direkt oder indirekt übernommen habe sind als solche kenntlich gemacht. Diese Arbeit hat in gleicher oder ähnlicher Form noch keiner Prüfungsbehörde vorgelegen und wurde bisher nicht veröf-fentlicht.

Ich erkläre mich damit einverstanden, dass die Arbeit durch den Lehrstuhl für Energiesysteme der Öffentlichkeit zugänglich gemacht werden kann.

München, den 06.10.2014 _____

Acknowledgements

I am using this opportunity to express my gratitude to everyone who supported me throughout the course of this Diploma Thesis.

I begin by thanking Prof. Dr.-Ing. Hartmut Spliethoff and Assistant Prof. Dr.-Ing. Sotirios Karellas for providing the opportunity to complete this thesis at the Institute of Energy Systems, TUM.

Furthermore, I would like to especially thank Dominik Meinel for his guidance and support during the entire period of this Thesis.

Finally I thank my parents Loukas and Margarita, for their constant support and trust all these years. Last but not least, I thank Sophia for standing by and believing in me.

Abstract

Geothermal Energy has the potential to provide a low CO_2 emission base-load power and heat by utilizing the natural hydrothermal resources of the planet. Moreover, the exploitable hot spots are worldwide distributed and have the potential to satisfy the world energy demand. Most of the widely distributed exploitable geothermal sources consist of low-temperature water in the range of 100-140 °C.

In this range, an effective and widely used technology is the Organic Rankine Cycle (ORC). The interest in the development and research of ORC units had a tremendous increase in the last decade, due to the wide scope of applications it can be used for. Geothermal plants, Waste Heat Recovery, Biomass Plants and Solar Thermal Plants are the main driving force behind the continuing increase in the interest in the ORC technology.

In the present study, MATLAB simulations were developed for the investigation of ORC units with different component configurations as well as with different HFOs as the working fluid. Furthermore, a detailed economic analysis was carried out, in order to assess the economic feasibility of each configuration.

Key words: Combined Heat and Power, Geothermal Energy, Organic Rankine Cycle, HFOs, MATLAB, Economic analysis.

Contents

List of Figures

List of Tables

Notation

A	$Capacity\ or\ size\ parameter\ for\ the\ equipment - Bare\ module\ method$
A_{HEX}	$Total\ heat\ transfer\ area\ of\ the\ heat\ exchanger\ [m^2]$
C_P^0	$Bare\ module\ cost\ (ambient\ operating\ pressure - carbon\ steel)$ [$]
C_{BM}	$Bare\ module\ cost$ [$]
CELF	Constant – escalation levelization factor
$CEPCI$	$Chemical\ Engineering\ Chemical\ Plant\ Cost\ Index$
CRF	Capital recovery factor
d_k^{SL}	$Depreciation - Straight\ line\ method$
F	$Heat\ transfer\ correction\ factor$
F_P	$Pressure\ factor$
F_M	$Material\ factor$
FCI_L	$Depreciable\ capital\ investment$
FLH	$Full\ load\ hours$
$h_{DH,in}$	$Enthalpy\ of\ the\ district\ heating\ water - entrance\ of\ the\ system\ [J/kg \cdot K]$
$h_{DH,out}$	$Enthalpy\ of\ the\ district\ heating\ water - exit\ of\ the\ system\ [J/kg \cdot K]$
$h_{gw,in}$	$Enthalpy\ of\ the\ geothermal\ fluid - entrance\ of\ the\ system\ [J/kg]$
$h_{gw,ref}$	$Enthalpy\ of\ the\ geothermal\ fluid - entrance\ of\ the\ system\ at\ T_{ref}\ [J/kg]$
$h_{P,in}$	$Enthalpy\ of\ the\ ORC\ fluid - entrance\ of\ the\ pump\ [J/kg]$
$h_{P,out}$	$Enthalpy\ of\ the\ ORC\ fluid - exit\ of\ the\ pump\ [J/kg]$
$h_{P,out,is}$	$Isentropic\ enthalpy\ of\ the\ ORC\ fluid - exit\ of\ the\ pump\ [J/kg]$
$h_{T,in}$	$Enthalpy\ of\ the\ ORC\ fluid - entrance\ of\ the\ steam\ turbine\ [J/kg]$
$h_{T,out}$	$Enthalpy\ of\ the\ ORC\ fluid - exit\ of\ the\ steam\ turbine\ [J/kg]$
$h_{T,out,is}$	$Isentropic\ enthalpy\ of\ the\ ORC\ fluid - exit\ of\ the\ steam\ turbine\ [J/kg]$
$h_{ECO,in}$	$Enthalpy\ of\ the\ ORC\ fluid - entrance\ of\ the\ preheater\ [J/kg]$

$h_{EVAP,out}$	$Enthalpy\ of\ the\ ORC\ fluid - exit\ of\ the\ evaporator\ [J\ /\ kg]$
i_{eff}	$Effective\ interest\ rate$
INW	$Injection\ Well\ (in\ Microsoft\ Visio\ figures)$
k	$Thermal\ conductivity\ [W/m\ K]$
$LMTD$	$Log\ mean\ temperature\ difference\ [K]$
$\dot{m}$	$Mass\ flow\ of\ the\ ORC\ fluid\ [kg\ /\ s]$
$\dot{m}_{gw}$	$Mass\ flow\ of\ the\ geothermal\ fluid\ [kg\ /\ s]$
$\dot{m}_N$	$Steam\ Turbine\ nominal\ mass\ flow\ of\ the\ ORC\ fluid\ [kg\ /\ s]$
$\dot{m}_{DH}$	$District\ heat\ water\ mass\ flow\ [kg\ /\ s]$
N	$Depreciation\ Life\ of\ the\ equipment$
NPV	$Net\ present\ value$
P	$Organic\ Rankine\ Cycle\ Pump\ (in\ Microsoft\ Visio\ figures)$
PEC	$Purchased\ Equipment\ Cost\ [\$]$
PWP	$Production\ well\ pump\ (in\ Microsoft\ Visio\ figures)$
$P_{el,P}$	$Pump - motor\ eletric\ power\ demand\ [W]$
$P_{el,T}$	$Turbine - generator\ eletric\ power\ output\ [W]$
$P_{el,ORC}$	$Total\ electric\ power\ output\ of\ the\ ORC\ unit\ [W]$
p_{Evap}	$Pressure\ in\ the\ evaporator\ [bar]$
p_{Cond}	$Pressure\ in\ the\ condenser\ [bar]$
$p_{Int,arith}$	$Intermediate\ pressure - arithmetic\ mean$
$p_{Int,geom}$	$Intermediate\ pressure - geometric\ mean$
PP_Evap	$Pinch\ point\ at\ the\ Evaporator\ [K]$
PP_Cond	$Pinch\ point\ at\ the\ Condenser\ [K]$
PP_DH	$Pinch\ point\ at\ the\ District\ heating\ heat\ exchanger\ [K]$
PEC	$Purchased\ Equipment\ Cost\ [\$]$
Q_{DH}	$Heat\ demand\ of\ the\ district\ heating\ network\ [W]$

Q_{max}	$Maximum\ heat\ demand\ of\ the\ district\ heating\ network\ [W]$
R_f	$Thermal\ resistance\ fouling\ effect$
r_i	$Internal\ radius\ of\ a\ bare\ tube\ [m]$
r_o	$External\ radius\ of\ a\ bare\ tube\ [m]$
r_n	$Escalation\ rate$
$s_{DH,in}$	$Entopy\ of\ the\ district\ heating\ water-entrance\ of\ the\ system\ [J\ /\ kg\cdot K]$
$s_{DH,out}$	$Entopy\ of\ the\ district\ heating\ water-exit\ of\ the\ system\ [J\ /\ kg\cdot K]$
$s_{gw,in}$	$Entropy\ of\ the\ geofluid-entrance\ of\ the\ system\ [J\ /\ kg\cdot K]$
$s_{gw,ref}$	$Entropy\ of\ the\ geofluid-entrance\ of\ the\ system\ at\ T_{ref}\ [J\ /\ kg\cdot K]$
ST	$Steam\ Turbine\ (in\ Microsoft\ Visio\ figures)$
S	$Salvage\ value\ of\ the\ equipment$
T_{c1}	$Cold-fluid\ inlet\ temperature\ [K]$
T_{c2}	$Cold-fluid\ outlet\ temperature\ [K]$
T_{h1}	$Hot-fluid\ inlet\ temperature\ [K]$
T_{h2}	$Hot-fluid\ outlet\ temperature\ [K]$
T_{c1}	$Cold-fluid\ inlet\ temperature\ [K]$
T_{ref}	$Ambient\ reference\ temperature\ [K]$
T_b	$Full\ load\ hours$
U	$Total\ heat\ transfer\ coefficient\ [W/m^2K]$

Greek symbols

α_i	$Heat\ tranfer\ coefficient\ for\ inside\ flow [W/m^2K]$
a_o	$Heat\ tranfer\ coefficient\ for\ outside\ flow\ [W/m^2K]$
Δx_e	$Turbine\ outlet\ steam\ quality$
η_m	$mechanical\ efficiency\ of\ the\ turbie - generator\ shaft$
η_{gen}	$eletric\ efficiency\ of\ the\ generator$
$\eta_{is,T}$	$Turbine\ isentropic\ efficiency$
$\eta_{is,T,corr}$	$Corrected\ turbine\ isentropic\ efficiency$
$\eta_{is,T,N}$	$Turbine\ nominal\ isentropic\ efficiency$
$\eta_{is,P}$	$Pump\ isentropic\ efficiency$
$\eta_{thermal}$	$Thermal\ efficiency\ [\%]$
η_{system}	$System\ efficiency\ [\%]$
η_{exergy}	$Exergy\ efficiency\ [\%]$

1 Introduction

1.1 Background

Nowadays, the world still relies heavily on fossil fuels to cover the energy demands, despite the increasing share of renewable energy that has been observed over the last years. The high share of fossil fuels creates a system that lacks diversity and security, threatens the health of the citizens, jeopardizes the stability of Earth's climate, and deprives the future generation of clean air, clean water and energy independence.

In Figure 1.1, the total consumption of energy in Germany and the energy mix used is depicted during the year 2013. In Figure 1.2, the Energy Import Dependency by fuel is depicted for the same country and year.

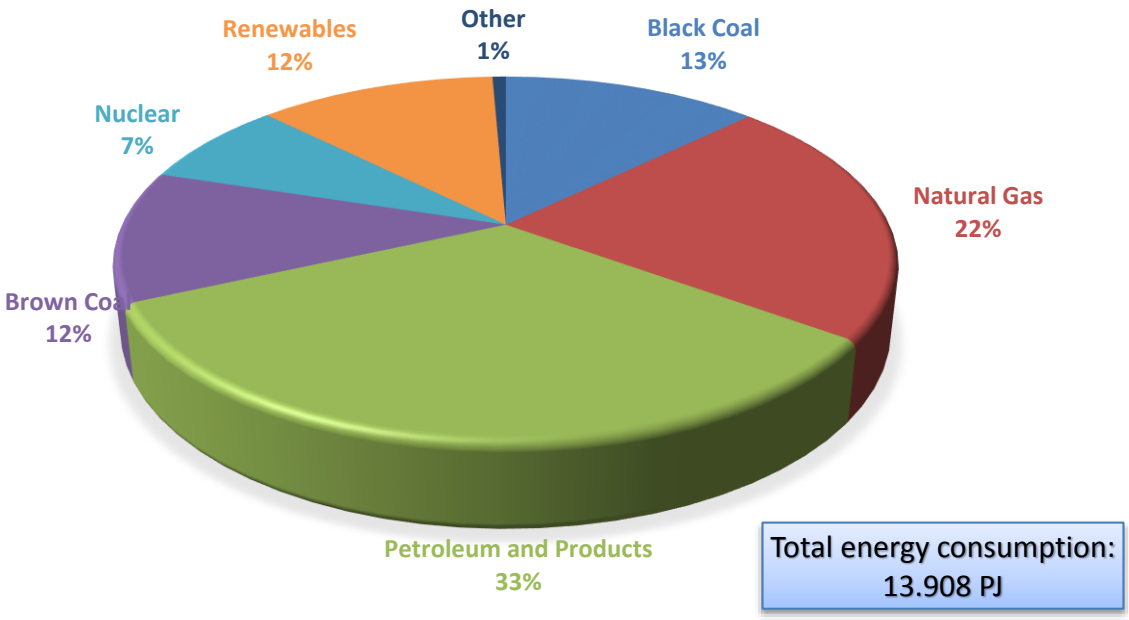

Figure 1.1 Primary Energy Consumption in Germany 2013 (Arbeitsgemeinschaft Energiebilanzen (AGEB), Arbeitsgruppe Erneuerbare Energien-Statistik)

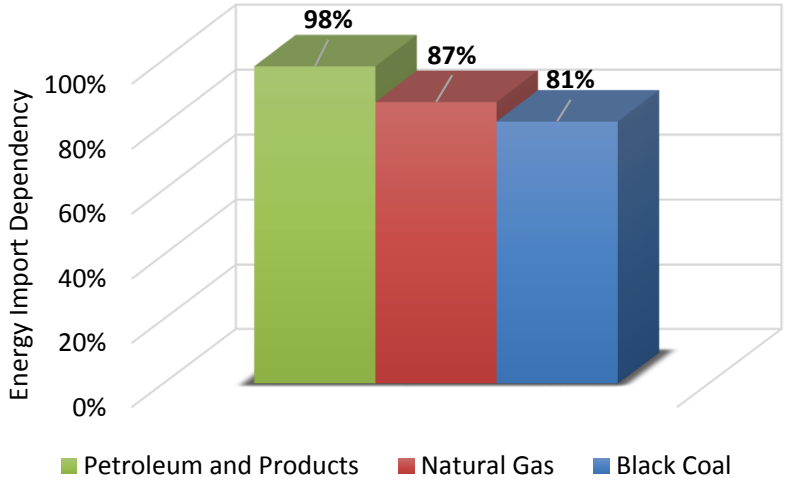

Figure 1.2 Energy Import Dependency by fuel in Germany (2013) (Arbeitsgemeinschaft Energiebilanzen)

As shown in Figure 1.2, 98% of Petroleum and Products, 87% of Natural Gas and 81% of Black Coal are imported. According to Figure 1.1, these three categories represent the 68% of the total energy consumption in year 2013. Consequently, the Energy Independence of Germany is highly compromised, since more than half of the total energy consumption is imported from other countries. However this situation is not limited just to Germany, but to the whole European Union, since most of Europe's countries import fossil fuels from countries outside the union. This is depicted in Figure 1.3:

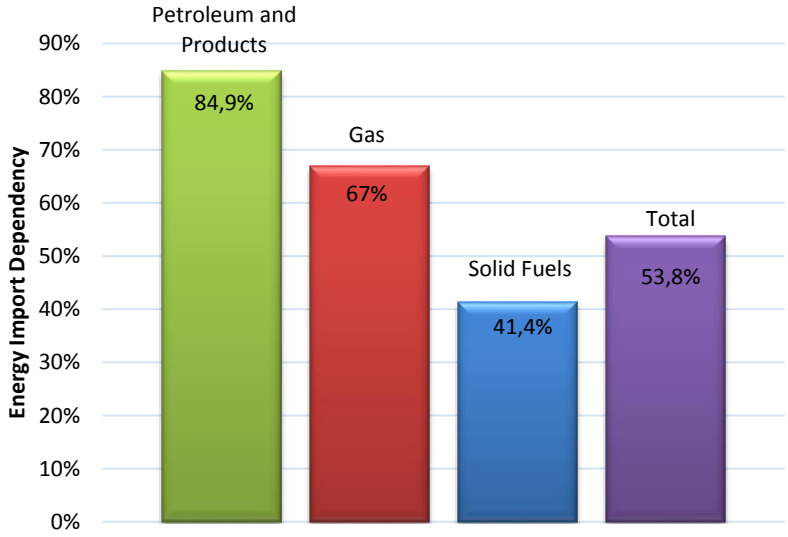

Figure 1.3 Energy Import Dependency by fuel in European Union 2013, (Eurostat)

On the other hand, aside from energy dependency, the other major drawback of fossil fuels, is the environmental impact. Global warming and Air Pollution are two direct consequences from the high consumption of fossil fuels.

The answer to these problems, is the use of renewable energy resources. Renewable energy resources such as wind, solar, bioenergy, and geothermal are capable of meeting a substantial proportion of Europe's energy needs, and can help alleviate many of the problems mentioned above while providing further significant benefits. This has already been recognized by the European Union and therefore a series of measures have been undertaken in order to support the clear energy development, like the Energy Transition or "Energiewende" in Germany. A strong dependence on renewable energy sources can contribute positively by:

- Protection of the environment and public health by avoiding or reducing emissions that contribute to air pollution, smog, acid rain, and global warming.
- Reduce a growing reliance on imported fuel and electricity.
- Creation of competition to help restrain fossil fuel price increases.
- Reduce the cost of complying with present and future environmental regulations.

However, renewable energy resources like wind or solar energy heavily depend on the weather fluctuations and thus cannot be simply used for base-load applications. On the other hand, geothermal energy is dispatchable, meaning that it is both available whenever needed, and can quickly adjust output to match demand. The US Energy Information Administration rates new geothermal plants as having a 92% capacity factor, higher than those of nuclear (90%), gas (87%), or coal (85%), and much higher than those of intermittent sources such as onshore wind (34%) or solar photovoltaic (25%). While the carrier medium for geothermal electricity (water) must be properly managed, the source of geothermal energy, the Earth's heat, will be constantly available for most intents and purposes (US Energy Information Administration 2013).

1.2 Motivation

The present study focuses on the design and evaluation of different Organic Rankine Cycle systems for geothermal Combined Heat and Power applications. These installations make more efficient use of the geothermal resources by cascading the geothermal fluid to successively lower temperature applications, thereby improving the economics of the entire system dramatically.

The technical and economic feasibility of the entire system is subject to many factors. Specifically, it depends heavily on the configuration of the systems components, the design of the individual components like the heat exchangers, the selection of the working fluid, the heat and power demands during the year and consequently the full and part load performance of the system. Therefore, the optimization and evaluation of such a system, is a complicated process, as each factor has to be taken in and be weighted accordingly to the specific boundary conditions.

The need of designing and optimizing such a system that will be technical and economical feasible for the efficient management of geothermal energy resources, is the motivation of this study.

1.3 Objectives

The objective of this study is to investigate and evaluate energetically and economically different Organic Rankine Cycle (ORC) configurations for use with geothermal medium temperature sources for the generation of electricity and heat. Therefore, in the first part of the study, the pure power generation concepts are developed and evaluated, while in the second part, the different Combined Heat and Power (CHP) concepts. Lastly, the economic evaluation of all the configurations takes place in order to assess the financial feasibility of the projects. The list of the objectives in this study can be summarized as follows:

- Design, simulation and energetic evaluation of Pure Power generation ORC concepts.
- Design, simulation and energetic evaluation of Combined Heat and Power ORC concepts.
- Comparison and economical evaluation of the systems.

1.4 Overview

The first part of this work is the literature study in chapter 2. The focus is on the Organic Rankine Cycle operation technology, the organic fluids used and the applications of the ORC technology. Furthermore, emphasis is placed on the geothermal Combined Heat and Power applications.

The Pure Power generation concepts are presented in chapter 3. The focus of this chapter is the design, simulation and energetic evaluation of the Pure Power generation ORC configurations. Likewise, in chapter 4, the Combined Heat and Power concepts are presented, while the focus is on the design, simulation and energetic evaluation of the CHP ORC configurations.

The Engineering Economic Analysis is presented in chapter 5. The focus of this chapter is a literature review about all the economic variables that affect the profitability of an investment. Emphasis is placed on the geothermal ORC investments.

The Economic Sensitivity Analysis Results are shown and explained in chapter 6, based on the boundary conditions and concepts given in the previous chapters. Finally, in chapter 7, the conclusions of this study are summarized and presented.

2 Literature study

2.1 Organic Rankine Cycle (ORC)

The Organic Rankine Cycle (ORC) is a Clausius – Rankine Cycle in which an organic working fluid is used instead of water – steam. The interest in the development and research of ORC units had a tremendous increase in the last decade, due to the wide scope of applications it can be used for. The core advantage of this technology, is the capability to use heat of low energy and temperature level for energy production processes.

The Rankine Cycle has been one of the most important ways of producing power since the 19th century, when the primary use was for transportation and industrial power production. Today, the Rankine Cycle remains the dominant power cycle for the production of electricity. Through the 20th century the Rankine Cycle continued to evolve in a number of ways including the development of the steam turbine and the use of different working fluids than water. The exploration of different working fluids has led to the field of Organic Rankine Cycles.

2.1.1 Operation

Conceptually, the basic mode of operation is essentially the same between the two cycles, since they are both based on the vaporization of a high pressure liquid, which is in turn expanded to a lower pressure thus releasing mechanical work. For the expansion, a scroll expander or a steam turbine may be used, for small or bigger scales respectively. After the expansion, the condensing of the low pressure steam takes place, in an air-cooled or water-cooled condenser. The second option is usually more preferable if available, due to lower costs.

The cycle is closed by pumping the working fluid back to the evaporator in high pressure. The three evaporation phases (preheating, vaporization and superheating) can either happen in a single heat exchanger, or in more than one, separately. Moreover, superheating may be avoided completely, with the use of some specific organic fluids, as explained later. Finally, depending on the fluid used, a recuperator can be installed as liquid preheater between the pump outlet and the expander outlet. This allows reducing the amount of heat needed to vaporize the fluid in the evaporator. These two basic variations which depend on the presence of a recuperator, are shown in Figure 2.1:

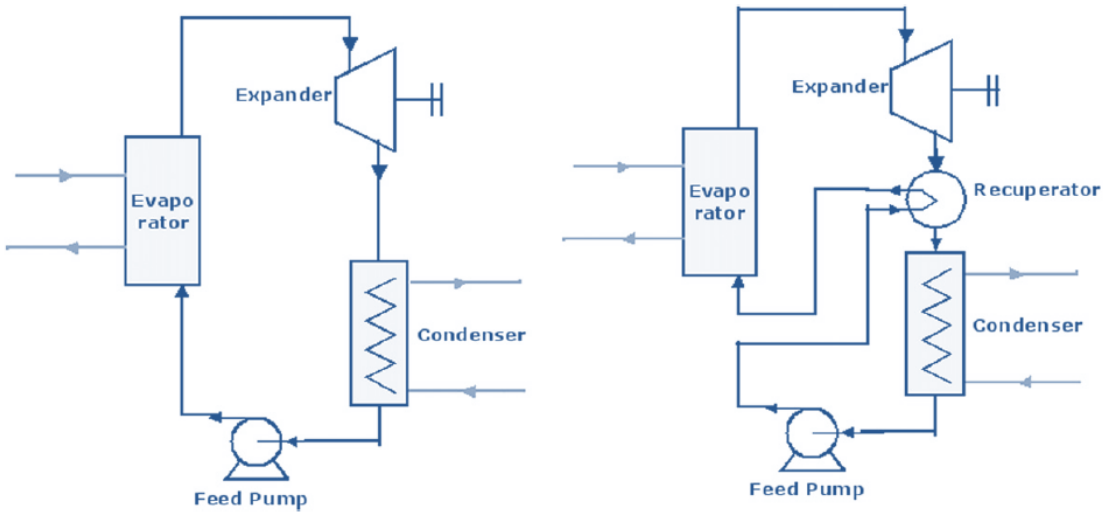

Figure 2.1 Schematic diagram of an ORC with (right) and without (left) recuperator.

2.1.2 Organic Fluids

The crucial characteristic, which makes the ORC technology appropriate for low heat energy applications is the use of an organic fluid, in contrast with the classic water-steam driven Rankine cycle. That is because a large number of organic fluids have lower boiling point than water and thus benefit from low heat energy inputs. The organic working fluids appropriate for ORC are generally common refrigerants with low-temperature boiling points, such as chlorofluorocarbons (CFCs), hydrochlorofluorocarbons (HCFCs), hydrofluorocarbons (HFCs), hydrofluoroethers (HFEs), hydrocarbons and more recently Hydrofluoroolefins (HFOs). The T-s diagram of some typical working fluids for the ORC cycle compared with water is shown in Figure 2.2:

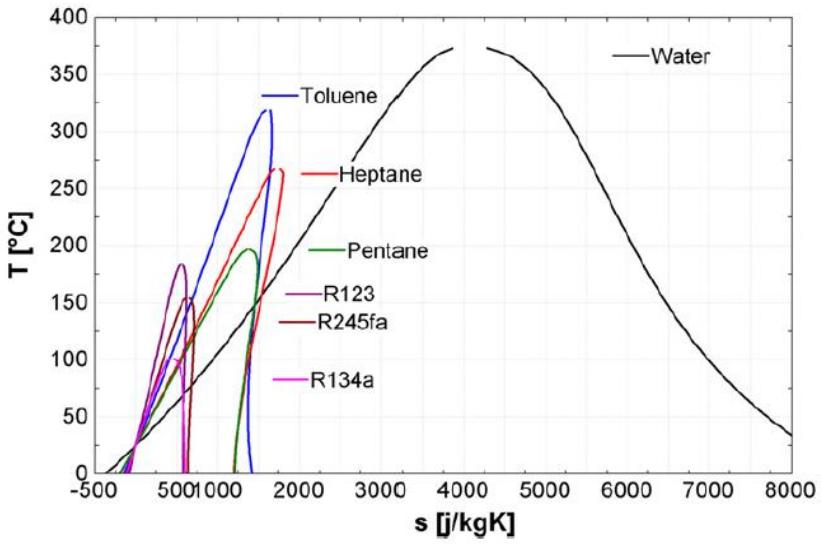

Figure 2.2 T-s diagram of working fluids for the ORC cycle, compared with water

Over the years there has been a progressive evolution of refrigerants from CFCs, HCFCs, to HFCs in order to produce more environmental friendly refrigerants. Today, the use of the first two generation refrigerants has been either banned or restricted due to high ODP (Ozone Depletion Potential) values.

The current third generation of refrigerants (HFCs), have no effect on the ozone layer but extremely high GWP (Global Warming Potential) values. In fact, they have been considered as one of the six main greenhouse gases according to Kyoto Protocol, which include Carbon dioxide (CO_2), Methane (CH_4), Nitrous oxide (N_2O), Hydrofluorocarbons (HFCs), Perfluorocarbons (PFCs) and Sulphur hexafluoride (SF6) (Kyoto Protocol Reference Manual 2008). Furthermore, HFCs are up to a thousand of times more harmful than CO_2. As shown in Figure 2.3, while CFC and HCFC emissions decrease, HFC emissions will surpass them by around 2025, and rapidly increase up towards 2050. Emissions are scaled to CO2-equivalent values, using 100-year GWPs (Velders 2009).

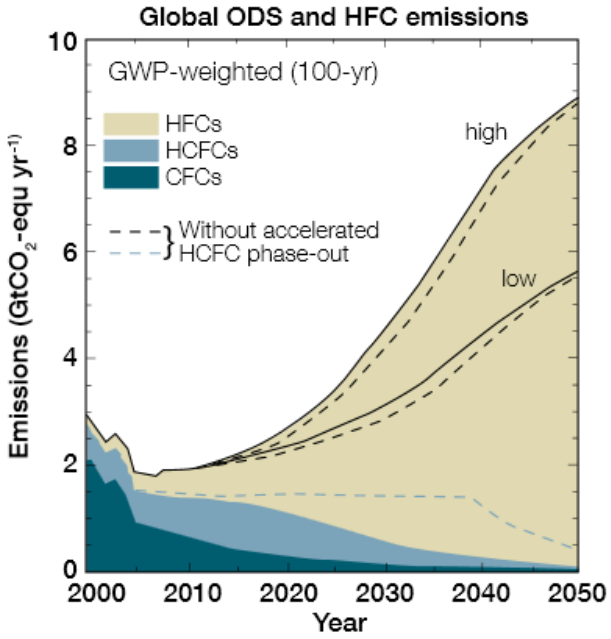

Figure 2.3 Global ozone depleting substances (ODS) and HFC emissions

In terms of the aforementioned environmental drawbacks of the current refrigerants, HFOs (hydrofluoroolefins) have been developed as the fourth generation refrigerants. Unlike HFCs, which are derivatives of alkanes, HFOs are derived from alkenes containing at least one double bond. For this reason, their atmospheric lifetimes can be greatly shortened to only few days compared to years for most of the other fluorinated compounds (Liu, et al. 2014). Moreover, an additional very promising aspect for HFO is the low GWP value, which is less than 10 (Brown 2009).

The encouraging aspects of HFOs have attracted an increasing number of development studies and two of them, i.e. R1234yf and R1234zeE, have been commercially available since 2013. More recently, both fluids have been added into some commercial software such as REFPROP 9.0, which allows realistic process simulations for various applications. For its application in refrigeration system, R1234yf has been considered to be an excellent replacement for the conventional refrigerant HFC-134a. In fact, some large automotive manufacturers in Europe are planning to gradually adopt R1234yf as one of the main refrigerants for the automotive refrigeration system (Automotive News 2013).

One other very important classification of the organic fluids, apart from their ODP or GWP values, is based on the slope (dT/ds) of the saturated vapor in T-s diagram. More specifically, the slope (dT/ds) of the saturated vapor curve of organic fluids in a T-s diagram can be negative, zero or positive and consequently the fluids are categorized into the following three groups (Qiu 2012):

- "Wet" fluids which have negative slope of the saturated vapor curve and are usually of low molecular mass, e.g. water M=18 kg/kmol, ammonia M=17 kg/kmol.

- "Isentropic" fluids which have nearly vertical saturated vapor curves and are commonly of medium molecular mass, such as R134a M=102 kg/kmol and R123 M=153 kg/kmol.

- "Dry" fluids which have positive slope of the saturated vapor curve and are usually of high molecular mass, e.g. HFE7000 M=200 kg/kmol and HFE7100 M=250 kg/kmol.

The slope of the saturation vapor curve for a dry, wet and isentropic fluid is shown in Figure 2.4:

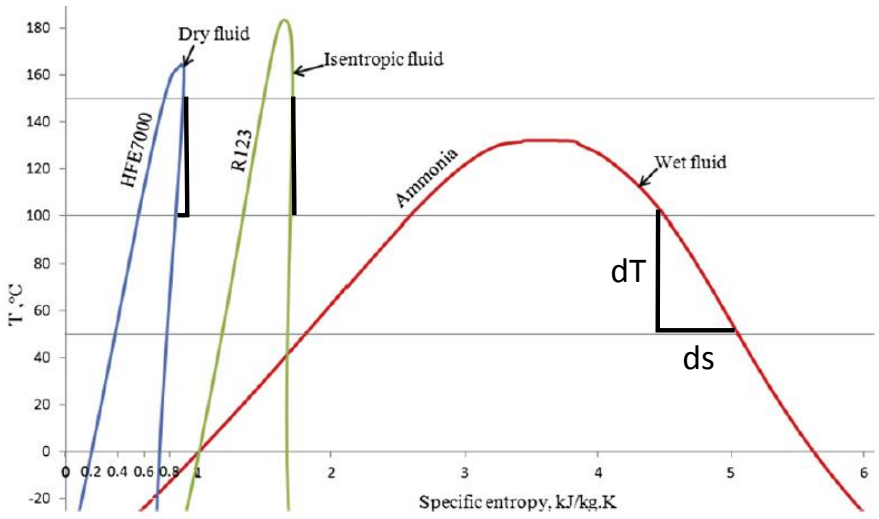

Figure 2.4 Ammonia, R123 and HFE7000 saturation curves (Qiu 2012)

Due to the negative slope of the saturation vapor curve for a wet fluid, outlet stream of the turbine typically contains lot of saturated liquid. Presence of liquid inside turbine may damage turbine blades and it also reduces the isentropic efficiency of the turbine. Typically, the minimum dryness fraction at the outlet of a turbine is kept above 85%. To satisfy the minimum dryness fraction at the outlet of the turbine, “Wet” fluids usually need to be superheated prior to entering the expander, while “isentropic” and “dry” fluids do not need superheating, thereby eliminating the concerns of impingement of liquid droplets on the expander blades.

Moreover, since the superheated apparatus is not needed, greater economic gain is achieved. The reason is that due to reduction of the heat transfer coefficient in the vapor phase, the heat transfer area and cost of the superheater increase significantly. Therefore, the working fluids of “dry” or “isentropic” type are more adequate for ORC systems (Qiu 2012).

In conclusion, the optimal characteristics of the organic working fluid could be summed up as follows:

- Isentropic or dry saturation vapor curve
- Low freezing point, high stability temperature
- High heat of vaporisation and density
- Low environmental impact
- Safety
- Good availability and low cost

2.2 ORC Applications

ORC units are used in applications which include low temperature heat sources, like binary geothermal power plants, solar thermal power systems, and waste heat recovery and biomass CHP plants. In the sections below, more information is provided for the wide scope of applications where ORC can be used in.

2.2.1 Geothermal binary power plants

Geothermal Energy applications of the Organic Rankine Cycle are the primary concern of this study and thus they are discussed separately in detail in the next chapter.

2.2.2 Biomass Combined Heat and Power

Biomass is biological material derived from living, or recently living organisms, and usually refers to plants or plant-based materials. Biomass is available all over the world from industrial processes such as wood industry or agricultural waste and can be used for the production of electricity on small to medium size scaled power plants. Among other means, it can be converted into electricity by combustion to obtain heat, which is in turn converted into electricity through a thermodynamic cycle.

The cost of biomass is significantly lower than that of fossil fuels. Yet, the investment necessary to achieve clean biomass combustion is more important than for classic boilers. For small decentralized units, the generation cost of electricity is not competitive and combined heat and power generation is required to ensure the profitability of the investment. Therefore, in order to achieve high energy conversion efficiency, biomass CHP plants are usually driven by the heat demand rather than by the electricity demand.

The possibility to use heat as a by-product is an important asset of biomass ORCs, highlighting the importance of a local heat demand, which can be fulfilled e.g. by industrial processes (such as wood drying) or space heating (usually district heating). Since heat is relatively difficult to transport across long distances, biomass CHP plants are most of the time limited to 6 – 10 MW thermal power, corresponding to 1 – 2 MW electrical power (Quoilin, et al. 2013).

A simplified diagram of such a cogeneration system is presented in Figure 2.5. Heat from the combustion is transferred from the flue gases to the heat transfer fluid (thermal oil) in two heat exchangers, at a temperature varying between 150 and 320 °C. The heat transfer fluid is then directed to the ORC loop to evaporate the working fluid, at a temperature slightly lower than 300 °C. Next, the evaporated fluid is expanded, passes through a recuperator to preheat the liquid and is finally condensed at a temperature around 90 °C. The condenser is used for hot water generation (Quoilin, et al. 2013).

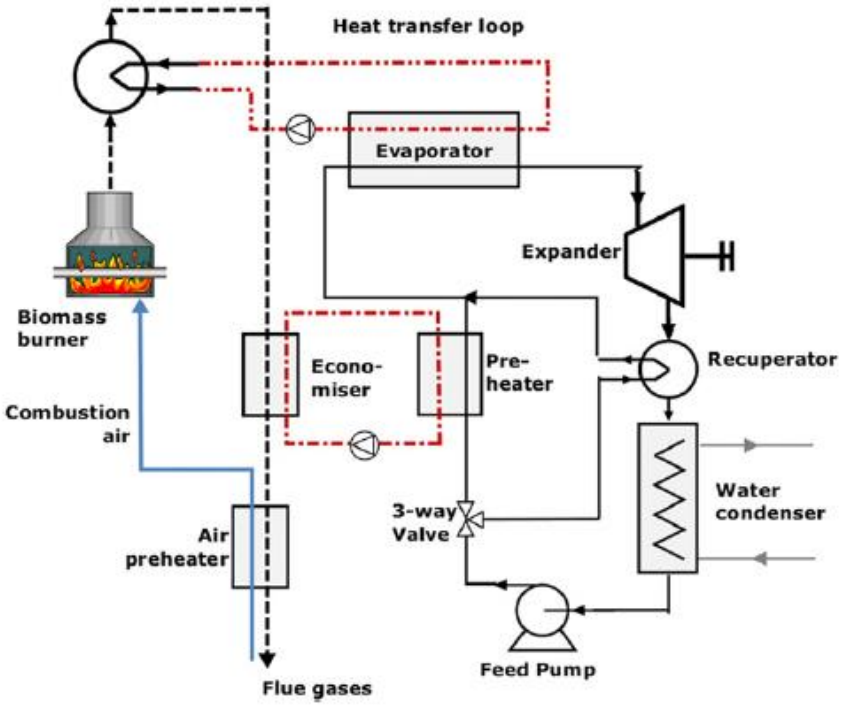

Figure 2.5 : Working principle of a biomass CHP-ORC system (Quoilin, et al. 2013)

2.2.3 Waste Heat Recovery

Waste heat recovery applications can be subdivided into two main categories: Heat recovery on mechanical equipment and industrial processes and Heat recovery on internal combustion engines.

2.2.3.1 Heat recovery on mechanical equipment and industrial processes

Numerous applications in the manufacturing industry reject heat at relatively low temperature. In many cases this heat is simply rejected to the atmosphere, since it cannot be reintegrated entirely on-site or used for district heating. This is not only an immense energy loss, but also causes two types of pollution: Firstly the pollutants in the flue gases generate health and environmental issues and secondly an uncontrolled heat rejection has a negative effect on aquatic equilibriums and biodiversity. Recovering waste heat alleviates these two types of pollution. It can moreover generate electricity to be consumed on-site or fed back to the grid. In such a system, the waste heat is usually recovered by an intermediate heat transfer loop and used to evaporate the working fluid of the ORC cycle.

Some industries present a particularly high potential for waste heat recovery. One example is the cement industry. In a typical cement producing procedure, 25% of the total energy used is electricity and 75% is thermal energy. However, the process is characterized by significant heat losses mainly by the flue gases and the ambient air stream used for cooling down the clinker, at about 35% - 40% of the process heat input and at 215-

315 °C. Approximately 26% of the heat input to the system is lost due to dust, clinker discharge, radiation and convection losses from the kiln and the preheaters (Karellas, et al. 2013). A heat recovery system could be used to increase the efficiency of the cement plant and thus contribute to emissions decrease. Other examples include the iron and steel industries (10% of the GHG emission in China for example), refineries and chemical industries. (Quoilin, et al. 2013). The heat recovery system of a typical cement plant is shown in Figure 2.6.

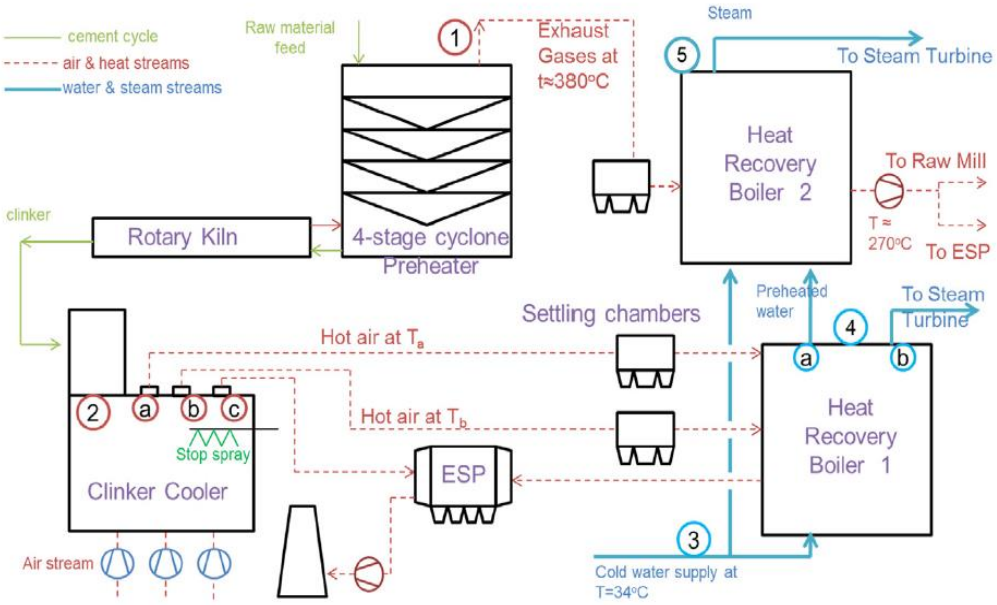

Figure 2.6 Heat recovery system of a typical cement plant (Karellas, et al. 2013)

2.2.3.2 Heat recovery on internal combustion engines

An Internal Combustion Engine (ICE) only converts about one-third of the fuel energy into mechanical power on typical driving cycles: A typical 1.4 l Spark Ignition ICE, with a thermal efficiency ranging from 15% to 32%, releases 1.7 – 45 kW of heat through the radiator, at a temperature close to 80 – 100 °C and 4.6 – 120 kW via the exhaust gas at temperatures between 400 – 900 °C (Chammas 2005).

Most of the systems under development recover heat from the exhaust gases and from the cooling circuit. An additional potential heat source is the exhaust gas recirculation (EGR) and charge air coolers, in which non-negligible amounts of waste heat are dissipated. The expander output can be mechanical or electrical. With a mechanical system, the expander shaft is directly connected to the engine drive belt, with a clutch to avoid power losses when the ORC power output is too low. The main drawback of this configuration is the imposed expander speed: this speed is a fixed ratio of the engine speed and is not necessarily the optimal speed for maximizing cycle efficiency. In the case of electricity generation, the expander is coupled to an alternator, used to refill the batteries or supply

auxiliary utilities, such as the air conditioning. The advantages and disadvantages of each power feedback are summarized in Figure 2.7 below:

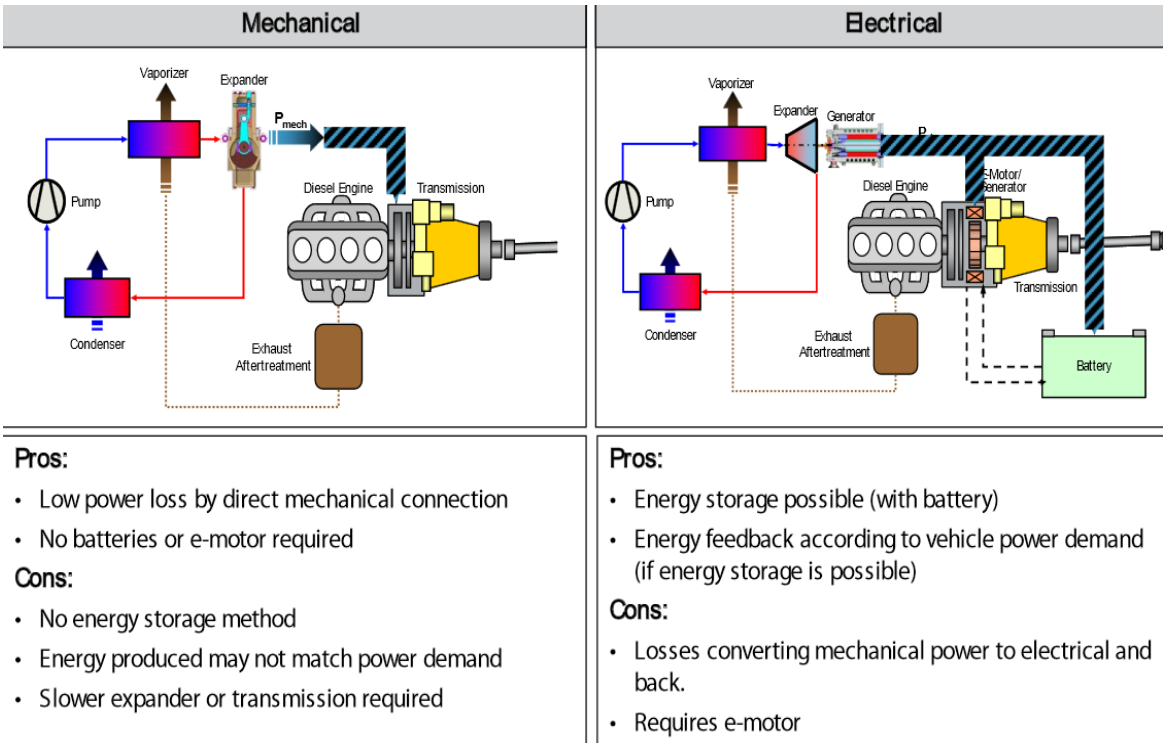

Figure 2.7 Mechanical and Electrical WHR power feedback Daimler's Super Truck Program, DEER Conference 2012

2.2.4 Solar Power plants

Concentrating solar power is a well-proven technology: the sun is tracked and its radiation reflected onto a linear or punctual collector, transferring heat to a fluid at high temperature. This heat is then used in a power cycle to generate electricity. The three main concentrating solar power technologies are the parabolic dish, the solar tower, and the parabolic trough. Parabolic dishes and solar towers are punctual concentration technologies, leading to a higher concentration factor and to higher temperatures. The most appropriate power cycles for these technologies are the Stirling engine (for small-scale plants), the steam cycle, or even the combined cycle (for solar towers).

Parabolic troughs work at a lower temperature (300 – 400°C) than point-focused CSP systems. The solar steam cycles are subject to the same limitations as in biomass power plants: steam cycles require high temperatures, high pressures, and therefore larger installed power to be profitable. Organic Rankine Cycles are a promising technology to decrease investment costs at small scale: they can work at lower temperatures, and the

total installed power can be scaled down to the kW levels. The working principle of such a system is presented in Figure 2.8. Technologies such as Fresnel linear concentrators are particularly suitable for solar ORCs since they require a lower investment cost, but work at lower temperature (Quoilin, et al. 2013).

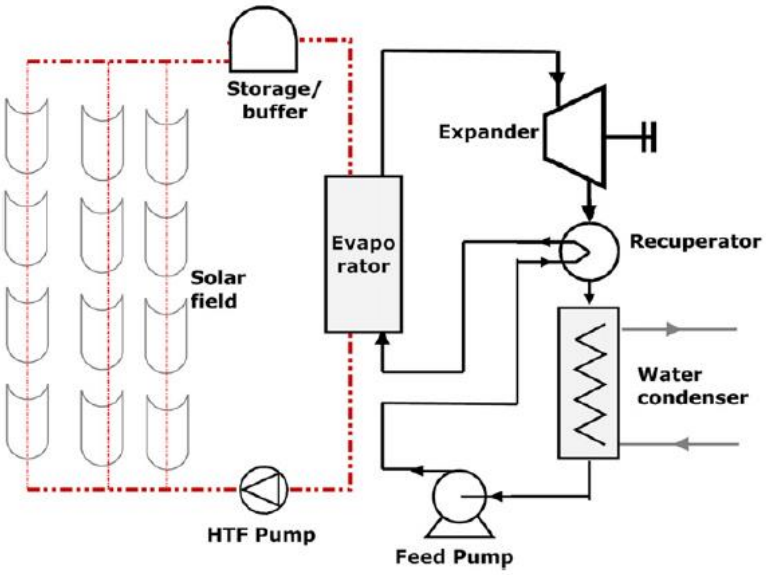

Figure 2.8 Working Principle of a solar ORC system (Quoilin, et al. 2013)

2.2.5 Other

Apart from the main ORC applications that have been discussed in the previous sections, other advanced applications are being currently studied in the form of prototypes or proof-of-concepts. These innovative applications include:

- Solar pond power systems, in which the ORC system takes advantage of temperature gradients in salt-gradient solar ponds (Tchanche, et al. 2011).

- Solar ORC-RO desalination systems, where the ORC is used to drive the pump of a reverse-osmosis desalination plant (Velez, et al. 2012).

- Ocean thermal energy conversion systems, utilizing the temperature gradients (of at least 20°C) in oceans to drive a binary cycle (Tchanche, et al. 2011).

- Cold production, where the shaft power of the ORC system is used to drive the compressor of a refrigeration system. Note that this layout can also be used to produce heat with a COP>1 if the ORC is coupled to a heat pump (Velez, et al. 2012).

2.3 Geothermal Energy

2.3.1 Introduction

Geothermal energy is the heat energy stored beneath the earth's surface. It originates from the formation of the planet, from radioactive decay of minerals, from volcanic activity, and from solar energy absorbed at the surface. The variance in the temperature between the core of the planet and its surface, also called the geothermal gradient, is the driving force behind the continuous conduction of thermal energy from the core to the surface (Turcotte 2002). In most of the world and away from tectonic plate boundaries, it is about 25 °C per km of depth (Fridleifsson, et al. 2008). The temperature profile of the inner earth, is shown in Figure 2.9:

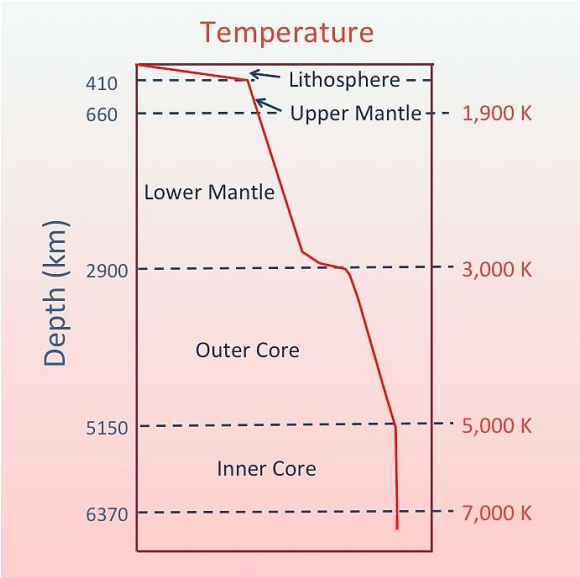

Figure 2.9 Temperature profile of the inner Earth (Fridleifsson, et al. 2008)

The heat outflows from the Earth's core, melting the rocks and forming the magma. Then, the magma rises toward the Earth's crust, carrying the heat from below through convective motions. It may flow as lava, smoothly or explosively, at the surface. In some areas, the magma remains below the crust, heating the surrounding rocks and hosted waters. Some of this hot geothermal water migrates upwards, through faults and cracks, reaching the surface as hot springs or geysers. Most of the geothermal water remains underground, trapped in cracks and porous rocks, forming the geothermal reservoirs. In such locations the geothermal heat flow can reach values ten times higher than normal.

Geothermal resources have been classified into low, medium and high enthalpy resources by their reservoir temperatures. Medium temperature geothermal resources where temperatures are typically in the range of 100 – 220 °C, are by far the most commonly available resources (Hettiarachchi, et al. 2007).

Europe has significant geothermal resources both in volcanic and sedimentary basin environment. The situation varies from country to country according to the geothermal technology that best suits the available natural resource. The spectrum varies from power generation from high enthalpy resources (Iceland, Italy, Greece), to direct use of hydrothermal resources in sedimentary basins (France, Germany, Poland, Italy, Hungary, Romania, and others). Shallow geothermal is available everywhere and is mostly harnessed by ground source heat pump installations. In Figure 2.10, the main geothermal resources of Europe are depicted (Antics 2007)

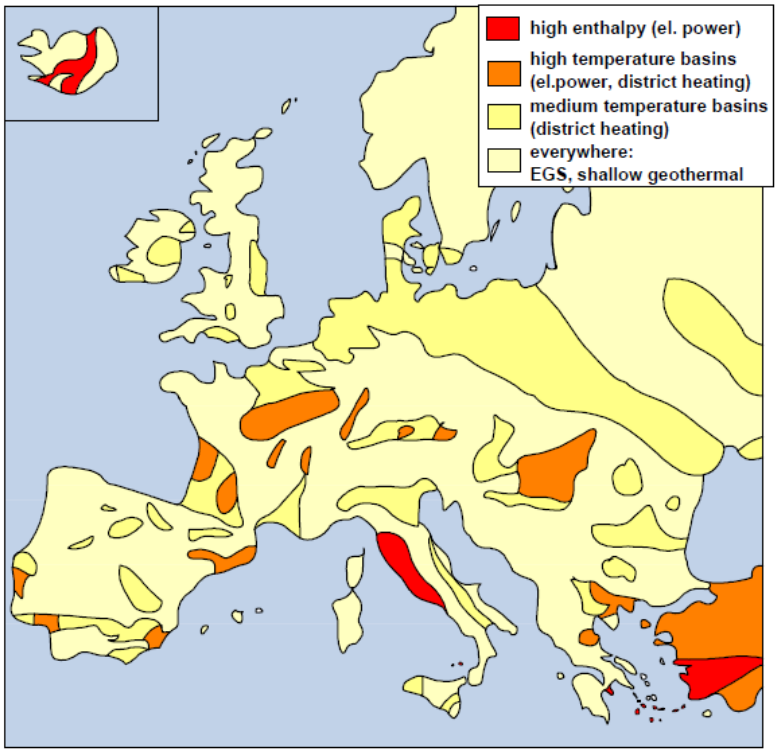

Figure 2.10 Main basins and geothermal resources of Europe

In Germany, many existing geothermal power plants are used for both power and heat generation. These are shown in Figure 2.11. Beneficial spots for geothermal plants can be found in the North German Basin, the Upper Rhine Rift and the South German Molasse Basin.

According to (Schulz 2005), who performed studies of the probability of success for hydrothermal wells in Molasse Basin in Germany, production from one well should, for economic reasons, exceed 50 l/s. In Germany, for 3.5-4 km deep wells the probability of success (POS) is usually calculated by the investor for flow rates of 65 l/s and 100 l/s. If performance of the well after stimulation is worse than the minimal POS requirement, the well is considered to be unsuccessful. If only the lower limit is reached, drilling is regarded as partially successful. Projects like Offenbach, Speyer and particularly Unterhaching, where a volumetric flow rate of 150 l/s was obtained from a single 3350 m deep production

well (Knapek 2007), have reached their goals. On the other hand, projects such as Bruchsal with a flow rate lower than 25 l/s are also present in the market.

The design of a standardized binary power plant should be based rather on successful projects, because with gained experience their share will be growing. However, in the geothermal industry a high risk of failed drilling will always exist and even in unsuccessful projects, where productivity of a well is low, geothermal water usually has to be utilized in order to minimize financial losses.

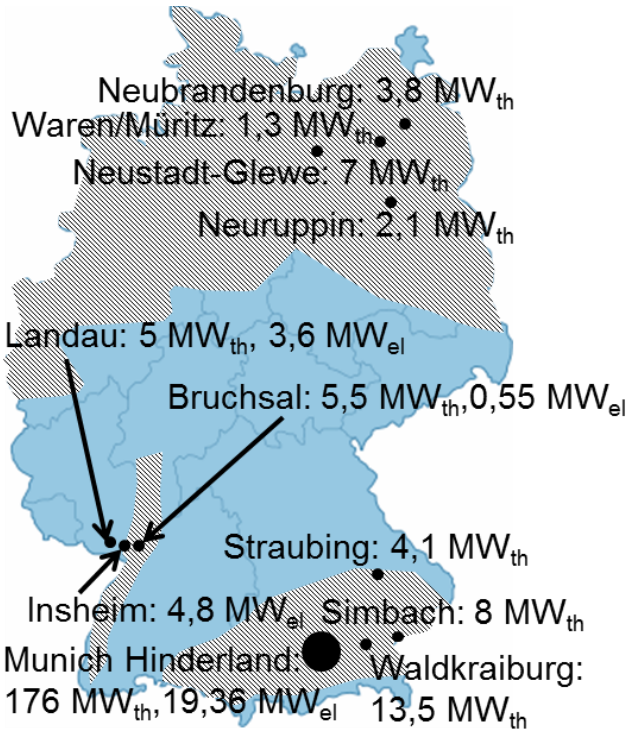

Figure 2.11 Geothermal Plants in Germany (Bundesverband Geothermie, Tiefe Geothermieprojekte in Deutschland)

2.3.2 Advantages of geothermal energy

Geothermal Energy has the potential to provide a low CO_2 emission base-load power and heat by utilizing the natural hydrothermal resources of the planet. Moreover, the exploitable hot spots are worldwide distributed and have the potential to satisfy the world energy demand.

In contrast to renewable energy sources like wind and solar energy, geothermal energy is not plagued by intermittency, which means that geothermal power plants can function as base load providers with great predictability. Geothermal has a higher capacity factor than many other power sources and is therefore suitable for base load demand.

The capacity factor of a power plant is defined as the ratio of its actual output over a period of time, to its potential output if it was possible to operate at full installed capacity constantly. The US Energy Information Administration rates new geothermal plants with a 92% capacity factor, higher than those of nuclear (90%), gas (87%), or coal (85%), and much higher than those of intermittent sources such as onshore wind (34%) or solar photovoltaic (25%). In Figure 2.12, the capacity factors of different renewable energies are presented. Geothermal energy, has the highest capacity of them all, with a minimum of 85%.

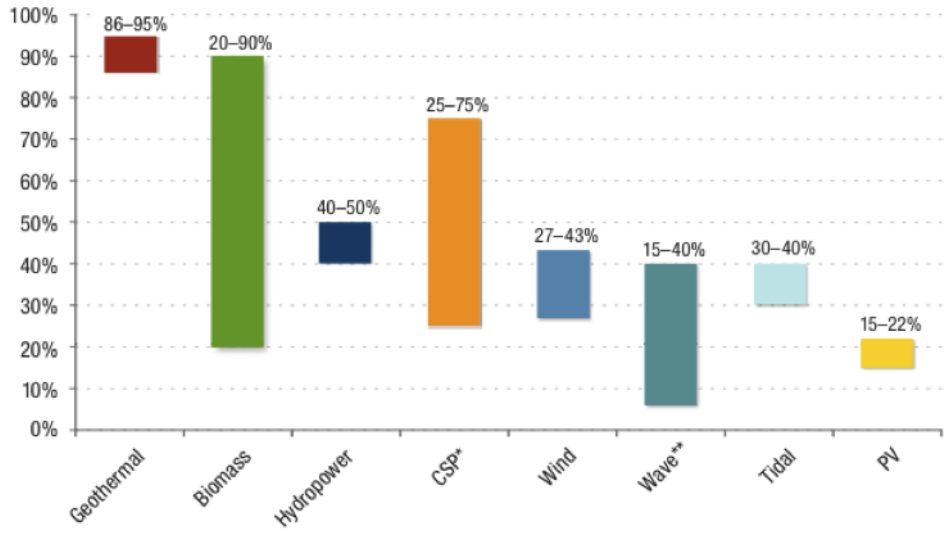

Figure 2.12 Capacity factor for Renewable Resources (U.S. Energy Background Information 2009)

While the carrier medium for geothermal electricity (water) must be properly managed to avoid local depletion, the source of geothermal energy, the Earth's heat, will be constantly available. That is because the energy removed from the resource is continuously replaced by more energy on time scales similar to those required for energy removal. Consequently, geothermal exploitation is not a “mining” process. (Rybach 2007)

2.3.3 Current technologies

There are several types of geothermal power technologies. Geothermal power plants today can use water in the vapor phase, a combination of vapor and liquid phases, or liquid phase only. The selection of the plant depends on the depth of the reservoir, and the temperature, pressure and nature of the entire geothermal resource. The three main types of plant are flash steam, dry steam and binary plants (Technology Roadmap: Geothermal Heat and Power 2011).

A simplified diagram of a typical geothermal plant, with a cross section of the inner earth and the geothermal water flow, is shown in Figure 2.13:

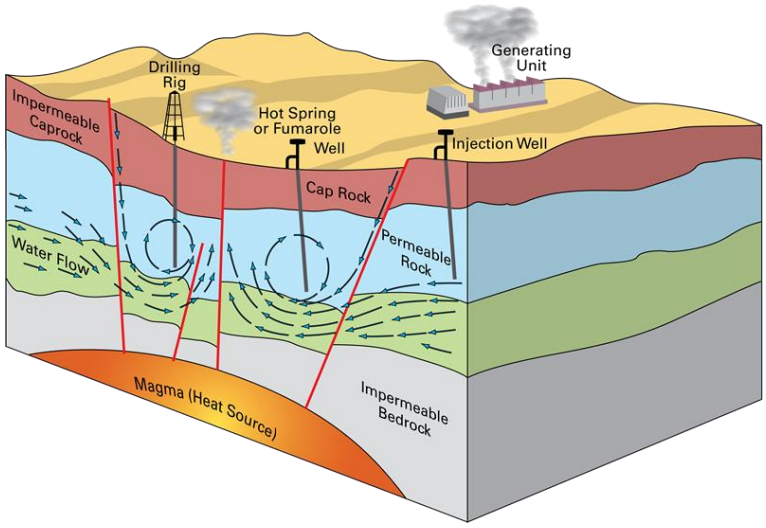

Figure 2.13 Simplified diagram of geothermal plant (British Geological Survey 2011)

2.3.3.1 Dry steam plants

Today, dry steam plants account for approximately one quarter of the geothermal capacity. They directly employ dry steam at a temperature above 150°C, which is piped from production wells to the plant and then to the turbine (Hohmeyer 2008). Control of steam flow to meet electricity demand fluctuations is easier than in flash steam plants, where continuous up-flow in the wells is required to avoid gravity collapse of the liquid phase. In dry steam plants, the condensate is usually re-injected into the reservoir or used for cooling. In Figure 2.14, the simplified configuration of a Dry Steam plant is depicted. The numbers in the graph correspond accordingly to: 1: Production Well, 2: Injection Well, 3: Turbine/Generator, 4: Condenser, 5: Pump.

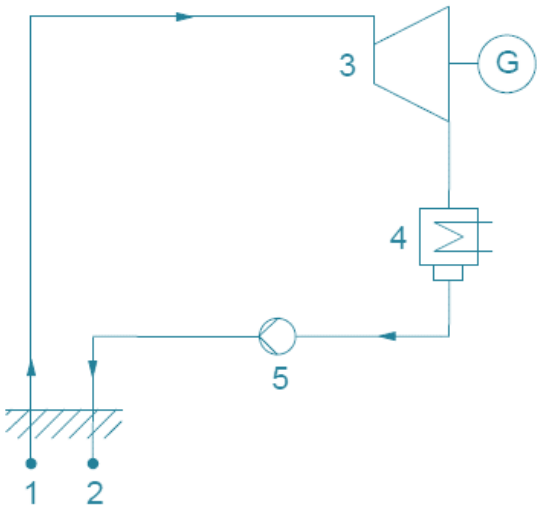

Figure 2.14: Dry Steam Configuration (Spliethoff, H., Wieland, C. 2012)

2.3.3.2 Flash steam plants

The most commonly found geothermal resources contain reservoir fluids with a mixture of hot liquid (water) and vapor (mostly steam) (Hohmeyer 2008). Flash steam plants, making up about two-thirds of geothermal installed capacity today, are used where water-dominated reservoirs have temperatures above 180°C. In these high-temperature reservoirs, the liquid water component boils, or "flashes," as pressure drops. Separated steam is piped to a turbine to generate electricity and the remaining hot water may be flashed again twice (double flash plant) or three times (triple flash) at progressively lower pressures and temperatures, to obtain more steam. The cooled brine and the condensate are usually sent back down into the reservoir through injection wells. Combined-cycle flash steam plants use the heat from the separated geothermal brine in binary plants to produce additional power before re-injection. In Figure 2.15, the simplified configuration of a Double Flash steam plant is shown. The numbers in the graph correspond accordingly to 1: Production well, 2: Injection Well, 3, 5: Throttle, 4, 6: Flash Tank 7: High pressure Turbine, 8: Low pressure Turbine, 9: Generator, 10: Condenser, 11: Pump.

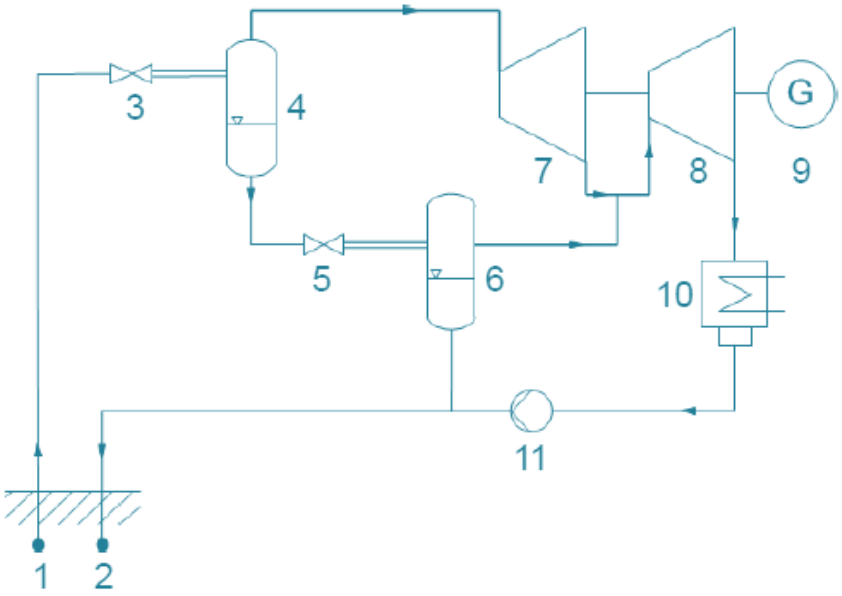

Figure 2.15 Configuration of a Double Flash (Spliethoff, H., Wieland, C. 2012)

2.3.3.3 Binary plants

Electrical power generation units using binary cycles constitute the fastest-growing group of geothermal plants, as they are able to use low- to medium-temperature resources, which are more prevalent. Binary plants, using an organic Rankine cycle (ORC) or a Kalina cycle, typically operate with temperatures varying from as low as 73 °C (at Chena Hot Springs, Alaska) up to 180°C. In these plants, heat is recovered from the geothermal fluid using heat exchangers to vaporize an organic fluid with a low boiling point (e.g. butane or pentane in the ORC cycle and an ammonia-water mixture in the Kalina

cycle), and drive a turbine. The Organic Rankine Cycle is the main focus of this study and was presented in detail in Chapter 2.2.

Although both cycles were developed in the mid-20th century, the ORC cycle has been the dominant technology used for low-temperature resources. The Kalina cycle can, under certain design conditions, operate at higher cycle efficiency than conventional ORC plants. The lower-temperature geothermal brine leaving the heat exchanger is reinjected back into the reservoir in a closed loop, thus promoting sustainable resource exploitation. Today, binary plants have an 11% share of the installed global generating capacity and a 44% share in terms of the number of plants (Bertani 2010).

A typical binary plant configuration is given in Figure 2.16, where 1: Production well, 2: Injection Well, 3: Evaporator, 4: Preheater 5: High pressure Turbine, 6: Recuperator, 7: Condenser, 8: Pump.

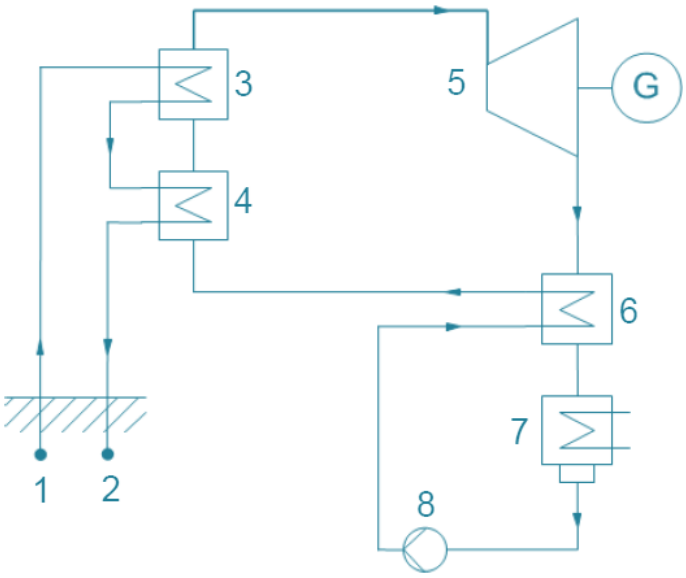

Figure 2.16 Binary plant configuration (Spliethoff, H., Wieland, C. 2012)

Nowadays, the main focus for binary plant configurations has been shifted from pure electrical power generation to combined heat and power (CHP) applications. Combined Heat and Power and Geothermal Energy is further investigated in the next chapter.

2.4 Geothermal Combined Heat and Power

Combined heat and power is the most effective way to make use of medium and low geothermal energy sources. The main reason is that CHP make more efficient use of the geothermal resources by cascading the geothermal fluid to successively lower temperature applications, thereby improving the economics of the entire system dramatically. Both high- and low-enthalpy geothermal resources can be directly used in a number of heating applications, such as space heating and cooling, industry, greenhouses, fish farming, health spas, etc. From the economic point of view, however, direct heat applications are site-sensitive as steam and hot water are hardly transported over long distances (Fridleifsson, et al. 2008). The most common application of the geothermal heat is for district heating schemes. The heat energy required may be regarded as a by-product of geothermal power production in terms of either waste heat released by the generating units or excess heat from the geothermal source.

The necessary condition required for the system to be cost effective, is the requirement of sufficient demand for heat production (e.g. district heating). In general, CHP plants are economically viable and largely used in colder climates, like Northern Europe where heating demand is significant and constant over the year. Therefore, in these areas, CHP is used more than power generation alone. The typical size of combined heat and power plants ranges from a few MWe up to 45 MWe (EGEC 2009). One of the first, and most well documented ORC-CHP units installed in Germany, is the one in Neustadt-Glewe. More details are given in the next section.

2.4.1 Neustadt-Glewe

The Neustadt-Glewe geothermal heating plant was commissioned in January 1995, supplying exclusively in direct-heat transition the base load of a district heating system amounting to a thermal output of approximately 11 MW, thus covering the demand of a major part of the town of Neustadt-Glewe. The installed geothermal capacity is 6 MW; a gas-fired boiler unit is operated to cover the peak-load. In the summer of 2003, the heating plant was extended by an ORC unit and in November of 2003, the first German geothermal power plant was connected to the grid, providing 210 kW_e gross capacity. The brine is produced from a 2100 to 2300 m deep sandstone aquifer. High salt contents of the brine (total dissolved solids = 227 g/L) require the use of resistant materials (e.g., titanium) for the heat exchanger equipment (Lund 2005).

The Neustadt-Glewe plant supplies heat and power using a parallel-series connection of power plant and heating station, as shown in Figure 2.17. The heating station takes priority over the power plant. The incoming mass flow rate of the brine is split and a part is fed to the power plant. The brine leaves the power plant at constant outlet temperature. The two flows, one at initial brine inlet temperature, the other at outlet temperature of the power plant, are joined upstream from the heating station. The mixing temperature should

be high enough to meet the heating demand. In summertime, a minimum temperature of 73°C is required. To meet the heating demand in wintertime, higher temperatures are necessary, amounting up to the initial maximum brine temperature 98°C, one of the lowest temperature used in the world. Unlike common combined heat and power plants with combustion or the plant setup realized with the Husavik plant, heating station and power plant are competing for the brine. The power plant is fed with variable mass flow rate of the brine at constant temperature; while, the heating station is provided with a constant mass flow rate at variable temperature (Lund 2005).

The power plant is a simple Organic Rankine Cycle (ORC) using n-Perfluorpentane (C_5F_{12}) as working fluid. An additional pump was installed in the geothermal loop to control the mass flow rate fed to the power plant and to overcome the pressure losses of the brine in the heat exchanging equipment of the power plant. Parasitic loads in the plant include all pumps (brine pump, feed pump 10 kW, cooling water pump in cooling circuit, 15 kW), the ventilators in the cooling tower (16 kW), the cooling water pump in the well and several dosing pumps in the make-up system for the cooling water. Only the downhole pump in the production well is not included in the parasitic loads. In Figure 2.17, the configuration of CHP plant Neustadt-Glewe is shown (Lund 2005).

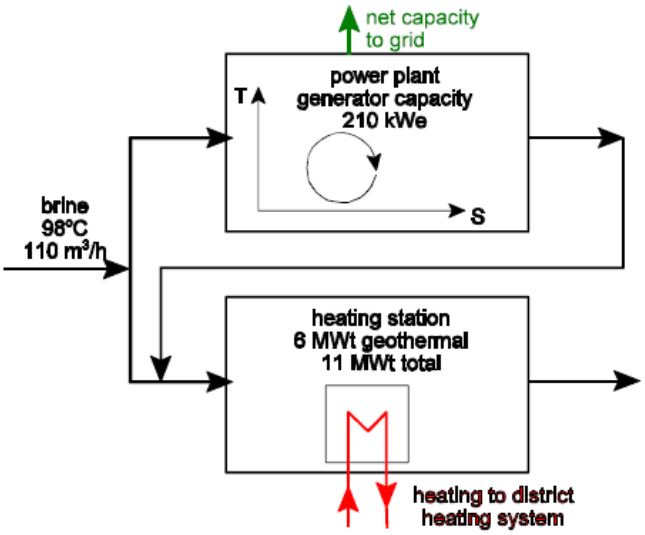

Figure 2.17 Combined heat and power supply in Neustadt-Glewe, serial/parallel connection of power plant and heating station (Lund 2005)

3 Organic Rankine Cycle Power Generation

3.1 Pure Power Generation Models

3.1.1 Standard / Simple Concept

The Organic Rankine Cycle pure power generation simple concept is the simplest configuration examined in this work. Although a description of the ORC operation has already taken place in the previous section, in the next paragraphs a more detailed report is given, thoroughly over the simple pure power generation concept.

The operating cycle begins when the stream of the heat source fluid, enters the system. In the case of geothermal applications, the source fluid is generally geothermal brine from a production well. This geothermal source fluid, flows through the network of heat exchangers, in which heat is transferred to the working fluid of the ORC unit. Usually, there are two stages of heat exchange: one occurring in a preheater, where the temperature of the working fluid is raised to its bubble point, and the other in an evaporator, where the working fluid is vaporized. However, in cases where the fluid is to reach a superheated state, a third heat exchanger known as superheater is required. The addition of superheater relies heavily on the properties of the working fluid. Dry or isentropic working fluids typically do not require superheating. On the other hand, wet fluids must be superheated in order to avoid corrosion damage in the turbine due to the formation of water droplets. Last but not least, a small superheating may occur in the last stages of the evaporator, even in the absence of separate superheating device. This is done on purpose, in order to mediate any following thermal losses and to maximize the heat capacity while avoiding any extra costs (Dinçer 2010) .

The heat addition takes place in the preheater and evaporator of the ORC unit. Ideally this is an isobaric process, however pressures losses occur in the heat exchangers and tubes. With detailed and optimal design, these losses can be minimized. Another approach is to assume a pressure drop between the outlet of the evaporator and the inlet of the turbine which will be considered as representative of all the pressure drops (Ibarra, et al. 2014). Moreover, with a simple feedback control loop the pump covers any losses with additional pressure increase, while consuming minimal extra power due to the thermodynamical properties of the working fluid state (Grundfos 2009) . In the present study a combination of the above methods is used. Firstly the pressure losses are assumed minimal and ignored and secondly the heat exchangers are designed and optimized. Lastly, the losses are assumed to be covered by the feedback control method of the pump.

The high-pressure vapor is then expanded in the steam turbine. The organic fluid exhaust vapor from this process is superheated steam, which is a result of the characteristic shape of the working fluid saturation line of dry and isentropic fluids. Moreover, this is also caused by the unavoidable irreversibilities of the expansion. In an ideal isentropic (and therefore vertical in the T-s diagram) expansion, more work would be produced, but also the danger of expanding in the wet zone would be greater.

The superheated stream of exhaust vapor may be sent directly to the condenser, where it is cooled and condensed. However, if economically feasible, the exhaust stream from the turbine is firstly directed to a recuperator. This heat exchanger recovers a part of the superheated vapor heat, which is consequently transferred to the liquid stream of working fluid entering the preheater. This is done in cases where the exhaust superheated steam has a sufficient enthalpy level after the expansion. In the present study, the working fluid is expanded close to the condensing temperature, rendering the addition of recuperator non-feasible. After leaving the condenser, the working fluid enters the pump, where its pressure is increased and returned directly, or through the regenerator, to the preheater and thus closing the thermodynamic cycle.

The pure power configuration follows the scheme shown in Figure 3.1. For a list of the abbreviations used in the figure, as well as all of this work, the reader may refer to the Notation in the beginning of this work.

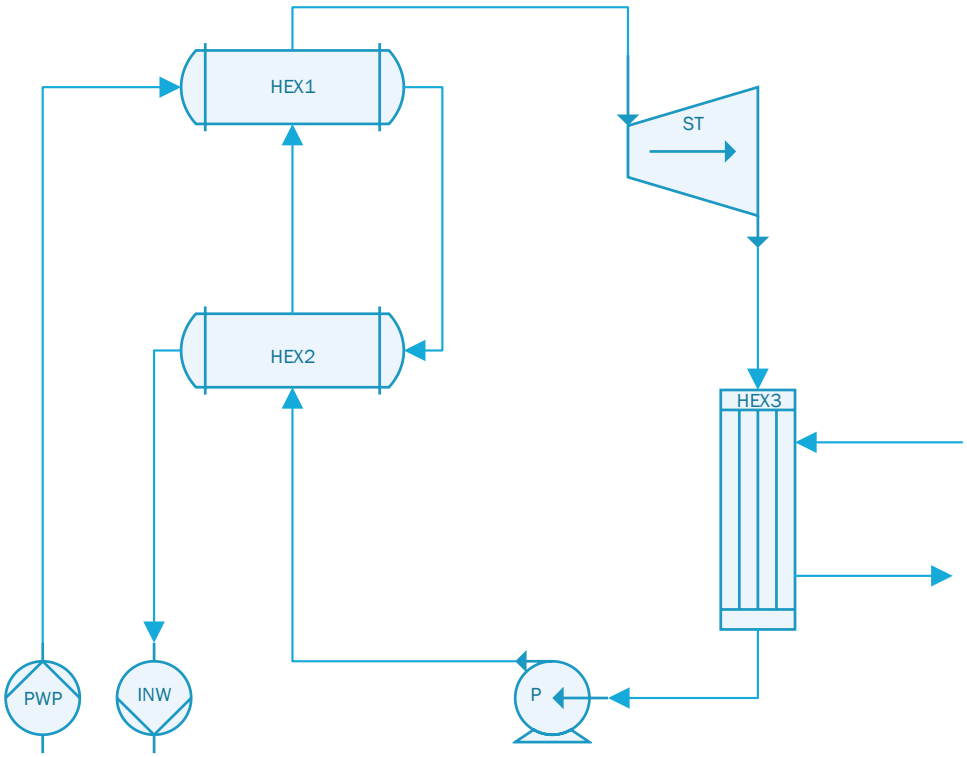

Figure 3.1 Standard / Simple power generation ORC configuration

3.1.2 Two Stage Turbine / “Bleed” Concept

The two stage pure power generation concept follows essentially the same operation method in comparison to the simple concept in Figure 3.1. Nevertheless, there are some essential variables and parameters, which change between the two concepts. The Idea of a two stage concept comes from the traditional water - steam power plants, where multi - staged steam turbines are used.

The operation cycle is mostly the same as the simple model. However, after the evaporator, the operation changes significantly. First and foremost, the steam turbine is not one-stage, but two-stage, which adds the feature of extracting steam from the turbine at an intermediate pressure. The remaining steam in the turbine expands until the condensation pressure is reached and consequently cools and condenses in the condenser. The condensate flows through the low pressure pump and reaches the intermediate pressure. It is then directed in a tank and mixed with fresh steam extracted from the two-stage turbine. The fluid at outlet of the tank is condensate in the intermediate pressure. Lastly, this condensate flows through the high pressure pump and consequently back in the preheater, closing the cycle.

In order to simplify the simulation model, the two stage turbine is modelled as two separate steam turbines. A splitter is added between the two turbines, in order to for the steam extraction to be modelled. In Figure 3.2, the two stage concept is illustrated.

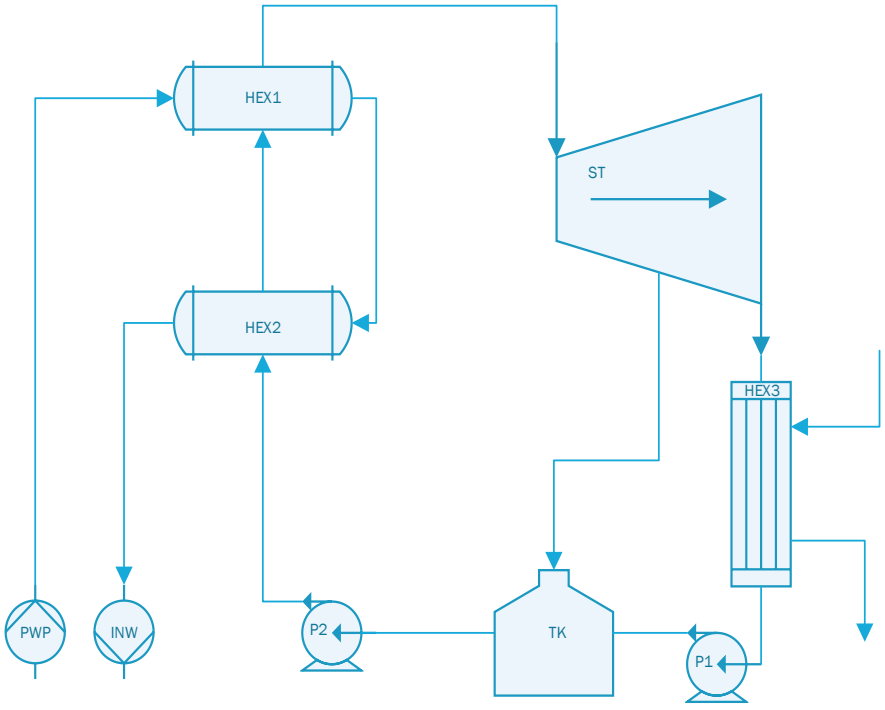

Figure 3.2 Pure Power Generation - Two Stage Concept / Model 1

3.2 Matlab Modelling

The modelling of the ORC configurations was done in MATLAB. The solving algorithm is based on the numbering of the pipelines and connection of components of each configuration, as was presented in the previous section.

In order to program the model, the most important step is to formulate the individual mass, pressure and energy balance equations of every component in the whole system. Thus the mass, pressure and energy matrices are formed. These represent the entire system and therefore are the heart of the model. The solving algorithm is presented in Figure 3.3.

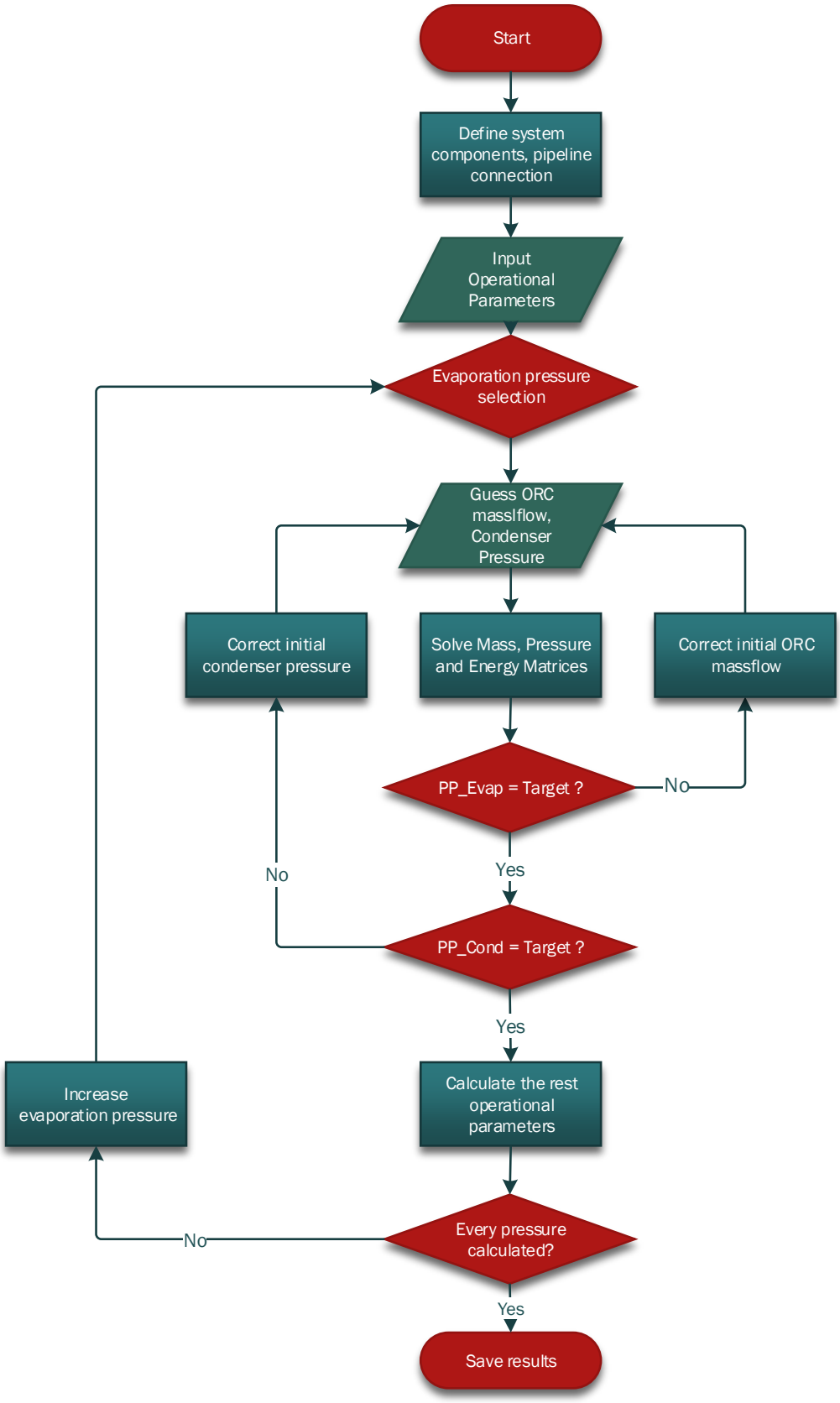

Figure 3.3 Pure power generation solving algorithm

3.3 Components of the ORC

In the sections below, information is given on the most important components of the organic rankine cycle configurations and how they are modeled in the simulations.

3.3.1 Steam Turbine

A steam turbine is a device that extracts thermal energy from pressurized steam and uses it to do mechanical work on a rotating output shaft. The stream of high-pressure vapor of organic fluid expands in the turbine, causing its internal part to rotate. The rotor is connected by a shaft to the generator which changes rotational kinetic energy into electricity. The expansion process is considered adiabatic and a steady sate of operation is assumed. The generated electric power can be calculated as follows:

$$P_{el,T} = \dot{m} \cdot \left(h_{T,in} - h_{T,out}\right) \cdot \eta_m \cdot \eta_{gen} = \dot{m} \cdot \left(h_{T,in} - h_{T,out,is}\right) \cdot \eta_m \cdot \eta_{gen} \cdot \eta_{is,T} \quad (3.1)$$

The mass flow of the working fluid as well as the enthalpy values, are calculated during the simulations, while the mechanical efficiency, generator electrical efficiency and turbine isentropic efficiency are given by the manufacturer of the equipment. Generally, the mechanical and electrical efficiencies maintain a constant value.

The turbine isentropic efficiency which, as can be seen in the previous equation, compares the real and ideal expansion in the turbine. For a steam turbine operating at off-design conditions, the characteristic curve describing the isentropic efficiency is a function of the mass flow rate (Jüdes 2009), (EBSILON Professional 7.00 n.d.):

$$\frac{\eta_{is,T}}{\eta_{is,T,N}} = -1.0176 \left(\frac{\dot{m}}{\dot{m}_N}\right)^4 + 2.4443 \left(\frac{\dot{m}}{\dot{m}_N}\right)^3 - 2.1812 \left(\frac{\dot{m}}{\dot{m}_N}\right)^2 + 1.0535 \frac{\dot{m}}{\dot{m}_N} + 0.701 \quad (3.2)$$

Where $\eta_{is,T,N}$ is the isentropic efficiency at the design point, at which the isentropic efficiency has the maximum value. At partial-load operation, the efficiency $\eta_{is,T}$ must be adjusted with respect to changes in the outlet steam quality (Δx_e). When the exiting steam quality is lower than 1, this adjustment is carried out using the following approximation:

$$\eta_{is,T,corr} = \eta_{is,T} - \frac{1}{2} \cdot \Delta x_e \quad (3.3)$$

Where $\eta_{is,T}$ denotes the isentropic efficiency in accordance with (3.2) and $\eta_{is,T,corr}$ denotes the resulting isentropic efficiency after the correction for steam quality.

An example is provided in Figure 3.4, where the isentropic efficiency is plotted for the design values of $\eta_{is,T,N} = 80\%$ and $\dot{m}_N = 185.56\ kg/s$ for a mass flow range of 50-210 kg/s.

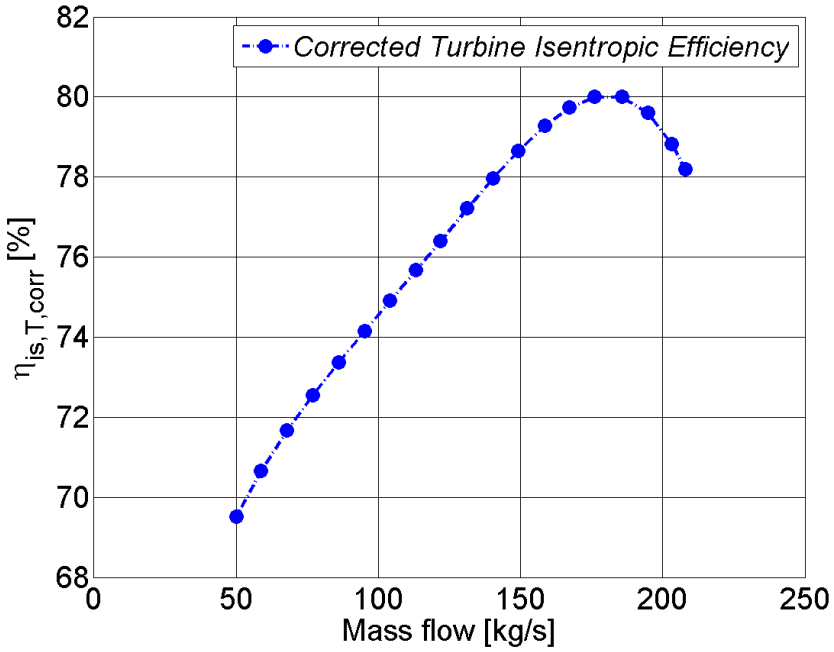

Figure 3.4 Turbine isentropic efficiency – mass flow rate

It is clear that the selection of the design point plays a very important role in the turbine efficiency. However, for small deviations of the mass flow from the design point, the efficiency is not changing significantly. Further simulations of the isentropic efficiency will be presented in the next sections.

3.3.2 Pump

The pumps are used in the cycle to raise the pressure of the working fluid after the expansion that occurs in the steam turbine. Using the same assumptions that were used for the turbine, power consumed by the feed pump can be calculated as:

$$P_{el,P} = \dot{m} \cdot \frac{h_{P,out} - h_{P,in}}{\eta_m \cdot \eta_{gen}} = \dot{m} \cdot \frac{h_{P,out,is} - h_{P,in}}{\eta_m \cdot \eta_{gen} \cdot \eta_{is,P}} \tag{3.4}$$

The mechanical efficiency, generator electrical efficiency and pump isentropic efficiency are given by the manufacturer of the equipment. The enthalpies and mass flows result from the simulations. However, in contrast with the steam turbine, there is not such a straightforward equation that connects mass flow and isentropic efficiency. Therefore, the pump isentropic efficiency will be assumed constant. This is further justified by the facts that the pump is a component that has relatively small power consumption due to thermodynamic and working fluid properties reasons and secondly, the isentropic efficiency of the commercial available pumps are very high, usually above 90%. Consequently, the pump efficiency will be considered constant in all simulations.

3.3.3 Heat exchangers

The heat exchangers are modeled by dividing them into a number of zones and calculating the properties of the working fluid for each zone as it flows through. The method which is used is the Log mean temperature difference (LMTD). The LMTD is a logarithmic average of the temperature difference between the hot and cold streams at each end of the exchanger. The use of the LMTD arises straightforwardly from the analysis of a heat exchanger with constant flow rate and fluid thermal properties. The LMTD is given by equation (3.5), where "1" and "2" correspond to the two ends of the heat exchanger at which the hot and cold streams enter or exit on either side.

$$LMTD = \frac{\Delta T_1 - \Delta T_2}{ln\left(\frac{\Delta T_1}{\Delta T_2}\right)} \tag{3.5}$$

The heat transferred in each zone is given by the equation:

$$Q = U \cdot A_{HEX} \cdot \ LMTD = UA_{HEX} \cdot \frac{(T_{h1} - T_{c2}) - (T_{h2} - T_{c1})}{\ln \frac{T_{h2} - T_{c1}}{T_{h1} - T_{c2}}} \tag{3.6}$$

At this point of analysis, the heat transfer coefficient (U) and the total area (A_{HEX}) separately, are not of interest. Therefore the total product ($U \cdot A_{HEX}$) for each zone will be calculated by the simulation.

The LMTD developed previously is not applicable for heat transfer analysis of cross-flow and multi-pass flow heat exchangers. A correction factor, F, is needed:

$$Q = \ U \cdot A \cdot \ LMTD \cdot F \tag{3.7}$$

The correction factors are available in chart form as prepared by Bowman et al. (1940) for practical use for all common multi-pass shell and tube and crossflow heat exchangers. The correction factor F is less than 1 for cross-flow and multi-pass arrangements; and 1 for a true counter-flow heat exchanger. F represents the degree of departure of the true mean temperature difference from LMTD for a counter-flow arrangement. In this thesis, the heat exchangers will be considered true counter-flow and therefore F=1.

3.4 Benchmarks for cycle evaluation

In this section the thermodynamic variables that are investigated are defined. In this work, these are the different efficiencies of the Organic Rankine Cycle and the pure power generation. These are used in order to evaluate the different concepts.

3.4.1 Power Generation

Power or electricity generation is the process of generating electric power from other sources of primary energy. In this work, this primary energy is the thermal energy of the geothermal fluid. Power is generated in the turbine of the ORC module. For more details about the turbines of the ORC module, the reader may refer to chapter 3.3.1. Generally, the power generation is defined as the net electrical power generated by the ORC module, which is the electrical power generated by the electrical generator coupled to the turbine minus the electrical power required by the motor of the pump. For the two stage concept power generation model, both turbine stages and pumps must be taken into account.

$$P_{el,ORC} = P_{el,T} - P_{el,P} = \dot{m} \cdot \left(h_{T,in} - h_{T,out}\right) \cdot \eta_{gen} \cdot \eta_{mech} + \dot{m} \cdot \frac{\left(h_{P,in} - h_{P,out}\right)}{\eta_{gen} \cdot \eta_{mech}} \quad (3.8)$$

3.4.2 Thermal Efficiency

The thermal efficiency is a dimensionless performance measure of a device that uses thermal energy. It generally indicates how well an energy conversion or transfer process is accomplished. In this case the device is the ORC module, and therefore the thermal energy input is defined as the total thermal energy input in the ORC cycle, which is occurs in the evaporator and preheater/economizer. The formula of the thermal efficiency is:

$$\eta_{thermal} = \frac{P_{output}}{Q_{input}} = \frac{P_{el,ORC}}{Q_{ORC}} = \frac{P_{el,ORC}}{\dot{m} \cdot \left(h_{EVAP,out} - h_{ECO,in}\right)} \quad (3.9)$$

3.4.3 System Efficiency

The system efficiency is similar to the thermal efficiency, but instead of defining the system boundaries as the ORC module, the whole system is considered. Therefore the energy input here is heat energy of the geothermal heat source in reference to the ambient temperatures, shown in equation (3.10).

$$\eta_{system} = \frac{P_{output}}{Q_{input}} = \frac{P_{el,ORC}}{Q_{system}} = \frac{P_{el,ORC}}{\dot{m}_{gw} \cdot \left(h_{gw,in} - h_{gw,ref}\right)} \tag{3.10}$$

3.4.4 Exergy Efficiency

The exergy efficiency (also known as the second-law efficiency or rational efficiency) computes the efficiency of a process taking the second law of thermodynamics into account. It can be demonstrated from the second law of thermodynamics, that no system can ever be 100% efficient. Therefore, when calculating the energy efficiency of a system, for example the thermal or system efficiency, the value found gives no indication of how the system compares to a thermodynamically perfect one operating under the same conditions. In comparison, the exergy efficiency of a system can reach 100% because the work output is compared to the potential of the input to do work. The energy efficiencies of a heat engine are always smaller than its exergy efficiency (Gilliland 1978). Therefore:

$$\eta_{exergy} = \frac{P_{output}}{Q_{input}} = \frac{P_{el,ORC} + E_{DH}}{E_{TWin}} \tag{3.11}$$

$$E_{DH} = \dot{m}_{DH} \cdot \left[h_{DH,out} - h_{DH,in} - T_{ref} \cdot \left(s_{DH,out} - s_{DH,in}\right)\right] \tag{3.12}$$

$$E_{TWin} = \dot{m}_{gw} \cdot \left[h_{gw,in} - h_{gw,ref} - T_{ref} \cdot \left(s_{gw,in} - s_{gw,ref}\right)\right] \tag{3.13}$$

3.5 Design boundary conditions

The design boundary conditions for the model of the ORC power plant must be cautiously chosen in order to assure the best performance of the unit under its future operating conditions. In the following sections are the factors which affect the performance of ORC power plant in the greatest way and have to be assessed before the simulation process:

3.5.1 Heat source conditions

The temperature and energy of the heat source fluid produced from the geothermal production well is one of the most important parameters of the power plant. In this work, the selected heat source temperature is 140 °C at a pressure of 10 bar, while the total geothermal power available is rated at 50 MWth. These are typical values for the area

of the South German Molasse Basin and the greater Munich area (Dominik Meinel, personal discussion 2014).

3.5.2 Cooling conditions

The condenser of the ORC units is considered water-cooled with an input water cooling temperature of 20°C. This temperature is equal to the ambient temperature and corresponds to an average high value of the southern Germany summer months (climatedata.eu 2014). Therefore this is a worst case scenario, since the lower the temperature, the lower the demand for cooling water will be. For the cooling water exiting the condenser, a maximum ΔT of 3°C increase is considered, due to environmental reasons.

3.5.3 Working fluids

The working fluids of the ORC unit that will be examined, are the R1234ze and R1234yf. These two are the only HFOs included in the REFPROP library and have been actually included only during the last years, where increasing interest for a fourth generation of refrigerants has increased. For more information about the refrigerants, the reader may refer to section 2.1.2.

The total boundary conditions used in the simulations are summarized in Table 3-1:

Table 3-1 ORC Pure power generation boundary conditions

Variable	***Value***
Geothermal Source	--
Geothermal heat power (MWth)	50
Production pressure (bar)	10
Temperature (°C)	140
Cooling Conditions	--
Cooling fluid input temperature (°C)	20
Maximum temperature increase (°C)	3
Efficiencies	--
Mechanical	0,98
Electrical	0,95
Isentropic pump	0,9
Isentropic Turbine (nominal)	0,8
Heat exchangers	--
Evaporator Pinch point (°C)	10
Condenser Pinch point (°C)	10
Working Fluids	--
Fluid 1	R1234ze
Fluid 2	R1234yf

3.6 Simulation Results

In the following sections, the results of the pure power generation simulations for variable evaporating pressure and heat source temperature are presented and discussed.

3.6.1 Standard / simple ORC concept power generation

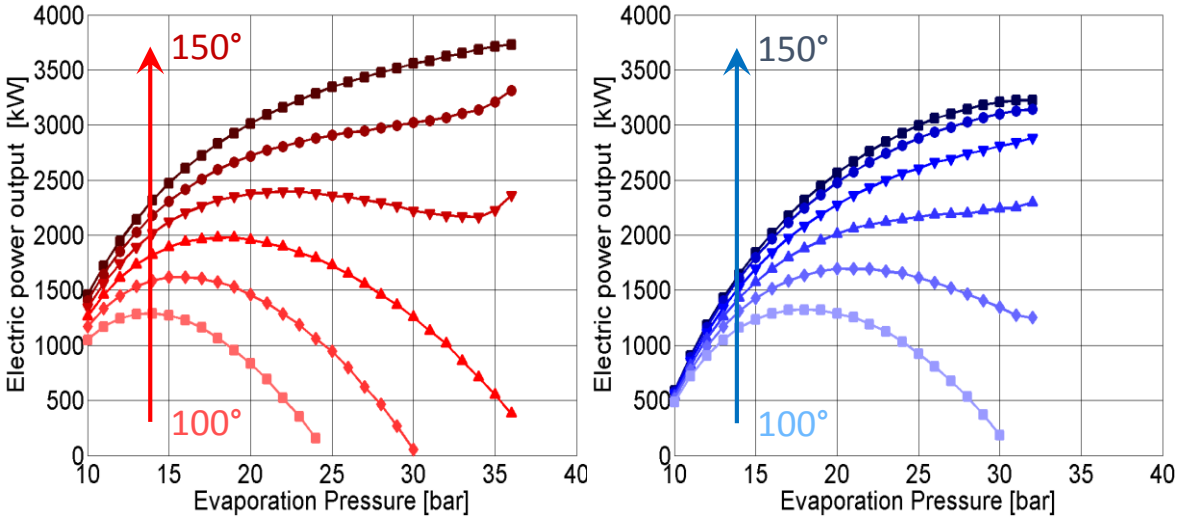

Figure 3.5 Pure power generation standard concept

As shown in Figure 3.5, for high temperatures of 140-150 °C, R1234ze produces more power. However for lower temperatures in the range of 120-130 °C, the R1234yf produces more power, while in the area of very low temperatures of 100-110°C both fluids produce approximately the same power. The reason for this variation at the given heat source temperatures, is due to the combination of two main causes:

First of all, due to the different properties of the two fluids, which affect the heat transfer in the preheater, evaporator and condenser, as well as the energy extracted in the turbine. The most important are summarized in the Table 3-2:

Table 3-2 Properties of R1234ze and R1234yf

	R1234ze	R1234yf
Molar mass (kg/kmol)	114,04	114,04
Triple point temperature (°C)	-104,53	-53,15
Normal boiling point temperature (°C)	-18,95	-29,45
Critical point temperature (°C)	109,37	94,7
Critical point pressure (bar)	36,363	33,822
Critical point density (kg/m³)	489,24	475,55
Acentric factor	0,313	0,276

The second cause, are the external parameters selected in the design phase, for example the pinch point temperature of the heat exchangers. The selected pinch point temperature, determines also the mass flow rate of the ORC unit. This is solved in the model with a repetition method (Section 3.2). For example, for the case of 130°C geothermal source, the evaporating temperature, the geothermal fluid temperature at ORC outlet and the ORC mass flow rate are shown in the Table 3-3:

Table 3-3 Evaporation temperature, ORC mass flow and geothermal stream exit temperature. Geothermal source temperature: 130 °C.

	R1234ze	R1234yf
Evaporation temperature (°C)	99,57	88,67
ORC mass flow rate (kg/s)	130,83	239,91
Geothermal fluid temperature at ORC outlet (°C)	78,66	52,18

As shown in Table 3-3, although the R1234ze has a higher evaporation temperature than the R1234yf, the mass flow rate is significantly lower. The higher mass flow rate of the R1234yf, results in more heat transfer in the preheater and evaporator and thus a lower geothermal fluid temperature at the ORC outlet. Therefore, R1234yf has higher power output at the temperatures of 120-130°C as seen in in Figure 3.5.

Moreover, in the range of 130-140°C of the R1234ze, the power generation curve has a different pattern than in the other temperatures. This is seen as an increase in low pressures, then a decrease for medium pressures, followed by a sudden increase in the highest pressures. An explanation of this behavior can be found by observing Figure 3.6:

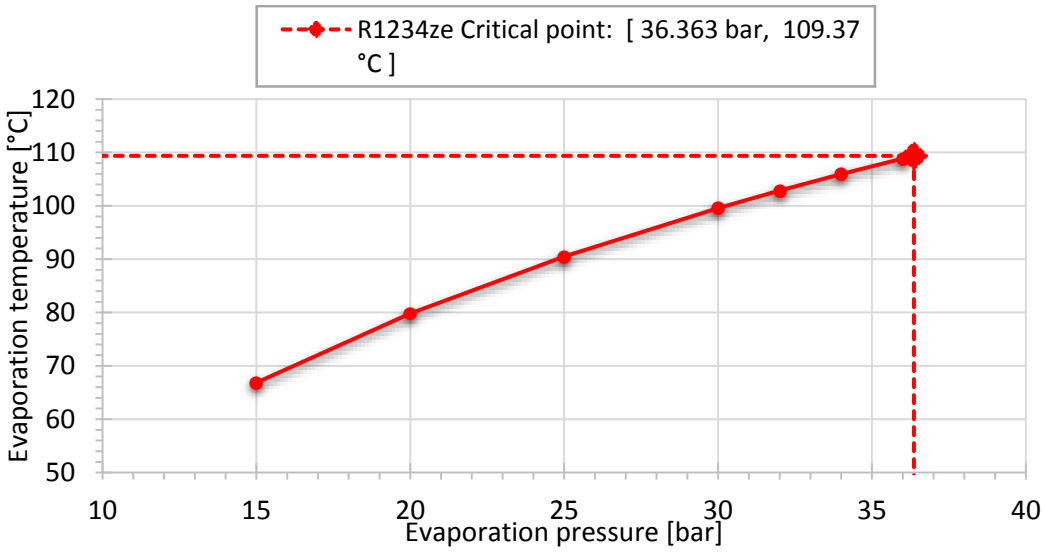

Figure 3.6 Evaporation pressure and corresponding evaporating temperature for a geothermal source temperature of 130 °C.

As shown in Figure 3.6, for increasing evaporating pressure, the R1234ze approaches the Critical point. At the critical point, the properties of the fluids change significantly since the phase boundaries stop to exist (Emsley 1991). Moreover, the REFPROP software has increased errors at critical and supercritical conditions. A consequence of approaching the critical conditions, is that the pinch point changes from the outlet of the preheater to the inlet. This is shown as a sudden increase in the power generation, as seen in Figure 3.5, for 130 ºC. Therefore the pinch point location, depends on the fluid used, the evaporating pressure and the temperature (Dominik Meinel, Personal Discussion).

3.6.2 Standard / simple ORC concept efficiency

Concerning the thermal and system efficiency, both are of quite low level and increase with increasing temperature and pressure. The low efficiencies achieved, are expected since it is known that the Organic Rankine Cycles achieve generally low energy efficiency levels. The efficiencies are presented in Figures 3.7 and 3.8.

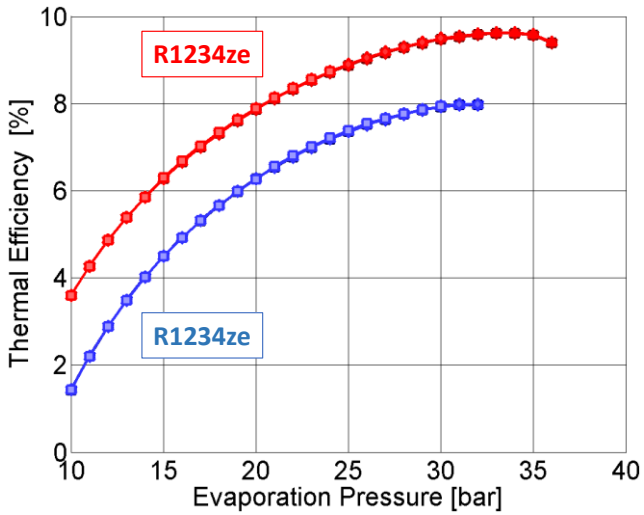

Figure 3.7 Thermal Efficiency Standard Concept

As is shown in Figure 3.7, the thermal efficiency of both fluids, is largely independent of the heat source temperature. For every heat source temperature, the thermal efficiency results in the same curve, with both fluids generally achieving low values. Because of the definition of the thermal efficiency, the conclusion is that the ORC configurations has a limited capacity of transforming the available heat energy into electrical energy.

The same applies to the system efficiency, depicted into Figure 3.8. The difference with the thermal efficiency, is that the system efficiency depends on the heat source temperature, in similar manner to the power generation in Figure 3.5. Nevertheless, both efficiencies have similarly low values, with the highest possible value of approximately 9%.

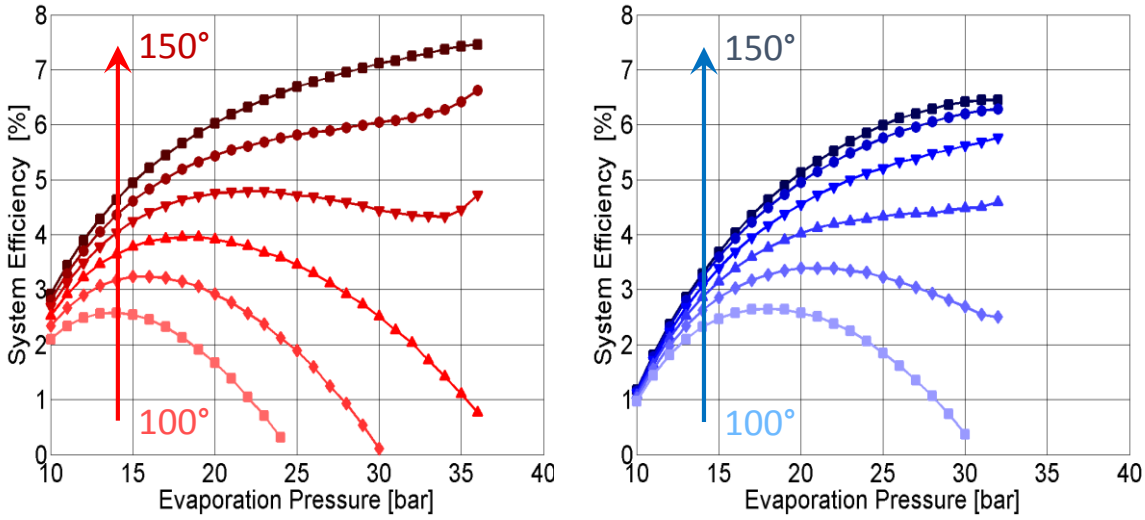

Figure 3.8 System Efficiency Standard Concept

However, the exergy efficiency (also known as the second-law efficiency) computes the efficiency of a process taking the second law of thermodynamics into account. As already mentioned before, when calculating the thermal or system efficiency above, the value found gives no indication of how the system compares to a thermodynamically perfect one operating under the same conditions. For this reason, the exergy efficiency is assumed more important than the others. The exergy efficiencies of both fluids, increase when the source temperature and evaporating pressure increase. Moreover, they are both of relative high value, with the R1234ze reaching almost up to 45% for a 150°C geothermal source. The exergy efficiency is shown in Figure 3.9:

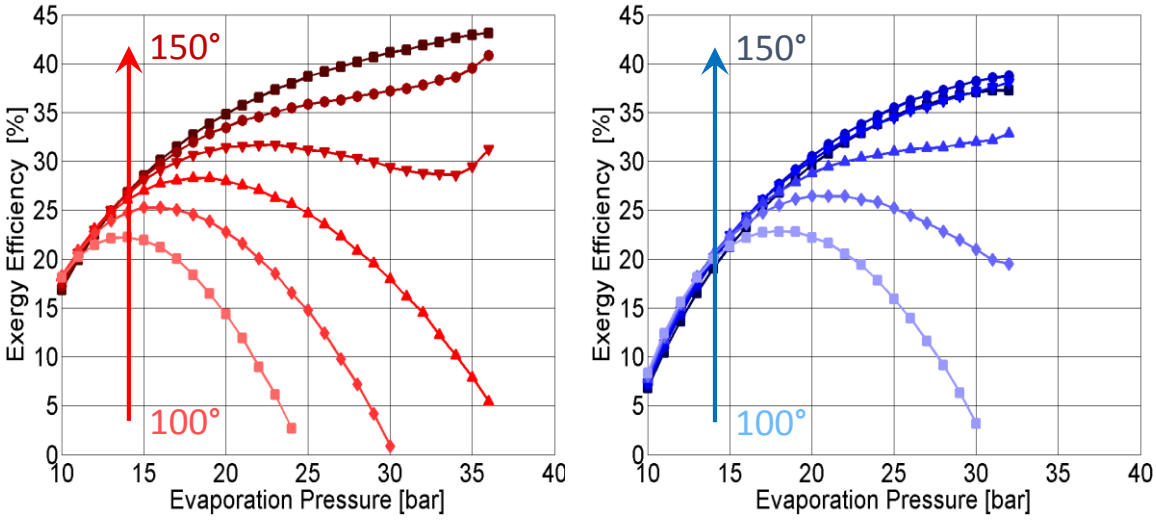

Figure 3.9 Exergy Efficiency Standard Concept

3.6.3 Two stage ORC concept results

The results of the two stage ORC concept are presented in this section. In Figure 3.10 the pure power generation is plotted for variable intermediate pressure, at 140 C°. The evaporation pressure on the other hand is fixed, and corresponds to the maximum power generation in the standard ORC according to Figure 3.5. These evaporation pressure values are summarized in the Table 3-4. The figures for other heat source temperatures follow the same pattern and therefore are given in the Appendix.

Table 3-4 Evaporation pressure of the two-stage ORC concept for different heat temperature sources.

Heat source temperature [C°]	Evaporation pressure [bar]
140	36
130	20
120	19
110	18
100	12

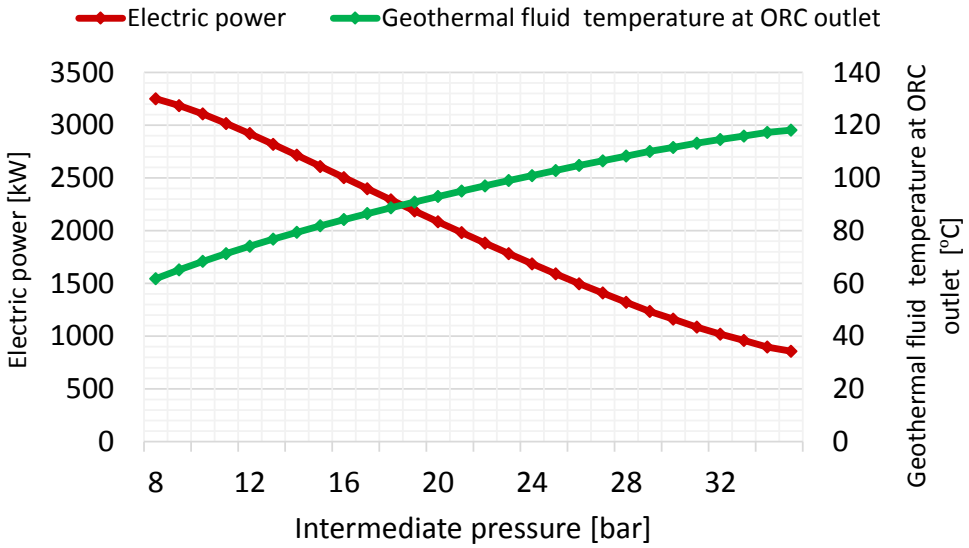

Figure 3.10 Power generation and geothermal fluid outlet temperature for variable intermediate pressure (Geothermal source at 140 C°)

As shown in Figure 3.10, the power generation is decreasing with increasing intermediate pressure. This is expected, since steam is extracted at an increasing high pressure, which could have been otherwise used for power production. On the other hand, with

decreasing intermediate pressure, the power generation increases and the model approaches the standard one stage operation. It further approaches completely, when the intermediate pressure is equal to the condenser pressure.

In Figure 3.11 the exergy and system efficiency for different heat source temperatures are presented. The value of the evaporation pressure is again according to Table 3-4 and corresponds to the maximum power generation as explained before.

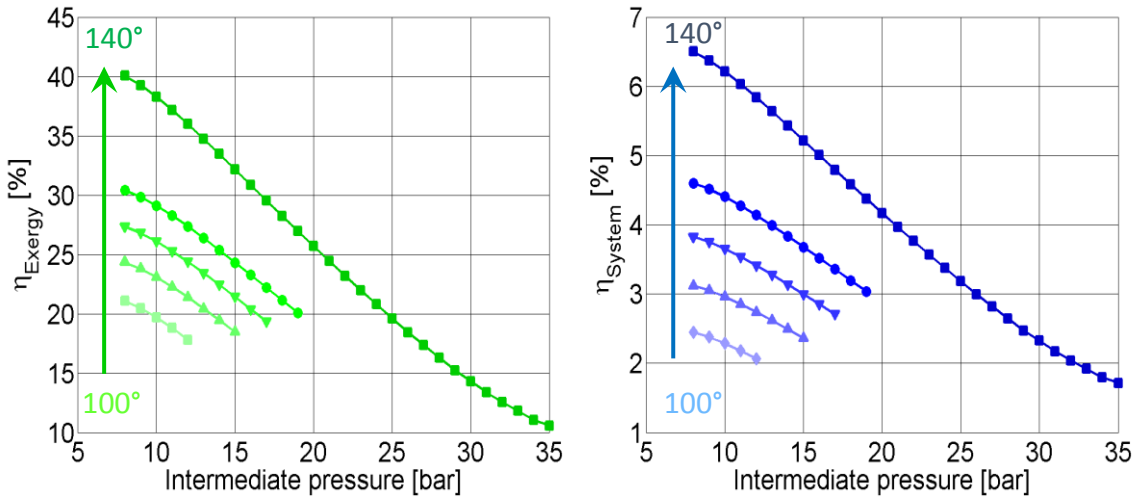

Figure 3.11 Exergy and system efficiency

As shown in Figure 3.11, both the exergy and system efficiency decrease with increasing intermediate pressure, in a similar way with the power generation in Figure 3.10. However, the thermal efficiency displays a completely different behavior and is therefore presented separately in the next section.

3.6.4 Two stage ORC thermal efficiency and optimum intermediate pressure

In contrast with the other efficiencies and power generation, the thermal efficiency displays a much different behavior, as shown in Figure 3.12:

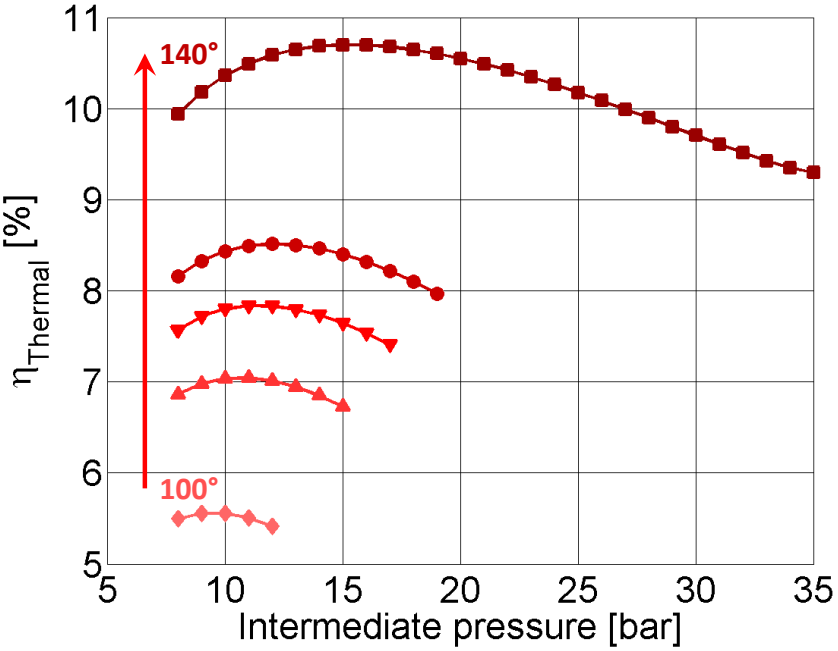

Figure 3.12 Thermal efficiency

The thermal efficiency achieves some topical maximum values, for an intermediate pressure that does not correspond to the higher power generation. Additionally, these values appear to be not random, but to follow a certain pattern. For comparison and the discovery of a possible relationship, the arithmetic and geometric mean between the evaporator and condenser pressure are calculated respectively according to equations (3.14) and (3.15).

$$p_{Int,arith} = \frac{p_{Evap} + p_{Cond}}{2} \tag{3.14}$$

$$p_{Int,geom} = \sqrt{p_{Evap} \cdot p_{Cond}} \tag{3.15}$$

The evaporation pressure is the same as before, presented in Table 3-4. The condenser pressure is calculated accordingly the pinch point temperature, as explained in section 3.2. In Table 3-5, the maximum thermal efficiency, the corresponding intermediate pressure, the calculated geometric mean and the arithmetic mean are given:

Table 3-5 Optimum intermediate pressure, geometric and arithmetic mean

Heat source temperature [C°]	Thermal efficiency [%]	Optimum intermediate pressure [bar]	Geometric mean [bar]	Arithmetic mean [bar]
140	10,699	15	15,018	21,132
130	8,512	12	11,194	13,132
120	7,835	11	10,619	12,132
110	7,042	11	10,012	11,132
100	5,557	10	9,025	9,632

As shown in Table 3-5, the geometric mean between the evaporator and condenser pressure, is very close to the intermediate pressure where the maximum thermal efficiency is achieved. The same relationship exists in the engineering field of refrigeration and air conditioning.

It is known that for an ideal gas, the compression work is minimal if the intermediate pressures are the geometric mean values. This relationship is given by the following equation, where p_1 and p_{N+1} are the lower and upper pressure limits of an N-Stage compression system, while $p_2, p_3 \ldots p_N$, are the intermediate pressures (Prasad 2003), (Domanski 1995).

$$\frac{p_1}{p_2} = \frac{p_2}{p_3} = \frac{p_3}{p_4} = \cdots = \frac{P_N}{p_N + 1} = \left(\frac{P_1}{p_N + 1}\right)^{1/N} \tag{3.16}$$

As stated in the same sources, for real gases the intermediate optimum pressures are usually much different from the geometric mean values. These can deviate up to 1 bar from the intermediate pressure, which is the maximum deviation observed in this analysis too. Therefore, a possible relationship between the two stage turbine ORC, and the two stage refrigeration cycles may exist. However, in order to validate this relationship, more simulations have to be carried out for many different operating points and working fluids, something which is not included into the objectives of this study.

3.6.5 Power generation and isentropic efficiency

The power generation of the one-stage ORC and the two-stage ORC, for both constant and variable isentropic turbine efficiency is given in Figure 3.13. The equations that were used for the variable turbine isentropic efficiency, are listed in section 3.3.1. The nominal turbine isentropic efficiency is set at 80%, while the nominal mass flow is set at the highest evaporation pressure. The other boundary conditions are the same as in the previous chapters. For the 2-Stage turbine, the intermediate pressure is set and corresponds to the highest thermal efficiency, according to the previous paragraph.

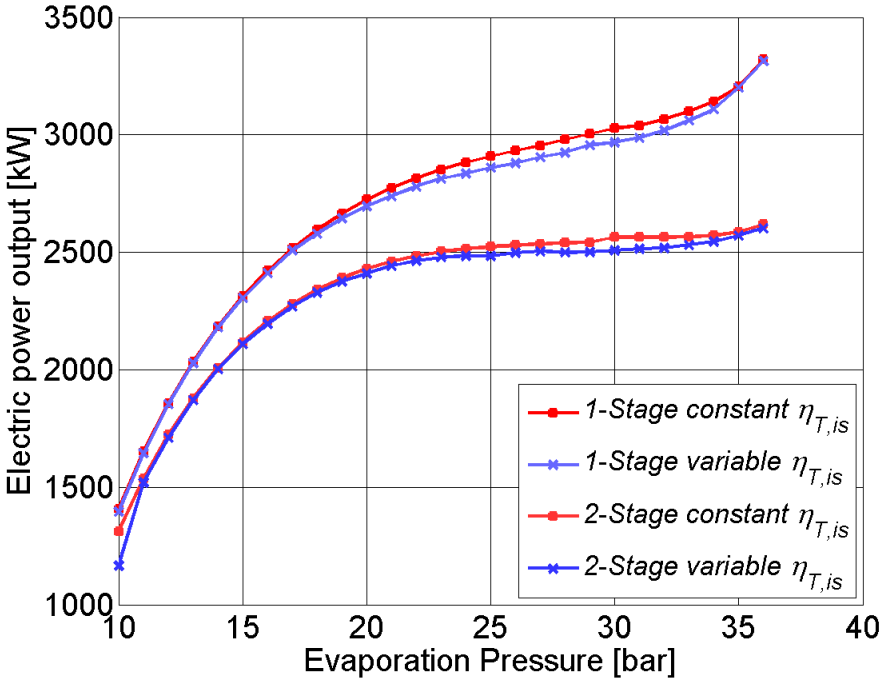

Figure 3.13 Power output with constant and variable turbine isentropic pressure.

As shown in Figure 3.13, the variable isentropic efficiency does not affect considerably the power generation, because the ORC mass flow does not change significantly enough. As already shown in Figure 3.4, the turbine isentropic efficiency remains relatively constant in a wide range of mass flows. Therefore, if the design point and nominal mass flow are selected carefully, the isentropic efficiency can be considered stable during the whole operation.

Lastly, as can be seen in Figure 3.13, the 2-stage ORC produces less power output. This, as already shown in Figure 3.10, is compensated by a temperature increase of the geothermal water at the ORC outlet. Therefore, the two-stage ORC is more suitable for CHP applications. This is investigated in the next chapter.

4 Combined Heat and Power

4.1 Combined Heat and Power Modelling

The Combined Heat and Power concepts are using the same algorithm for modelling and simulation as the in the pure power generation, with a few modifications. The formation of the mass, pressure and energy matrices follows the same rules and of course takes in account the new components required like the splitters, district heating heat exchanger etc. This means that the matrices will contain more rows and columns, as more balance equations are added.

The main difference is instead of looping for all the possible evaporation pressure levels, this is done for all the possible heat demand levels. In contrast with the pure power generation, the evaporation pressure is fixed, and selected according to the results of the pure power generation results, to correspond to the maximum power generation.

The primary variables that are examined, are the same as in the pure power generation case. These are the thermal efficiency, system efficiency, exergy efficiency and power generation. However in the Combined Heat and Power applications one more efficiency can be defined, the combined efficiency. The solving algorithm for the CHP concepts is shown in Figure 4.1.

4.1.1 Combined Efficiency

The combined efficiency is performance measure of a device that uses thermal energy for the production of both electrical and thermal energy. In geothermal combined heat and power applications is defined similar to the thermal efficiency, with the difference being that also the thermal energy supplied to the district heating is included in the numerator of the fraction.

$$\eta_{CHP} = \frac{P_{el,ORC} + Q_{DH}}{Q_{ORC}} = \frac{P_{el,ORC} + Q_{DH}}{\dot{m} \cdot \left(h_{EVAP,out} - h_{ECO,in}\right)} \tag{4.1}$$

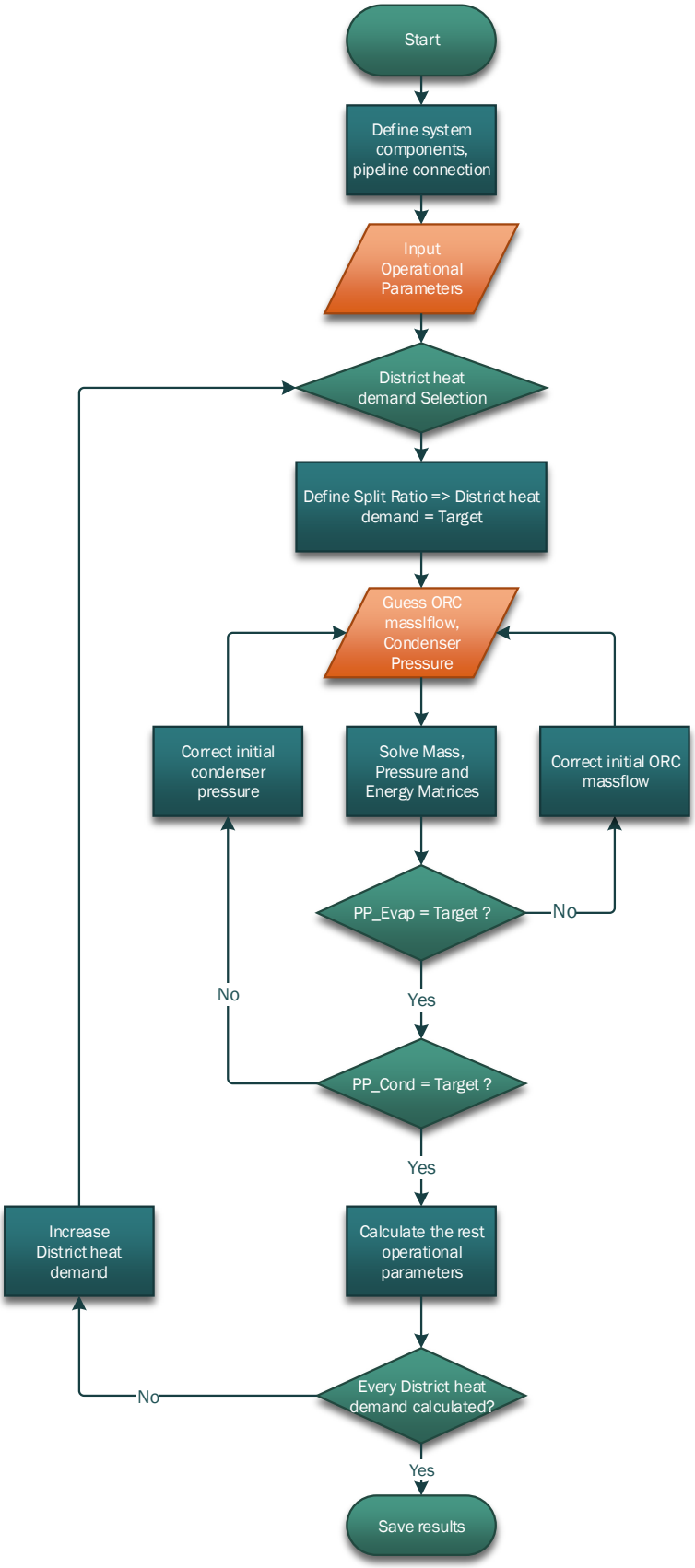

Figure 4.1 Combined heat and power solving algorithm

4.1.2 Combined Heat and Power - Parallel Concept

The parallel configuration is the simplest CHP concept investigated in this study. A part of the geothermal water is directed into the district heating heat exchanger and then reinjected into the earth through an injection well. The second stream of geothermal water is directed into the ORC unit, for power generation. It is then injected into the same injection well, or a separate one. Two parallel concepts are investigated, one with a one-stage ORC and one a two-stage ORC. These are shown in Figures 4.2 and 4.3:

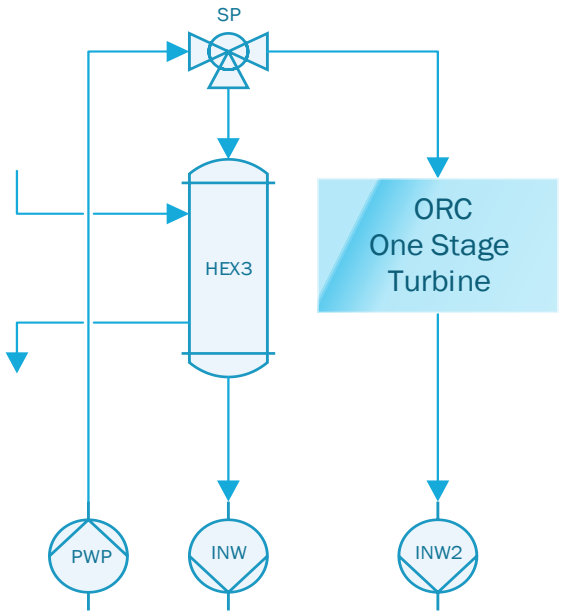

Figure 4.2 CHP Parallel one-stage ORC concept

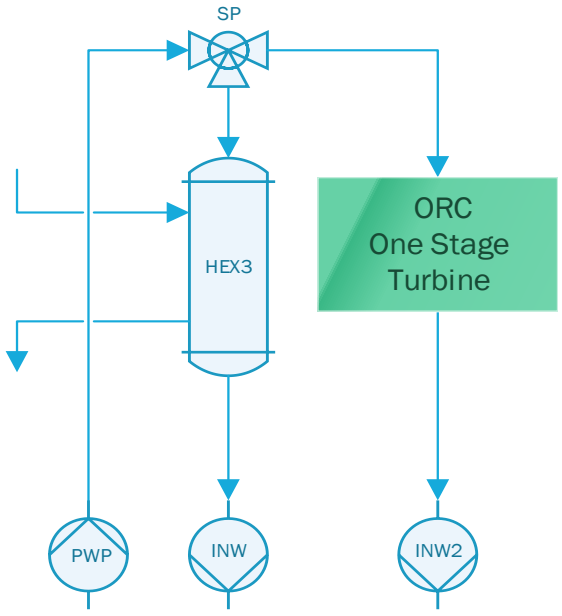

Figure 4.3 CHP Parallel two-stage ORC concept

4.1.3 Combined Heat and Power - Serial / Parallel “Combi” Concept

The serial / parallel or for short “Combi” concept, is the combination of the serial and parallel connection of the district heating to the ORC module. The parallel connection was described in section 4.1.2, while a serial concept is not investigated. This is due to the fact that the geothermal water energy at the ORC outlet is very low and therefore the serial concept is unable to fully cover the district heating demand. In the “Combi” concept, the geothermal water from the ORC outlet is combined with hot geothermal water in a mixer. Then they are both directed into the district heating heat exchanger and afterwards into the injection well. The Combi concepts are shown in Figures 4.4 and 4.5:

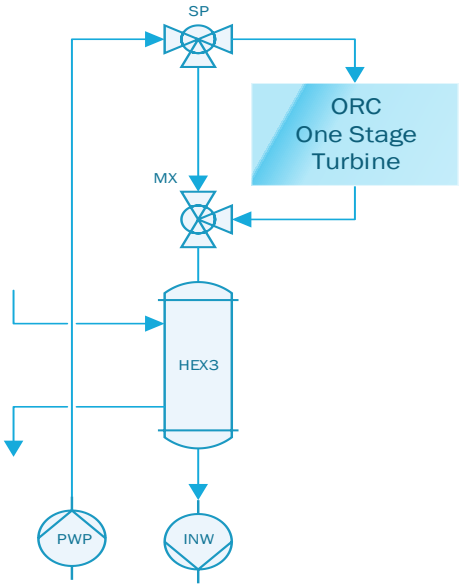

Figure 4.4 CHP Serial / Parallel “Combi” one-stage ORC concept

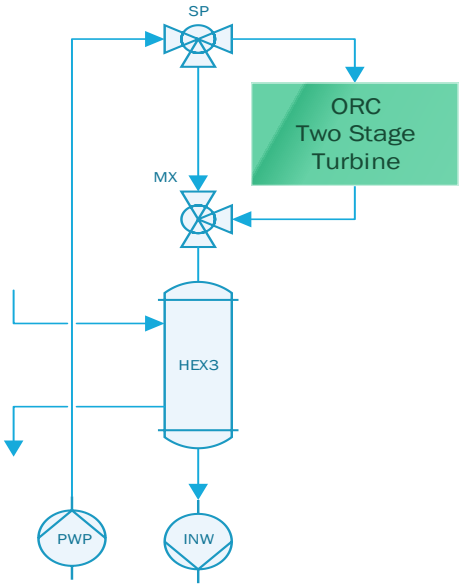

Figure 4.5 CHP Serial / Parallel “Combi” two-stage ORC concept

4.1.4 Boundary conditions

The main boundary conditions are equal to the ones that were assumed in the pure power generation simulations. However there are some additional conditions that have to be assumed, since the operation has changed to both power and heat generation. These are summarized in Table 4-1:

Table 4-1 CHP boundary conditions

Geothermal Source	--
Geothermal heat power [MWth]	50
Production pressure [bar]	10
Temperature [°C]	140
Cooling Conditions	--
Cooling fluid input temperature [°C]	20
Maximum temperature increase [°C]	3
Efficiencies	--
Mechanical	0,98
Electrical	0,95
Isentropic pump	0,9
Isentropic Turbine (nominal)	0,8
Heat exchangers	--
Evaporator Pinch point [°C]	10
Condenser Pinch point [°C]	10
Working Fluids	--
Fluid 1	R1234ze
Fluid 2	R1234yf
Evaporation pressure [bar]	Fixed - maximum power generation
Intermediate pressure [bar]	Fixed - maximum thermal efficiency
District Heating	--
Operating pressure [bar]	5
Supply temperature [°C]	80
Return temperature [°C]	50
Heat exchanger Pinch point [°C]	5

The values used for the district heating are regarded as typical for the European conditions and are considered appropriate for the purposes of this Thesis (Dominik Meinel, Personal Discussion).

4.2 Combined Heat and Power results

In this section, the results of the combined heat and power simulations are discussed for the design geothermal source temperature of 140 °C. In Figure 4.6 and 4.7 the power generation and exergy efficiency for all the investigated concepts are presented with R1234ze as the working fluid. In the Appendix, the power generation and all the efficiencies are presented for both R1234ze and R1234yf.

As shown in Figure 4.6, the power output for the parallel concepts, starts from a high value and constantly decreases with increasing heat district demand. In comparison, in the serial/parallel "Combi" concepts, the power generation starts from a relatively lower power output, but remains constant until a certain heat district demand, after which it decreases. For the specific boundary conditions this corresponds to 12.5 MWth. Moreover at this operating point, the pinch point changes from the inlet of the district heating heat exchanger to the outlet.

The system and thermal efficiencies have typically low values. The system efficiency follows the same pattern as the power generation, while the thermal efficiencies remain constant for all the district heating demands. This is due to the fact that although the ORC variables change according to the CHP operating point, they retain the same "scale". Both efficiencies are generally lower than the pure power generation models, since the power output is lower due to the CHP operation.

The exergy and combined efficiencies greatly increase in comparison to the pure power generation. This happens because both efficiencies take into account the district heating, something which the thermal and system efficiency do not. Moreover, the exergy efficiency, as stated in section 3.4, takes into account the second thermodynamic law and therefore is more suitable to universally evaluate the concepts. The exergy efficiency is thus presented in Figure 4.7, while for the system, thermal and combined efficiency, the reader can refer to the Appendix.

Therefore, the parallel one-stage ORC concept is more suitable for low district heating demands, and up to 9 MWth. For higher values, the serial/parallel two-stage ORC concept produces more power. Finally, all concepts approach for high heat demands. Based on these results, a new model is proposed, which combines the best configurations. The target is to achieve a higher gain of power for both low and high heat district demands. The proposed model is presented in the next section.

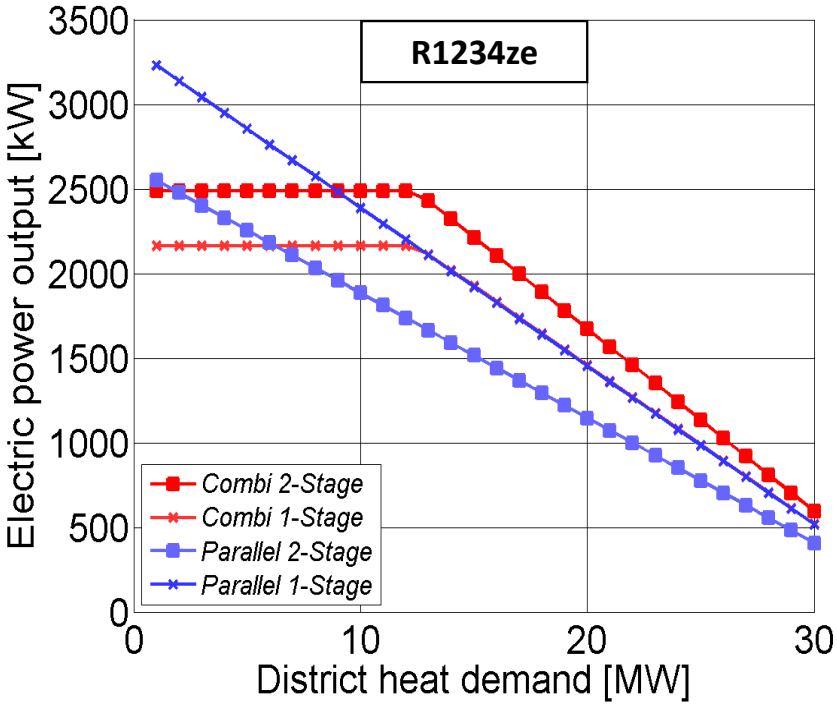

Figure 4.6 CHP concepts power generation

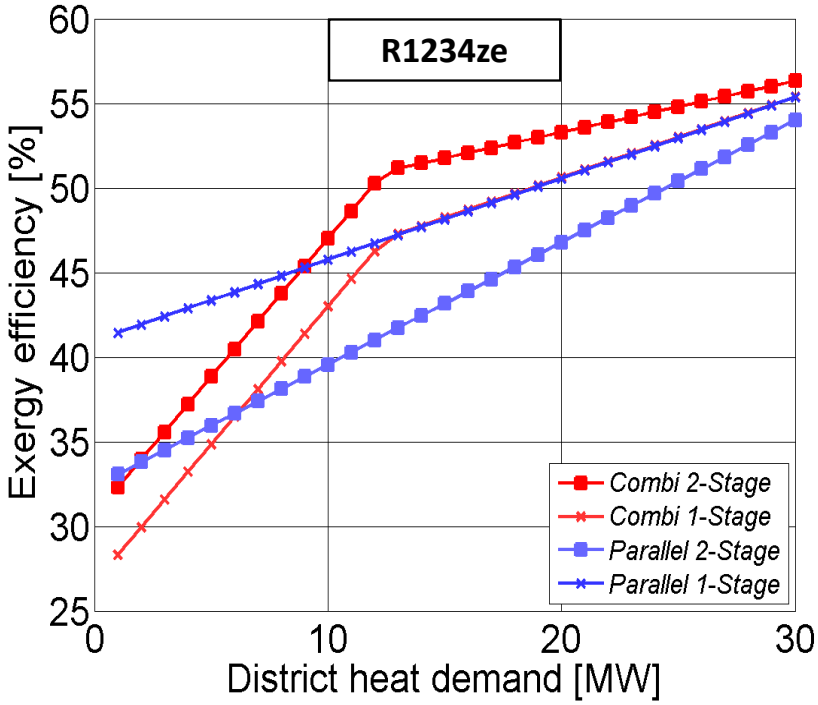

Figure 4.7 CHP concepts exergy efficiency

4.2.1 Combined heat and power combination concept

In section, a combination concept is proposed, which is based on the previous configurations presented. This configuration is presented in Figure 4.8, and shall be called “serial/parallel multi” or simply “Multi” configuration. The Multi configuration can operate as a parallel one stage concept for low heat demands, while for higher heat demands the operation changes into the serial/parallel two-stage configuration. This is achieved by automatically closing and opening the corresponding valves.

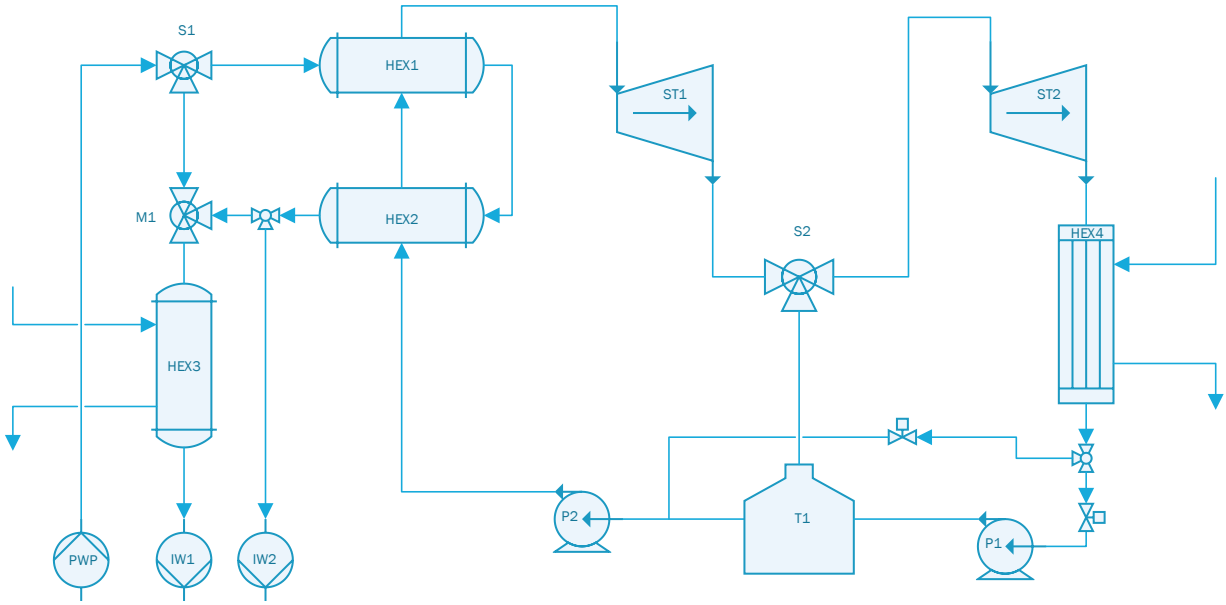

Figure 4.8 Combination configuration „Serial/Parallel Multi“

The electric power output and the exergy efficiency for this combination concept are presented in Figure 4.11. For comparison also the parallel and serial/parallel results are given, for the same temperatures in Figures 4.9 and 4.10. Only the exergy efficiency is presented for comparison, since from the previous analysis, it is established that it’s the only efficiency that takes into account the most factors, and therefore can be used to evaluate the configuration objectively.

As can be seen in Figure 4.11, the “Serial/Parallel Multi”, or simply Multi configuration, has a gain in the electricity output in both low and high head demand districts. Another remark, is that the change between the two operation modes, from parallel 1-stage to serial/parallel 2-stage, occurs at higher district heating demands, for lower heat sources temperatures. For example at 140 °C degrees the change occurs at 10 MW_{th} while at 100 °C at 19MWth.

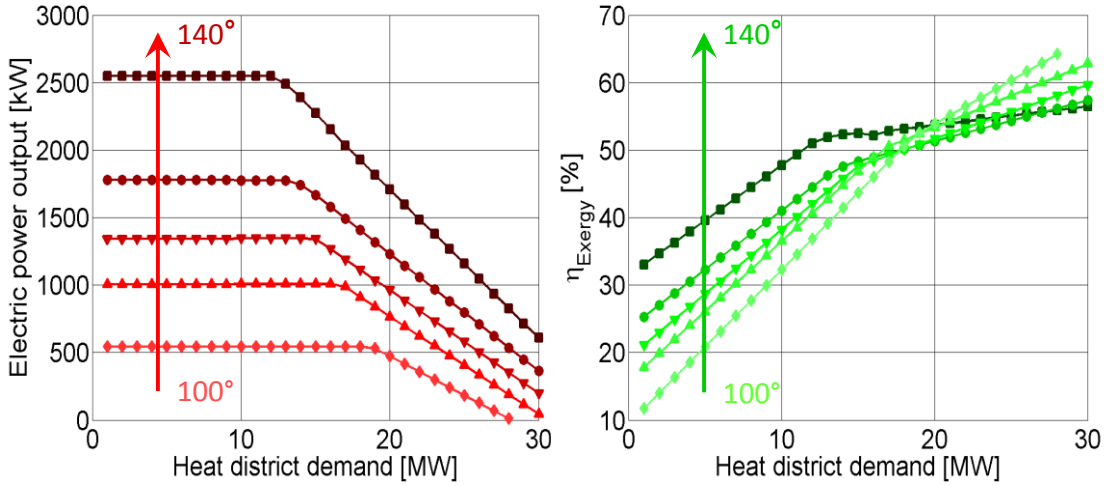

Figure 4.9 Serial/Parallel concept

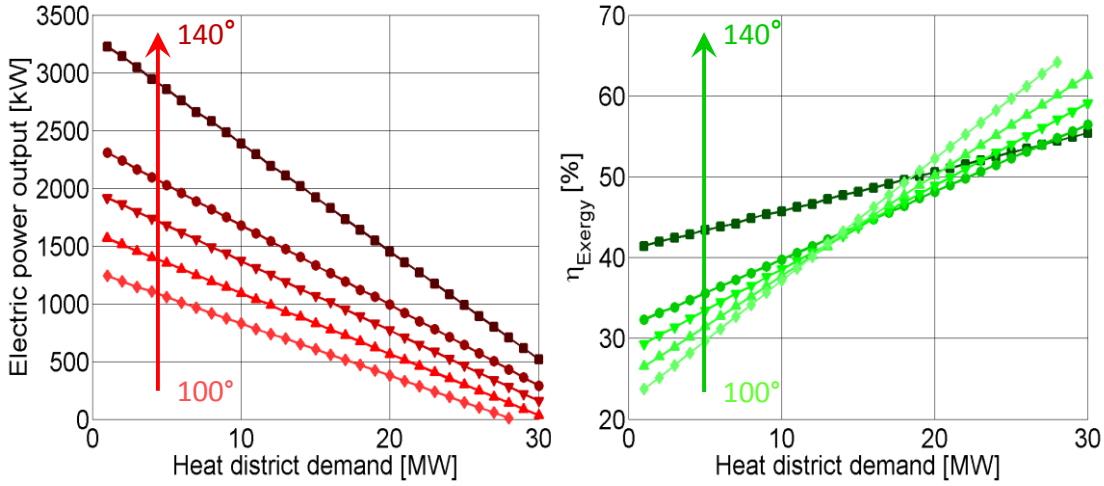

Figure 4.10 Parallel concept

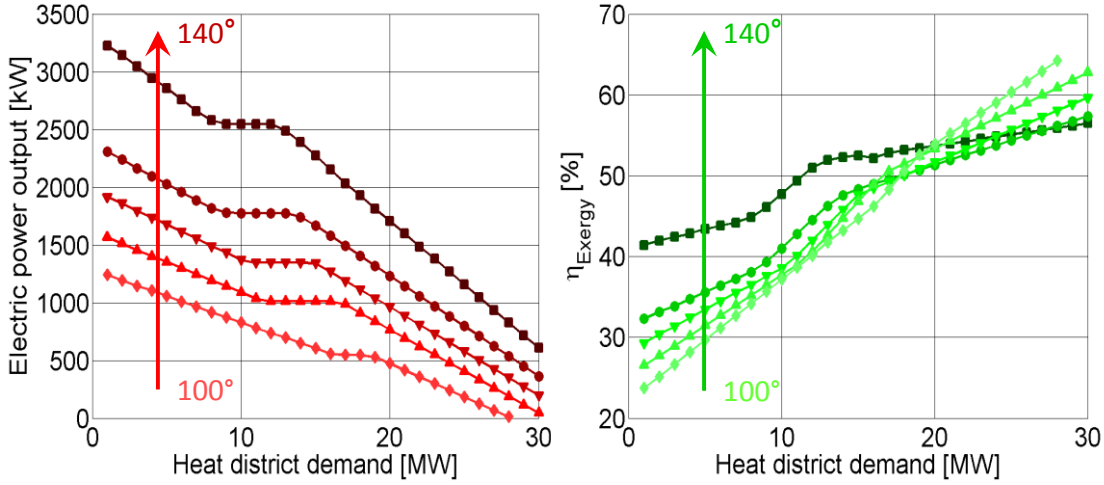

Figure 4.11 Multi concept

5 Engineering Economic Analysis

In this chapter, the focus is on the evaluation of the economics of the Organic Rankine Cycle installations. The primary objective of every project is to be profitable. The investment must always be profitable during the engineering economic analysis, to proceed to the next phase of actual construction. In order to carry out a detailed economic analysis, all factors that contribute to the costs and revenue of the project have to be taken into account. These are discussed in detail in the following sections.

5.1 Estimation of the Total Capital Investment

The Total Capital Investment (TCI) of an ORC Power Plant is calculated according to Formula 5.1 (Bejan 1996):

$$TCI = FCI + SUC + WC + LRD + AFUDC \tag{5.1}$$

Where FCI is the fixed capital investment, SUC the startup costs, WC the working capital, LRD the costs of licensing, research and development and AFUDC the allowance for funds used during construction.

5.2 Fixed Capital Investment

The fixed capital investment is defined as an investment in physical assets such as machinery, land, buildings, installations, vehicles, or technology. Therefore it consists of direct and indirect costs. The first type, direct cost, represents all equipment, materials and labor involved in the creation of permanent facilities. Indirect costs are costs that are not directly accountable to a cost object (such as equipment) and include administration, personnel and security costs (Association for the Advancement of Cost Engineering 2010).

5.2.1 Estimation of Purchased Equipment Costs

To obtain an estimate of the capital cost of the geothermal plant, the costs associated with major plant equipment must be known. The most accurate estimate of the purchased cost of a piece of major equipment is provided by a current price quote from a suitable vendor (a seller of equipment). The next best alternative is to use cost data on previously purchased equipment of the same type. Another technique, sufficiently accurate for study and preliminary cost estimates, utilizes summary graphs available for various types of common equipment. Any cost data must be adjusted for any difference in unit capacity and for any elapsed time since the cost data were generated. There are several

cost indices used by the chemical industry to adjust for the effects of inflation. The indices most generally accepted in the chemical industry and reported in the back page of every issue of Chemical Engineering are the Marshall and Swift Equipment Cost Index and the Chemical Engineering Plant Cost Index (Turton 2012).

5.2.2 Module Costing Technique & Plant Purchased Equipment Cost

The equipment module costing technique is a common technique to estimate the cost of a new chemical plant. It is generally accepted as the best for making preliminary cost estimates and is used extensively. This approach, introduced in the late 1960s and early 1970s, forms the basis of many of the equipment module techniques in use today. This costing technique relates all costs back to the purchased cost of equipment evaluated for some base conditions. Deviations from these base conditions are handled by using multiplying factors that depend on the following:

1. The specific equipment type

2. The specific system pressure

3. The specific materials of construction

The material provided in the next section is based upon information in (Guthrie 1974) , (Ulrich 1984) and (Navarrete 1995).

5.2.2.1 Bare Module Cost for Equipment at Base Conditions

The bare module equipment cost represents the sum of direct and indirect costs. In order to estimate bare module costs for equipment, purchased costs for the equipment at base case conditions (ambient pressure, carbon steel) must be available along with the corresponding bare module factor and factors to account for different operating pressures and materials of construction. These data are made available for a variety of common gas/liquid processing equipment in Appendix A in (Turton 2012). These data were compiled during the summer of 2001 from information obtained from manufacturers and also from the R-Books software marketed by Richardson Engineering Services.

Data for the purchased cost of the equipment, at ambient operating pressure and with carbon steel construction (C_P^0) were fitted to the following equation:

$$\log_{10} C_P^0 = K_1 + K_2 \cdot \log_{10}(A) + K_3 \cdot [\log_{10}(A)]^2 \qquad (5.2)$$

Where A is the capacity or size parameter for the equipment. The data for K_1, K_2, and K_3, along with the maximum and minimum values used in the correlation, are given in Table 5-1 (Turton 2012).

Table 5-1 Constants K_1, K_2, and K_3 according to equipment size parameter A. Excerpt from: (Turton 2012)

	Steam turbine	fixed tube HEX	U-tube HEX	Kettle Reboiler	Positive displacement pump	Reciprocate pump
A	75-7500 kW	10-10^3 m^2	10-10^3 m^2	10-100 m^2	1 -100 KW	0.1 -200 KW
K_1	2.6259	4.3247	4.1884	4.4646	3.4771	3.8696
K_2	1.4398	-0.3030	-0.2503	-0.5277	0.1350	0.3161
K_3	-0.1776	0.1634	0.1974	0.3955	0.1438	0.1220

5.2.2.2 Pressure Factors

The costs of equipment increase with increasing operating pressure. In this section, the method of accounting for changes in operating pressure through the use of pressure factors is covered. The pressure factors (F_P) for the equipment are given by the following general form:

$$\log_{10} F_P = C_1 + C_2 \cdot \log_{10}(P) + C_3 \cdot [\log_{10}(P)]^2 \qquad (5.3)$$

The units of pressure, P, are bar gauge or barg (1 bar = 0.0 barg) unless stated otherwise. The pressure factors are always greater than unity. The values of constants in Equation (5.3) for different equipment are given in Tables 5-2 and 5-3. Also shown are the ranges of pressures over which the correlations are valid. Some equipment does not have pressure ratings and therefore has values of C_1–C_3 equal to zero.

Table 5-2 Constants C_1, C_2, and C_3 for p < 5 barg (HEX); p < 10 barg (Pump) Excerpt from: (Turton 2012)

	Steam turbine	fixed tube HEX	U-tube HEX	Kettle Reboiler	Positive displacement pump	Reciprocate pump
C_1	0	0	0	0	0	0
C_2	0	0	0	0	0	0
C_3	0	0	0	0	0	0

Table 5-3 Constants C_1, C_2, and C_3 for 5 barg < p < 140 barg (HEX); 10 barg < p < 100 barg (pump) Excerpt from: (Turton 2012)

	Steam turbine	fixed tube HEX	U-tube HEX	Kettle Reboiler	Positive displacement pump	Reciprocate pump
C_1	0	0.03881	0.03881	0.03881	-0.24538	-0.24538
C_2	0	-0.11272	-0.11272	-0.11272	0.225902	0.225902
C_3	0	0.08183	0.08183	0.08183	-0.01363	-0.01363

5.2.2.3 Material Factors and Bare Module Factor

The costs of equipment change with changes in the material of construction. In this section, the method of accounting for different materials of construction is covered. The bare module factors for the equipment are given by the following equation:

$$F_{BM} = C_p^0 \cdot (B_1 + B_2 \cdot F_M \cdot F_P) \tag{5.4}$$

The values of the constants B_1 and B_2 and the material factors F_M for the equipment of the ORC plant are given in Table 5-4. For ambient pressure conditions and carbon steel construction, the bare module factor for the equipment at these conditions (F_{BM}) is found by setting F_M and F_P equal to unity. The data for the constants and the material factors are obtained from following references: (Turton 2012), (Guthrie, Capital Cost Estimating 1969), (Navarrete 1995).

Table 5-4 Material factors FM and constants B_1 and B_2 Excerpt from: (Turton 2012)

	Steam turbine	fixed tube HEX	U-tube HEX	Kettle Reboiler	Positive displacement pump	Reciprocate pump
F_M	0	1.38	1.38	1.38	1.41	1.4
B_1	0	1.63	1.63	1.63	1.89	1.89
B_2	0	1.66	1.66	1.66	1.35	1.35

5.2.2.4 Bare Module Cost and Plant Cost Index

Finally the bare module cost is given by the following equation:

$$C_{BM} = C_p^0 \cdot F_{BM} \tag{5.5}$$

However, as already described in section 5.2.1, the data used to obtain the above correlations was compiled during the summer of 2001, therefore is not suitable for later years, due to inflation effects. The indices most generally accepted in the chemical industry and reported in the back page of every issue of Chemical Engineering are the Marshall and Swift Equipment Cost Index and the Chemical Engineering Plant Cost Index.

Therefore, the Chemical Engineering Chemical Plant Cost Index (CEPCI) is obtained according to year, from following references: (Chemical Engineering, VOL. 121, NO. 3 March 2014), (Turton 2012) . It must be said that although the first source is published during the March of 2014, the most recent and accurate annual value of CEPCI it contains is in year 2012, therefore this one will be used. Of course there. From the above, the CEPCI in year 2012 is equal to 584.6 while in the year 2001 is equal to 397.

Consequently, the final Purchased Equipment Cost (PEC) in dollars, is given by the equation (5.6). In order to calculate the currency in Euros, an exchange rate of 1 $ = 0.78996 € is used, which was latest updated in October 2014.

$$PEC = C_{BM} \cdot \frac{CEPCI_{2014}}{CEPCI_{2001}} \tag{5.6}$$

5.2.3 Heat Exchangers Cost

In order to calculate the cost of the heat exchangers, the area and consequently the heat transfer coefficient must be known. This is more complicated in comparison with the Turbomachinery which require only the power output. Therefore to acquire accurate values of the heat transfer coefficient, the heat exchangers are designed and optimized at a specific design point. The heat transfer coefficient, will then be used for the whole operational range. In this study, no off-design analysis is carried out. Moreover, all heat exchangers are considered shell and tube type. These include the evaporator, the preheater, the condenser and in the case of CHP, also the district heating heat exchanger.

Shell-and-tube heat exchangers can be assembled with many different configurations. In this thesis only the TEMA E type is investigated. This is the most basic type, with a single shell pass and with the inlet and the outlet at the opposite ends of the shell. The working fluid flows on the shell side with the exception of the condenser, where condensation was chosen to take place in the tube side. Therefore, on the one hand models for the pressure drop and heat transfer coefficient in single-phase flow and two-phase evaporation flow in the shell side are needed. On the other hand, models for the pressure drop and heat transfer coefficient in two-phase condensation flow and single-phase flow in the tube side are also required.

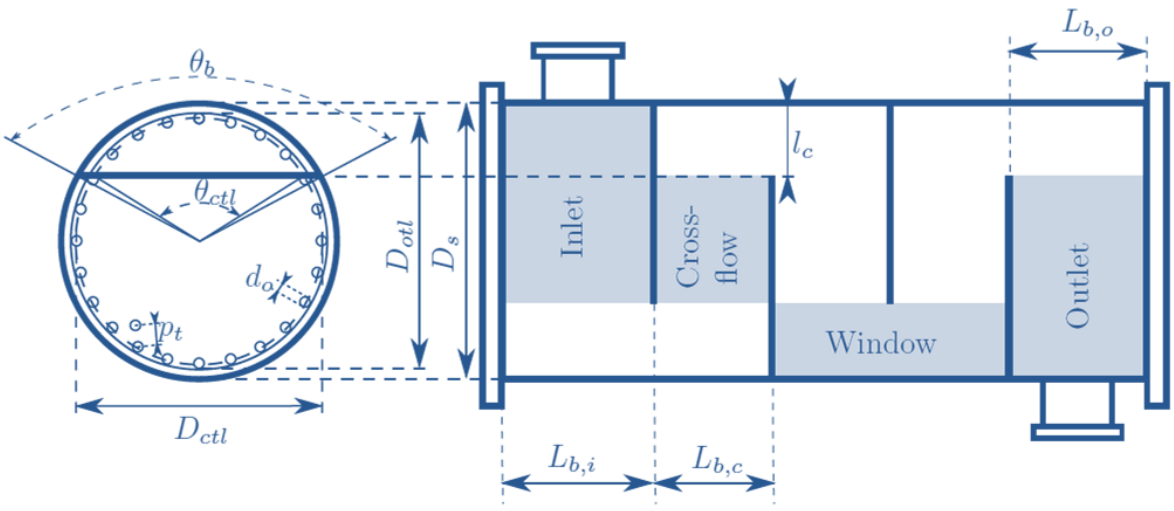

Figure 5.1 Shell-and-tube geometrical characteristics (Shah 2003)

In Figure 5.1, the basic geometrical characteristics of a shell-and-tube heat exchanger are shown. These are the shell outside diameter Ds, the outside diameter of a tube do, the pitch between the tubes pt, the baffle cut length lc and the baffle spacing at the inlet Lb,i, outlet Lb,o and the center Lb,c. The expressions to calculate other geometrical characteristics can be found in the literature (Hewitt 1990), (Shah 2003).

5.2.3.1 Overall Heat Transfer Coefficient

The overall heat transfer coefficient takes into account the heat transfer coefficients of both the tube and shell side. Moreover, most heat exchangers surfaces tend to acquire an additional heat transfer resistance that increases with time. This either may be a very thin layer of oxidation, or may be a thick crust deposit, such as that which results from a salt-water coolant in steam condensers. This fouling effect can be taken into consideration by introducing an additional thermal resistance (R_f). Its value depends on the type of fluid, fluid velocity, type of surface, and length of service of the heat exchanger (Kakaç and Liu 1998).

For unfinned, tubular heat exchangers the overall heat transfer coefficient can be determined from the inside and outside heat transfer coefficients, fouling factors and appropriate geometric parameters. The formula is given by the following equation:

$$U = \frac{1}{\frac{r_o}{r_i}\frac{1}{a_i} + \frac{r_o}{r_i}R_{fi} + \frac{r_o \ln(r_o/r_i)}{k} + R_{fo} + \frac{1}{a_o}} \tag{5.7}$$

Then the required heat exchanged area can be calculated by the heat transfer equations presented already in paragraph 3.3. For correlations of the shell and tube sides heat transfer coefficients for single phase, two-phase condensation in tubes and two-phase evaporation the reader can refer to the following sources: (Thome 2010), (Vera-Garcia 2010).

5.2.3.2 Heat exchanger models optimization

For this thesis, models that are based on the correlations from Wolverine Engineering Data Book and are programmed in MATLAB were used. These then were optimizing by the use of evolutionary algorithms in MATLAB. A genetic algorithm (GA) is a method for solving both constrained and unconstrained optimization problems based on a natural selection process that mimics biological evolution. The algorithm repeatedly modifies a population of individual solutions. At each step, the genetic algorithm randomly selects individuals from the current population and uses them as parents to produce the children for the next generation. Over successive generations, the population "evolves" toward an optimal solution.

The variables to be optimized and minimized are the:

- Shell pressure drop
- Tube pressure drop
- Cost
- (Calculated geometrical area – Required thermodynamical area)

On the other hand, the control variables are selected as the:

- Effective length
- Shell inside diameter
- Tube inside diameter (manually)

In Figure 5.2 the solving algorithm which was used in Matlab is presented. The left section corresponds to the heat exchanger model while the right section corresponds is the MATLAB evolutionary algorithm.

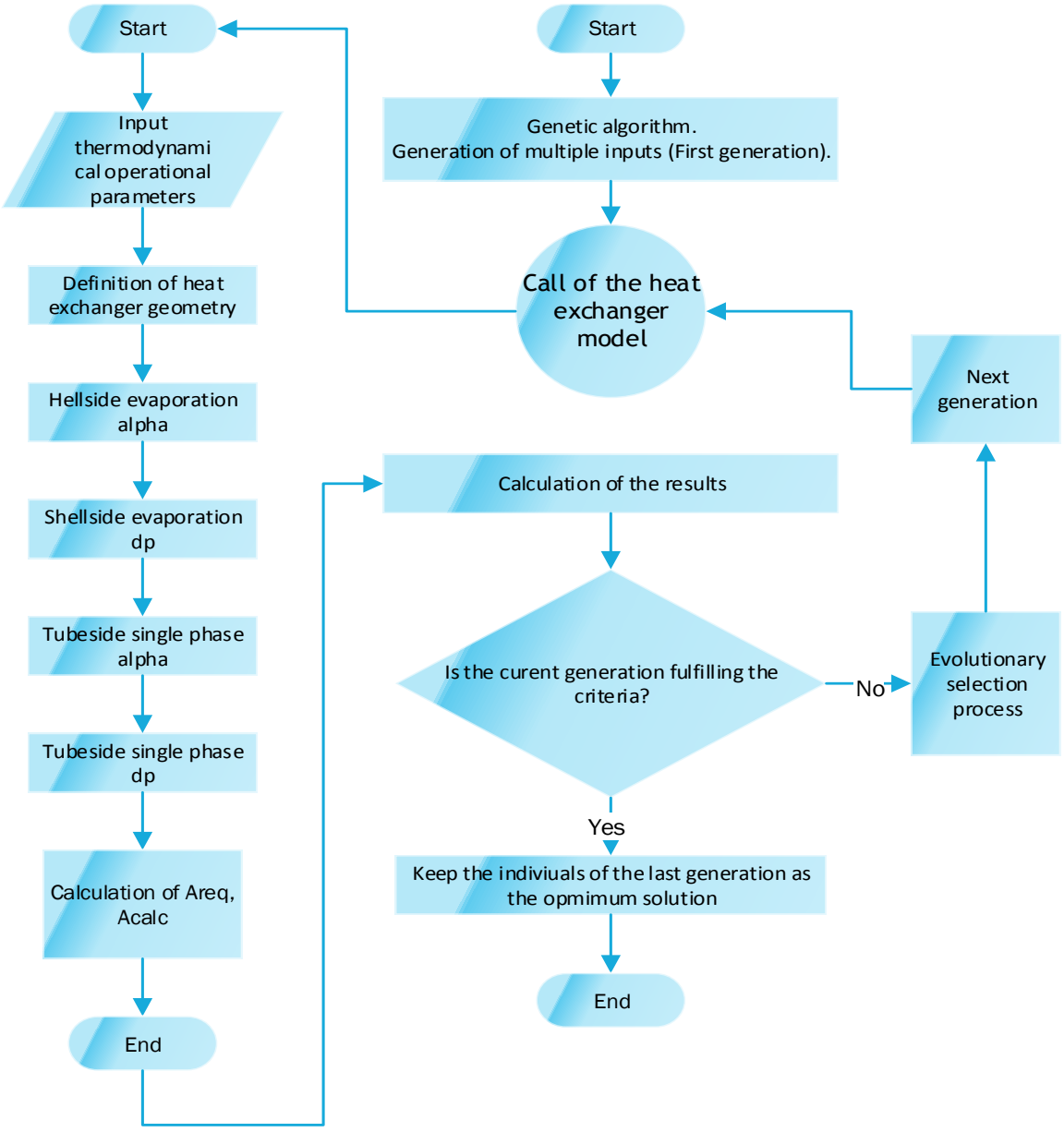

Figure 5.2 Heat exchanger optimization algorithm

The optimization algorithm were run for the operating point of 15 MW_{th} for the parallel single-stage model. The results from the simulations are presented graphical in Figures 5.3 and 5.4.

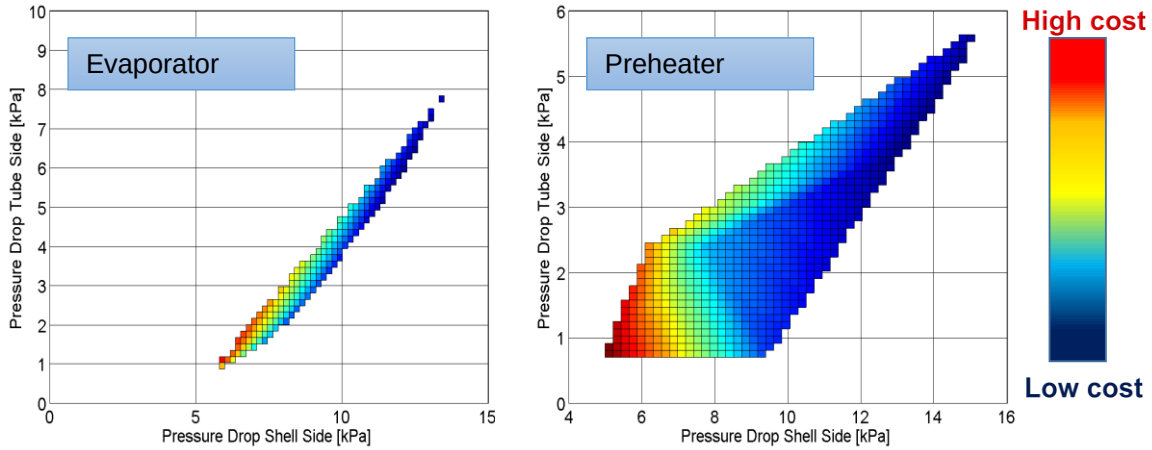

Figure 5.3 Optimization results for evaporator (left) and preheater (right)

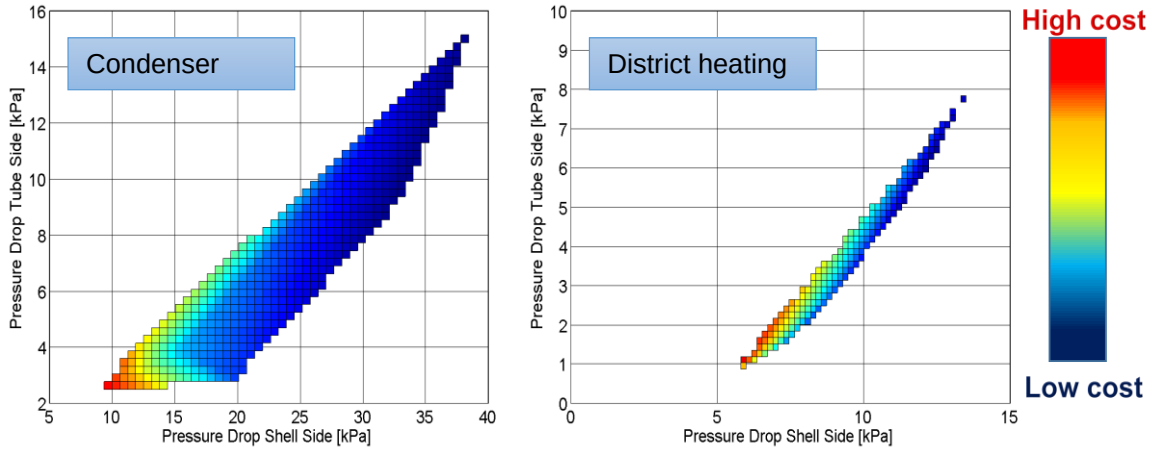

Figure 5.4 Optimization results for condenser (left) and district heating (right)

The above charts are only for qualitative purposes, since the only variable retained for the next chapter is the heat transfer coefficient. Of course, the heat transfer coefficient is expected to change with each different operating load. In this thesis however no off-design analysis is carried out, and the heat transfers coefficients calculated are assumed to be constant for all the operating points. These are summarized together with the control variables and the pressure drops in the Table 5-5:

Table 5-5 Optimization results

	Evaporator	Preheater	District Heating	Condenser	Units
U	2293	657	914	1360	[W/m^{2}K]
Shell inside diameter	0,9	1,5	0,76	1,5	[m]
Effective Length	4,37	10	5,5	12,5	[m]
Pressure drop shell	3,8	12	8	36	[kPa]
Pressure drop tubes	2,1	1,7	2	8	[kPa]

From the qualitative charts in Figure 5.4 and data of Table 5-5, it is shown that:

- The preheater is bigger and thus more expensive than the evaporator. This happens because of the worse heat transfer coefficient, and also due to the fact that the preheater has to transfer a higher thermal load than the evaporator because of the thermodynamical properties and T-S diagram of the R1234ze at these conditions (At high pressures, lower energy is required for evaporation).

- The condenser is also bigger relatively to the other heat exchangers. This happens mainly because of the huge cooling load which has to be transferred. Moreover, because of the small allowable increase of temperature in the cooling water, this results into a very high mass flow of cooling water, which in turn results into higher pressure drops and cost.

In the next sections, the above U values will be considered constant for each heat exchanger correspondingly. The area required will be calculated according to equation 3.7, and the final heat exchanger cost, according to equation 6.5.

5.2.4 Plant PEC

The total cost of the whole plant is calculated by the following equation:

$$PEC_{Plant} = PEC^{0}_{Plant}(1 + F_C + AUX_C + Cont_C) \quad (5.8)$$

Where the total purchased equipment cost of all the components (PEC^{0}_{Plant}), given by the following equation:

$$PEC^{0}_{Plant} = PEC_{EVAP} + PEC_{ECO} + PEC_{COND} + PEC_{DH} + PEC_T + PEC_{FP} + PEC_{TP} \quad (5.9)$$

In Equation (5.9), PEC_{EVAP} is the Evaporator purchased equipment cost, PEC_{PRE} the Preheater purchased equipment cost, $PEC_{COND}$the Condenser purchased equipment cost, PEC_{DH} the District heating heat exchanger purchased equipment cost, PEC_T Turbine purchased equipment cost, PEC_{FP} ORC pump purchased equipment cost and PEC_{TP} the geothermal fluid pump purchased equipment cost.

Moreover, the additional costs required in Equation (5.8) are: The fee for the completion of the plant (F_C) which is rated at 3% of the PEC^{0}_{Plant}, the auxiliary facility cost AUX_C which is rated at 50% of the PEC^{0}_{Plant} and the contingency cost ($Cont_C$) which it is rated at 15% of the PEC^{0}_{Plant} (Turton 2012).

5.2.5 Remaining FCI costs

In this section the remaining Fixed Capital Investment Cost are presented. The estimations below are generally adapted to the European conditions and are obtained from the following references: (Lukawski 2009), (Bejan 1996).

5.2.5.1 Piping and Heating Network

The piping costs collectively are comprised of the piping system in the power plant, and in the cases of Combined Heat and Power, also of the district heating. In the power plants alone is usually in the range of 10-70% of the purchased-equipment cost (PEC). For geothermal power plants the relative cost of piping is usually much lower. It is caused by lower piping diameters and the high cost of other components in binary units (Lukawski 2009), (Bejan 1996). The total cost of piping is assumed to be equal to 7% of PEC for geothermal applications. The cost of the district heating network is estimated to 500.000 €/km of district heating network (Heberle 2014), (Ehrig 2011).

5.2.5.2 Installation of equipment

This cost accounts for transportation of equipment from the factory, insurance, costs of labor, foundations, insulation, cost of working fluid, and all other expenses related to the construction of a power plant. Installation costs of fossil fuel power plants account usually for 20-90% of the purchased equipment costs. However, the designed ORC power plant is assembled into one unit when it is manufactured and its transportation is relatively

cheap and easy because of its small size. On average, the transportation cost alone accounts only for 5% of PEC for power plants in general. For these calculations, a value of 3% of PEC is assumed for this category.

5.2.5.3 Instrumentation, controls and electrical equipment

For instrumentation, controls and electrical equipment a cost of 5% of PEC is assumed. The cost of electrical equipment, which for power plants usually includes distribution lines, emergency power supplies and switch gears is relatively low for the designed plant. It is however variable depending on the place of installation, but in this work a close proximity of the electric grid is assumed (Lukawski 2009).

5.2.5.4 Cost of land

Direct costs also include so-called offsite costs, i.e. cost of land, civil and structural work. The cost of land is highly site-dependent. It is suggested (Bejan) that if land is to be purchased, cost may contribute up to 10% of PEC. However, specific land use for a binary power plant is significantly lower than for any other type of power plant. For this study, a value of 7% of PEC is assumed (Lukawski 2009).

5.2.5.5 Infrastructure, civil and structural work

This category includes the costs of all needed roads, buildings etc. These costs are site specific and vary significantly between different projects. For geothermal projects, although in reality they are still highly variable, these costs are fixed in this thesis and equal to 5% of PEC (Lukawski 2009).

5.2.5.6 Engineering and supervision

This category of costs includes the cost of planning and the design of the power plant as well as the manufacturer's profit, the engineering supervisor, inspection and administration. Bejan suggests that for power plants in general, these costs range between 25 and 75% of PEC. Since the ORC power plant described in this thesis is preassembled by manufacturer it can be assumed that the only cost of design and planning is the manufacturer's profit. Costs of supervision should also be lower as the time of construction is shorter compared to traditionally designed plants. Moreover, highly specialized staff is not required. All these factors make the final cost of engineering and supervision to be set at the relatively low level of 6% of PEC (Lukawski 2009).

5.2.5.7 Construction

Expenses for construction include all the costs of temporary facilities and contractor's profits. This is yet another phase in which universally designed units hold an advantage over those which are individually designed. Usually for power plants these costs account for about 15% of direct costs (Bejan 1996). However, the placement of an already

assembled and frame-mounted unit into its place of operation is much cheaper than assembly on the spot. In this thesis construction is assumed to account for 4% of direct costs.

5.2.6 Other outlays

Other outlays consist of the startup costs, working capital and allowance for funds during construction (Bejan 1996).

5.2.6.1 Startup costs

Startup costs are the expenses that have to be spent after the construction of the power plant but before the unit can operate in full load. They have to cover not only the cost of equipment and work during startup time, but mainly the difference in income which is the result of part load operation during this time. Some sources show a comprehensive and detailed approach to estimate these costs on the basis of the cost of fuel (Bejan 1996). However, such methodology does not apply in the geothermal industry since the investment in fuel is done before the erection of the power plant. Finally, a contribution of 1% of FCI was assumed for geothermal applications (Lukawski 2009).

5.2.6.2 Working capital

Working capital is the amount of money needed to cover the costs of power plant operation before receiving payment for electricity sold to the grid. According to (Bejan 1996), working capital for power plants is calculated as the sum of costs representing two months of fuel at full load and three months of labor. The first of these costs may obviously be neglected in a geothermal power plant, where the investment in fuel is made before the plant starts to operate. The unit should also work without permanent supervision; therefore labor costs are relatively low. Finally, working capital is assumed to be very low and set at 3% of PEC.

5.2.6.3 Allowance for funds used during construction (AFUDC)

With this category of capital investment costs comes another advantage of universally designed power plants. In site-specific design, the construction period is long. An allowance of funds used during construction time compensates for different time values of money. In the investigated unit, foregoing costs are relatively low since construction time is short. Thus AFUDC is ignored in this study (Lukawski 2009).

5.3 Cost of geothermal wells

The cost of drilling is site-specific and varies drastically for different projects. Moreover, for a geothermal binary plant utilizing low-temperature water as a heat source it is usually not surface equipment, but drilling that has the highest share in total investment cost. For low temperature fields, estimations found in literature vary significantly. Based on the majority of reports, 17-47% of the total project cost is allocated to drilling (Geothermal Energy Association). Generally the cost of drilling can be divided into three individual phases: Exploration, confirmation and site development.

Exploration is the initial development phase and includes prospecting and field analyses aiming to locate a productive geothermal reservoir. The cost reported by ORMAT (Geothermal Energy Association), which is equal to $250/kWe, will be also considered for this study.

The confirmation phase consists of the drilling of production wells until approximately 25% of the needed resource capacity is confirmed. Cost of the confirmation phase for commercially viable projects average around $150/kWe (Lukawski 2009).

The most expensive of these three phases is the last one: site development, in which, for large-scale projects, approximately 75% of required brine flow is obtained. Sensible cost estimates for drilling are very difficult to provide. For European conditions, the best cost approximation which is also assumed in this work, is estimated to be $3200 per kW, according to (Gerber 2012)

According to the Geothermal Energy Association, a minimum of 3 to 5 years is required to put a geothermal power plant on line. Therefore it is assumed that capital investment in a geothermal power plant occurs during the period of 3 years.

5.4 Operation and maintenance costs

Operation and maintenance costs consist of all expenses ensued during the operation phase of the power plant. Generally operational maintenance is the care and minor maintenance of equipment using procedures that do not require detailed technical knowledge of the equipment's or system's function and design. This category of operational maintenance normally consists of inspecting, cleaning, servicing, preserving, lubricating, and adjusting, as required. They encompass expenses related to labor, chemicals, spare parts, etc. In geothermal power plants these costs are usually very low compared to the initial investment. In this work, an average price of 4% of the total equipment cost is assumed (Lukawski 2009).

5.5 Time value of money

It is commonly known that the value of money changes in time and that typically the same amount of money now is worth more than it will be in the future. Because economic analysis of the project requires comparison of many flows of money occurring in different points in time, a method of converting these flows into an equivalent constant quantity has to be used. Such a concept is called levelization and is used in this thesis to calculate costs of operation, maintenance and levelized total cost of electricity. Costs of fuel and capital investment are also expressed in the form of annuities. To account for change in the value of money over time, the effective rate of return (i_{eff}) is used.

Annuity is a series of equal cash flows occurring during some period of time. To determine annuity (A) taking place once a year during n years from the present value P, the capital recovery factor (CRF) is used (Bejan 1996) :

$$A = CRF \cdot P = \frac{i_{eff}\left(1 + i_{eff}\right)^{n}}{\left(1 + i_{eff}\right)^{n} - 1} P \tag{5.10}$$

Due to inflation, changes in the market situation, technological advances etc., O&M costs rates vary in time. This phenomenon is known as escalation in engineering economics. In order to transform a nonlinear series of O&M costs into an equivalent series of annuities called levelized values, the constant-escalation levelization factor (CELF) is used (Bejan 1996):

$$A = CELF\ P_0 = k\frac{1 - k^{n}}{1 - k} CRF\ P_0 \tag{5.11}$$

Where P_0 is the expenditure for O&M in the first year and r_n the escalation rate. Moreover the constant k is defined as:

$$k = \frac{1 + r_n}{1 + i_{eff}} \tag{5.12}$$

5.6 Depreciation of Capital Investment

The depreciation of a capital investment is a method of allocating the cost of a tangible asset over its useful life. Businesses depreciate long-term assets for both tax and accounting purposes. For accounting purposes, depreciation indicates how much of an asset's value has been used up. For tax purposes, businesses can deduct the cost of the tangible assets they purchase as business expenses; however, businesses must depreciate these assets in accordance with rules about how and when the deduction may be taken based on what the asset is and how long it will last. These rules are set by the local revenue agency or taxation authority and therefore greatly change between different countries.

Specifically for a chemical process plant, the physical plant (equipment and buildings) associated with the process has a finite life. The value or worth of this physical plant decreases with time. Some of the equipment wears out and has to be replaced during the life of the plant. Even if the equipment is seldom used and is well maintained, it becomes obsolete and of little value. When the plant is closed, the plant equipment can be salvaged and sold for only a fraction of the original cost.

There are generally different methods for depreciation which are based on the type of the specific investment, and rules set by the local taxation authority. The one most extensively used, which is also used in the current work, is described below (Zervos 2009), (Turton 2012).

5.6.1 Straight-Line Depreciation Method, SL

This is the simplest method, and yet is being used widely for applications ranging from wind parks to chemical process plants. This method is approved by most taxation authorities since it provides balanced benefits to both the investor and the revenue agency (Zervos 2009).

An equal amount of depreciation is charged each year over the depreciation period allowed. The formula for calculating the SL Method depreciation is:

$$d_k^{SL} = \frac{FCI_L - S}{N} \tag{5.13}$$

Where FCI_L is the depreciable capital investment, S the salvage value of the equipment and N the depreciation life of the equipment.

The depreciable capital investment (FCI_L) represents the fixed capital investment to build the plant minus the cost of land and represents the depreciable capital investment. The salvage value of the equipment (S) represents the fixed capital investment of the plant, minus the value of the land, evaluated at the end of the plant life. Usually, the equipment salvage (scrap) value represents a small fraction of the initial fixed capital investment. Often the salvage value of the equipment is assumed to be zero, as is done in this work. Lastly, the depreciation life of the equipment (N) does not reflect the actual working life of the equipment but rather the time allowed by the taxation authority for equipment depreciation. For example the U.S. Internal Revenue Service (IRS) currently allows for chemical process equipment a depreciation class life of 9.5 years (Turton 2012). Similarly in this work, the depreciation time is set equal to 10 years.

5.6.2 Geothermal Energy Tax Rate

In economics, the tax rate describes the ratio (usually expressed as a percentage) at which a business or person is taxed. The tax rate is set by the local revenue agency or taxation authority and therefore highly varies by country, like the depreciation.

Moreover, the tax rate may change also over the course of time. Generally, deferred tax assets and liabilities are, in principle, measured using the tax rates valid as at the balance sheet date. Future tax rate changes are taken into account if substantial prerequisites for its future applicability have been met on the balance sheet date, always within the scope of a legislative procedure. In this work, the tax rate will be considered constant during the whole lifetime of the project.

In the case of geothermal energy taxation in Germany, a flat rate of 30.0%, which includes the standard corporation tax rate of 15%, the solidarity surcharge of 5.5% and an average trade tax rate of 14.2%, can be used (Annual Report of Daldrup & Söhne AG, Geothermal power plants 2013).

5.7 Financing Mechanism

The ultimate product of the economic analysis, is affected not only by capital investment, but also by the origin of these funds. The cost, amount and way in which money is borrowed varies significantly in every investment. They depend on the type of the project, the situation in financial markets, the company borrowing the money, the financial institution lending the money and other conditions.

Most of the projects are financed from two sources: debt and equity. The proportion of equity and debt the company is using to finance its assets, is called Debt/Equity Ratio and it represents a measure of a company's financial leverage. The cost of debt is lower, however in the case of project failure the debt provider is usually the first one to get its money back. Moreover it is usually expected by the bank to secure the debt with some share of money from equity. This one, however, is more expensive.

The debt/equity ratio also depends on the industry in which the company operates. For example, capital-intensive industries such as auto manufacturing tend to have a debt/equity ratio above 2 while personal computer companies have a debt/equity of under 0.5 (Investopedia 2014). According to the Geothermal Energy Association, in geothermal projects usually 30% of financing comes from equity and 70% from debt, namely a Debt-to-Equity Ratio of ~2.3. In this study, this ratio will be assumed.

5.7.1 Interest Rates

The interest rate is defined as the rate at which interest is paid by a borrower (debtor) for the use of money that they borrow from a lender (creditor). Both of these interest rates are highly influenced by the estimated risk of failure of the project. Investors usually compensate for increased danger by raising interest rates. Geothermal plants, because of factors like the uncertainty of well productivity and chemistry of geothermal fluid, are currently considered by financial institution as relatively risky investments. Therefore, it is expected that the effective rate of return is also higher for geothermal projects in comparison for example with wind energy projects. Typical interest rates in the geothermal industry are around 6-8% for debt and approximately 17% for equity (Geothermal Energy Association). Taking into account the 30%-70% equity-debt ratio as mentioned before, this produces a final interest rate of approximately 9%-11%. In this work, the effective rate of return is set to equal 10%.

5.7.2 Loan Financing Mechanism

There are two basic loan financing mechanisms, which in turn are based on the financial institution that lends the money. These are known as fixed-rate loans and adjustable-rate loans. If the loan is a fixed-rate loan, each fully amortizing payment will be equal an amount. If the loan is an adjustable-rate loan, the fully amortizing payment may change as the interest rate on the loan changes. The fully amortizing payment is simply defined as the periodic loan payment, part of which is principal and part of which is interest, where if the borrower makes payment according to the loan's amortization schedule, the loan will be paid-off by the end of its set term. In this work, fixed-rate loans will be used.

The amount of the total investment that is covered by the loan also varies greatly based on the individual projects and investors. According to the U.S. Department of Energy, the debt-to-capital ratios vary within the 60% – 80% range. This rendered its weighted average highest among all the utility-scale technologies according to Renewable Energy Finance Tracking Initiative (REFTI) and U.S. Department of energy. Wind and large photovoltaics each displayed an aggregate debt-to- capital ratio of about 50% (large PV coming in slightly above, wind slightly below), while concentrated solar power had the lowest ratio of 40% (Alliance for Sustainable Energy 2012).

The Debt Term for geothermal power plants is relatively long and can be compared with the actual estimated operating lifetime of the project. Similar investments from Ormat Technologies, had a debt term of 18 years (Ormat Technologies Long-Term Debt Financing 2012). In this study the Debt Term is assumed as 15 years.

The operating lifetime of geothermal power plants ranges between 20-30 years. However, approximately 50% of the current global installed capacity has been in operation for more than 25 years, and two power plants for more than 50 years (International Energy Agency 2010). The great difference between the actual expected time of operation and its

financial planned lifetime, is that the second is much shorter. Investors' expectations concerning the money return period are also different for each type of project and originate in the different nature of developers. Therefore, the lifetime of the designed plant is assumed to be 20 years.

5.8 Revenue / Electric and Thermal power sales

The revenue of a geothermal Organic Rankine Cycle plant originates from the sale of electric power, or in the case of CHP plant, of both electric and thermal power. Therefore the knowledge of these sale prices are essential to the economic success of the investment. Moreover, the purchase price of electricity must be known, since it is assumed that the pump of the geothermal production well, is powered by electricity from the net and not from the electricity generated.

The Sale and Purchase prices for electricity and heat which were assumed in this work are presented in Figure 5.5 according to the following sources: (Gesetz für den Ausbau erneuerbarer Energien, Erneuerbare-Energien-Gesetz August 2014), (VEA Bundesverband der Energieabnehmer e.V. 2013). For the purposes of this thesis, these prices are considered constant during the whole operational lifetime of the ORC Plant.

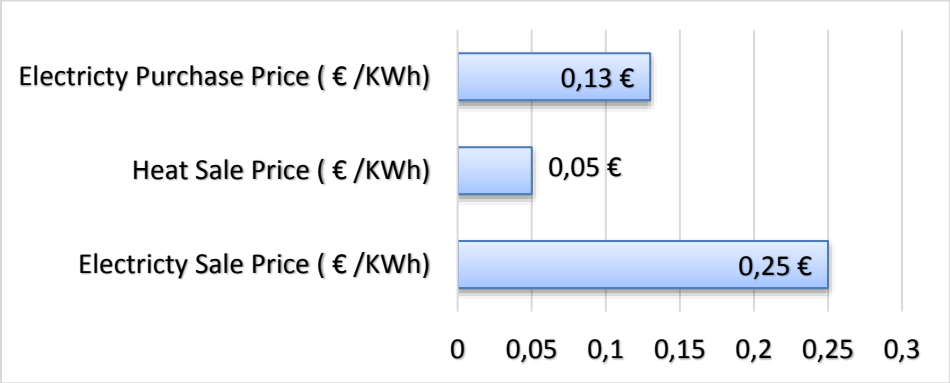

Figure 5.5 Electric and thermal power prices

5.8.1 Load Duration Curve

In order to calculate the different operation parameters of the CHP power plant, the knowledge of the Yearly Load Duration Curve is necessary. Specifically, a load duration curve illustrates the variation of a certain load in a descending arrangement such that the maximum load is plotted on the left and the smallest one on the right. Generally, a duration curve represents the relationship between a certain magnitude and its frequency over a certain period of time.

However, if there is no empirical data for a load duration curve, certain mathematical approximations can be taken into account. For a heat load duration curve, the most

well-known formula has been developed by Sochinsky, (Holzheizwerke 2004). This approach describes an exponential dependence of the heat power required with the time.

The function developed by Sochinsky is shown in formula (5.14) where Q(t) corresponds to the heat load demand, a_0 to the minimum Load and a_m to the average Load. Q_{min} is the minimal required heat demand, Q_{max} is the maximum required heat demand and T_b the full load hours. The working hours t_b are the annual working hours of the District Heating System, which are normally less than all hours of the year, because of maintenance.

$$\mathrm{Q(t)} = \mathrm{Q_{max}}\left(1 - (1 - \mathrm{a_0})\,\mathrm{T}^{\frac{\mathrm{a_m} - \mathrm{a_0}}{1 - \mathrm{a_0}}}\right) \tag{5.14}$$

$$T = \frac{t}{t_b} \quad (t_b < 8760\ hours) \tag{5.15}$$

$$a_0 = \frac{Q_{min}}{Q_{max}} \tag{5.16}$$

$$a_m = \frac{Q_m}{Q_{max}} = \frac{Q_{max}\,T_b}{Q_{max}\,t_b} = \frac{T_b}{t_b} \tag{5.17}$$

The mathematical model proposed by Sochinsky has been proven to validate the real empirical data of thermal district heating networks. In Figure 5.6, the heat load duration curve is depicted for the district head demand in Lemgo, Nordrhein-Westfalen, Germany, where the site experimental data and the Sochinsky mathematical model are compared. As can be clearly seen, the model approaches the real curve with great precision. However since the mathematical approximation is continuous and exponential, it will not be able to predict precisely some other duration curves, like the heat district in Neustadt-Glewe, in Figure 5.7. These charts were obtained from the following work: (Schallenberg 1996).

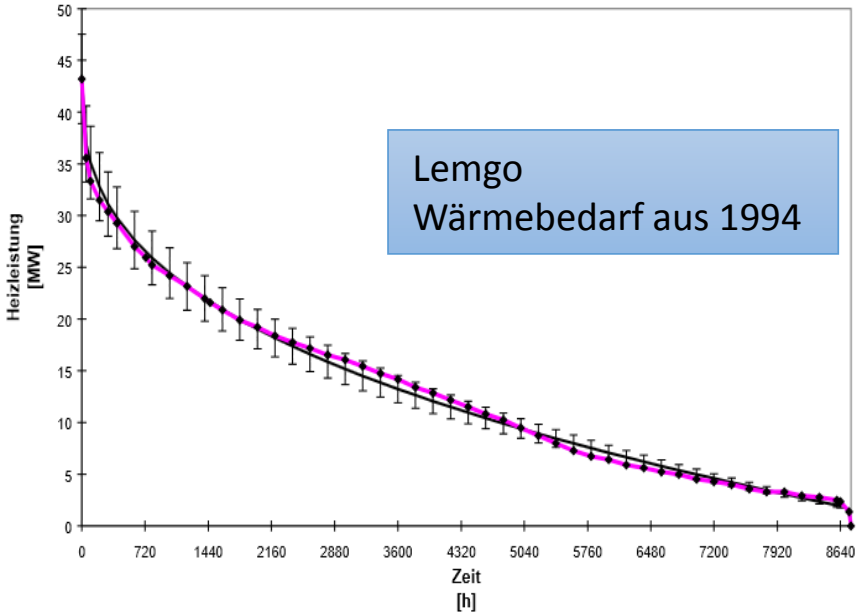

Figure 5.6 Load duration curve and heat district demand in Lemgo, Germany 1994. (Schallenberg 1996)

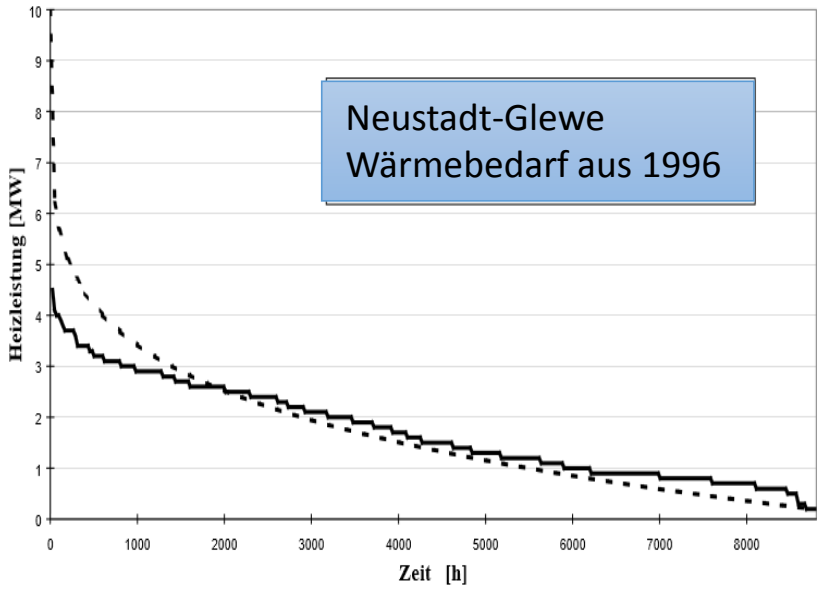

Figure 5.7 Load duration curve and heat district demand in Neustadt-Glewe, Germany 1996. (Schallenberg 1996)

5.9 Profitability Criteria for Project Evaluation

In this section the profitability criteria are discussed, which in turn are used to assess the investment. Generally speaking, there are three bases used for the evaluation of profitability: Time, Cash and Interest Rate. For each of these bases, discounted or non-discounted techniques may be considered. The nondiscounted techniques do not take into account the time value of money and are not recommended for evaluating new projects with a long planned operation lifetime. A summary of all the profitability criteria can be found in the Appendix, in Table A-1. In the following sections, the criteria that will be used in this study are presented.

5.9.1 Payback period

Payback period in capital budgeting refers to the period of time required to recoup the funds expended in an investment, or to reach the break-even point. As a tool of analysis, the Payback period is often used because it is easy to apply and easy to understand for most individuals. When used carefully or to compare similar investments, it can be quite useful.

5.9.2 Net Present Value - NPV

Net present value is defined as the difference between the present value of cash inflows and the present value of cash outflows. NPV is used in capital budgeting to analyze the profitability of an investment or project. The following is the formula for calculating NPV:

$$NPV = \sum_{t=1}^{T} \frac{C_t}{(1+r)^t} - C_0 \tag{5.18}$$

Where C_t the net cash inflow during the period, C_0 the initial investment, r the discount rate, and t the number of time periods. Determining the value of a project is challenging because there are different ways to measure the value of future cash flows. Because of the time value of money, a dollar earned in the future won't be worth as much as one earned today. The discount rate in the NPV formula is a way to account for this. Companies have different ways of identifying the discount rate, although a common method is using the expected return of other investment choices with a similar level of risk.

5.9.3 Internal Rate of Return - IRR

The internal rate of return (IRR) or economic rate of return (ERR) is a rate of return used in capital budgeting to measure and compare the profitability of investments. It is defined as the discount rate that makes the net present value of all cash flows from a

particular project equal to zero. Generally speaking, the higher a project's internal rate of return, the more desirable it is to undertake the project. As such, IRR can be used to rank several prospective projects a firm is considering. Assuming all other factors are equal among the various projects, the project with the highest IRR would probably be considered the best and undertaken first.

5.10 Summary of economic boundary conditions

In Tables 5-6 and 5-7 the economic boundary conditions are summarized:

Table 5-6 Summary of financial mechanism

Financing Mechanism	
Debt-to-equity ratio	2,33
Debt / equity interest rate	7% / 17%
Effective interest rate	10%
Inflation Rate	2%
Debt to Capital Ratio	60%
Loan Payment Method	Fixed-rate
Amount of 2nd year	50%
Debt Term (Years)	10
Depreciation Method	Straight-Line
Depreciation Time (Years)	10
Tax Rate	30%

Table 5-7 Summary of Total Capital Investment costs

Total Capital Investment	
Final Plant PEC	***% of Purchase Equipment Cost***
Fee	3%
auxiliary facility cost	50%
Contingency	15%
Maintenance	**4 % Final Plant PEC**
Geothermal Drilling	***Cost per KWh generated ($/KWh)***
Exploration	250
Confirmation	150
Drilling (3000 m)	3200
Other Costs	***% of Total Investment Cost***
Piping	7%
Electrical equipment	5%
Installation	3%
Infrastructure	5%
Engineering	6%
Construction	4%
Land	7%
Startup	1%
Work Cap	3%
District Heating (8 km)	**500000 € / km of district heating network**

6 Economic Sensitivity Analysis Results

6.1 District heating demand sensitivity analysis

In the first section, the sensitivity analysis focuses on the effect of the heat load duration curve. In total 16 different cases are tested, consisting of 4 different maximum loads (10, 15, 20, 25 MW) and each of 4 different cases of maximum load hours (1000, 1500, 2000, 2500 hours). The heat load duration curves that correspond to the 10 MW case is shown in Figure 6.1. The curves of the other maximum loads, preserve the same graphs, since the vertical axis has been normalized. The full load hours were limited to the 1000-2500 range, because of the similarity of the duration curves to the real data from Lemgo and Neustadt-Glewe, which were presented in the previous section.

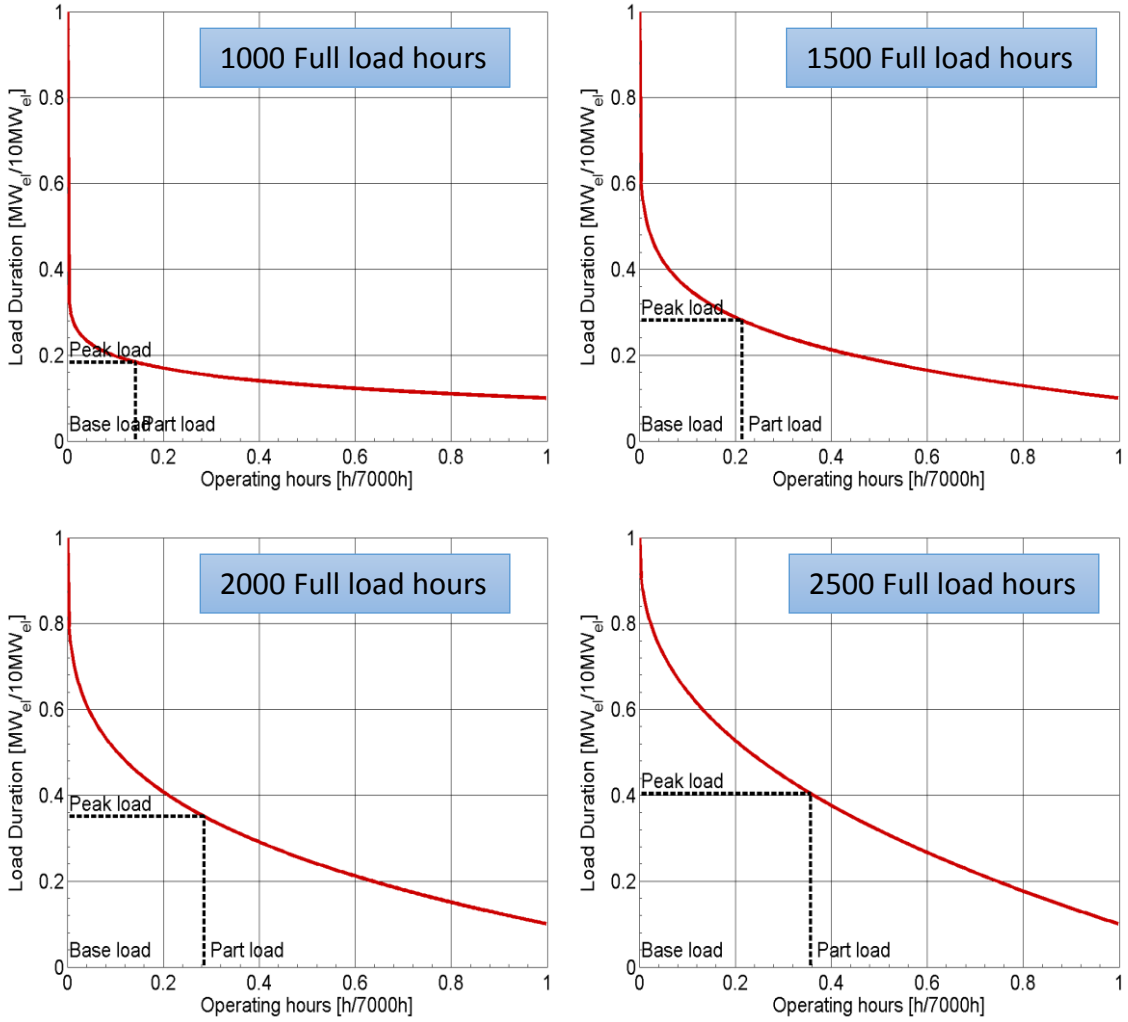

Figure 6.1 Heat load duration curve – sensitivity analysis

In Figure 6.2, the NPV sensitivity analysis results are presented:

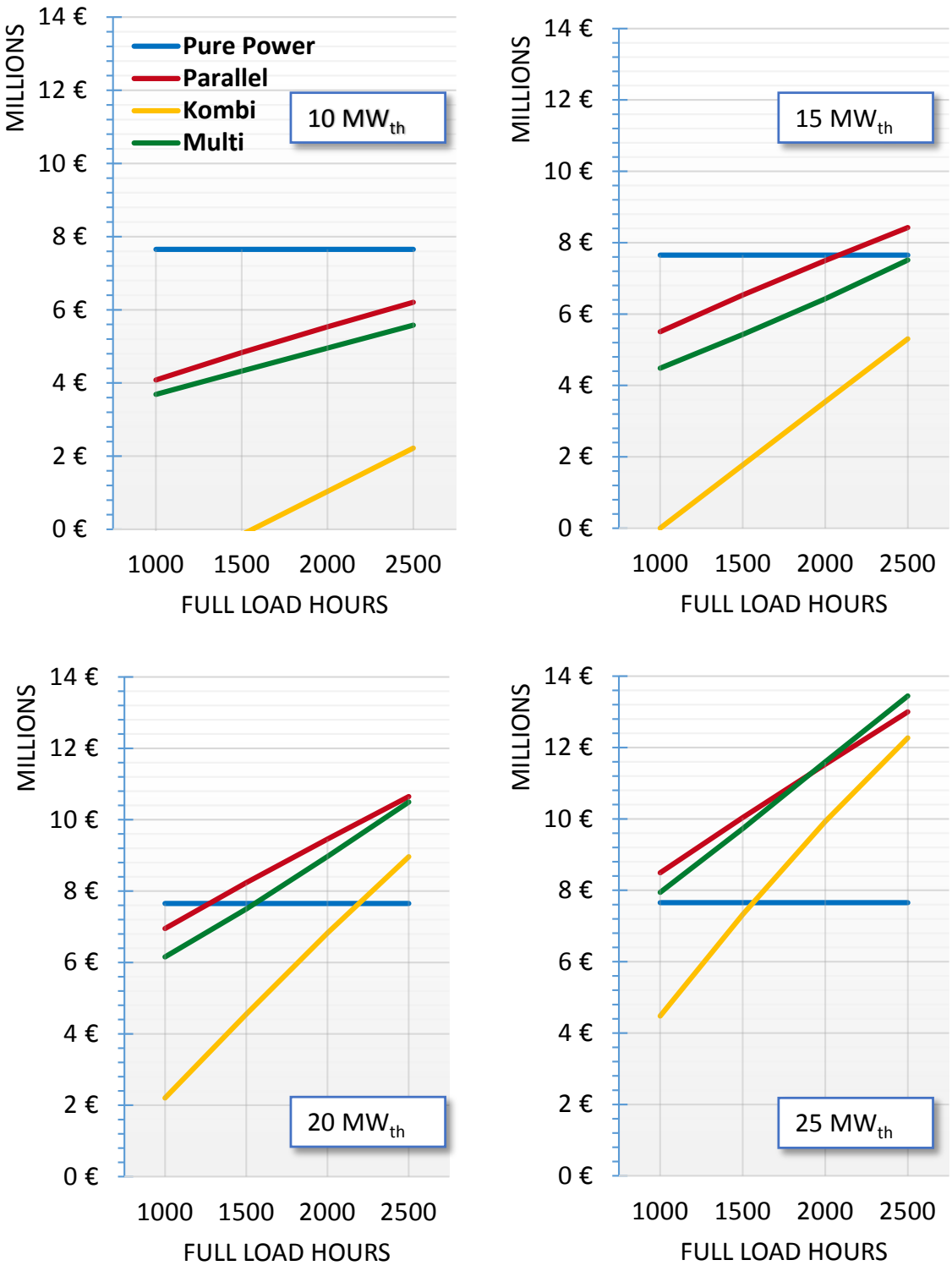

Figure 6.2 NPV sensitivity analysis – variable load duration curve

As can be seen in Figure 6.2, for low heat demands only the pure power generation is profitable. The gains from the district heating demand sales of the CHP configurations, are not high enough to compensate for the extra heat district equipment costs. Only from 20 MW_{th} and 1200 FLH the parallel configuration has a higher NPV, followed by the Multi configuration, while the serial/parallel configuration remains uneconomical since it only benefits in higher heat demands. At very high heat demands, from 25 MWth and 1700 FLH, the Multi configuration is the most profitable of all configurations, since due to design, it has high gains in both low and high heat demand.

On the next page, in Figure 6.3, the IRR sensitivity analysis results are presented. As can be seen, the IRR values are also improving with increasing heat demands, but at slower rates than the NPV. For example, the NPV for the parallel concept is getting higher than the NPV for pure power concept at 20 MW_{th} and 1200FLH. However, the IRR is getting better at 20 MW_{th} and 1800FLH. Moreover, the Multi concept has the best NPV value at 25 MWth and 1700 FLH, but around 25 MWth and 2500 FLH attains the best IRR value.

The reason of the slower increase of the IRR, in comparison with the NPV is due to the definitions of these financial variables. The IRR, reflects also the “risk” of the investment. Profits that come that earlier in the lifetime of a project are more valuable than profits towards the far future. This has to be taken into account for the geothermal power plants, since they have relative long payback periods, as shown in Figures 6.4 and 6.5, in the next section.

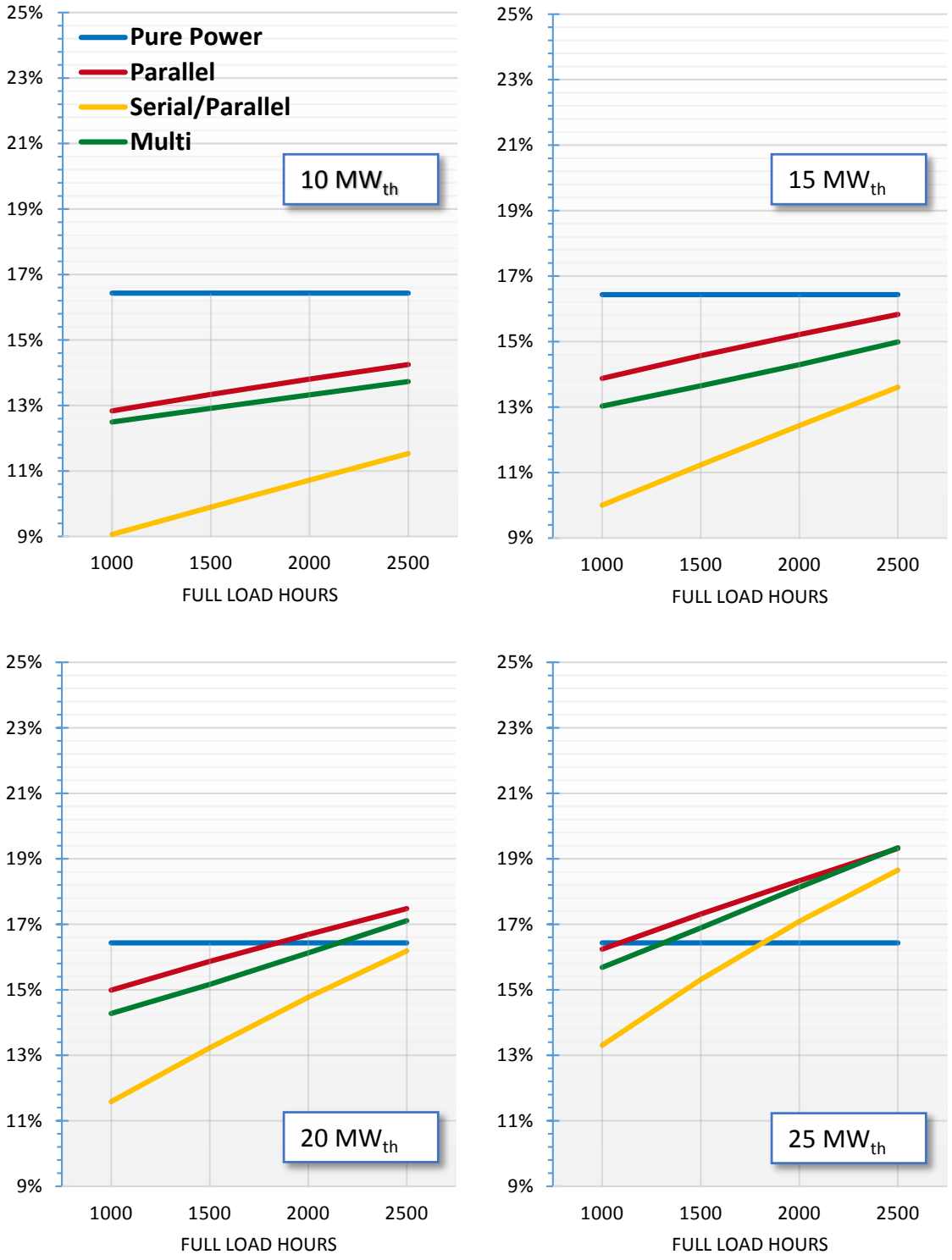

Figure 6.3 IRR sensitivity analysis – variable load duration curve

The cash flow analysis, which includes the individual cash flows and cumulative cash flows, can provide more details for the profitability of the investment. As already discussed in section 5.9, two methods can be used: Discounted and nondiscounted.

In Figure 6.4 the cash flows (represented by bars) and the cumulative cash flows (represented by lines) are given, for a heat district demand of 10 MW_{th} and 1000FLH. Both nondiscounted and discounted methods are used. Moreover, in the same figure, the discounted and nondiscounted payback period can be estimated. This is the period of time required reach the break-even point, or in other words, the time period where the cumulative cash flow becomes positive for the first time.

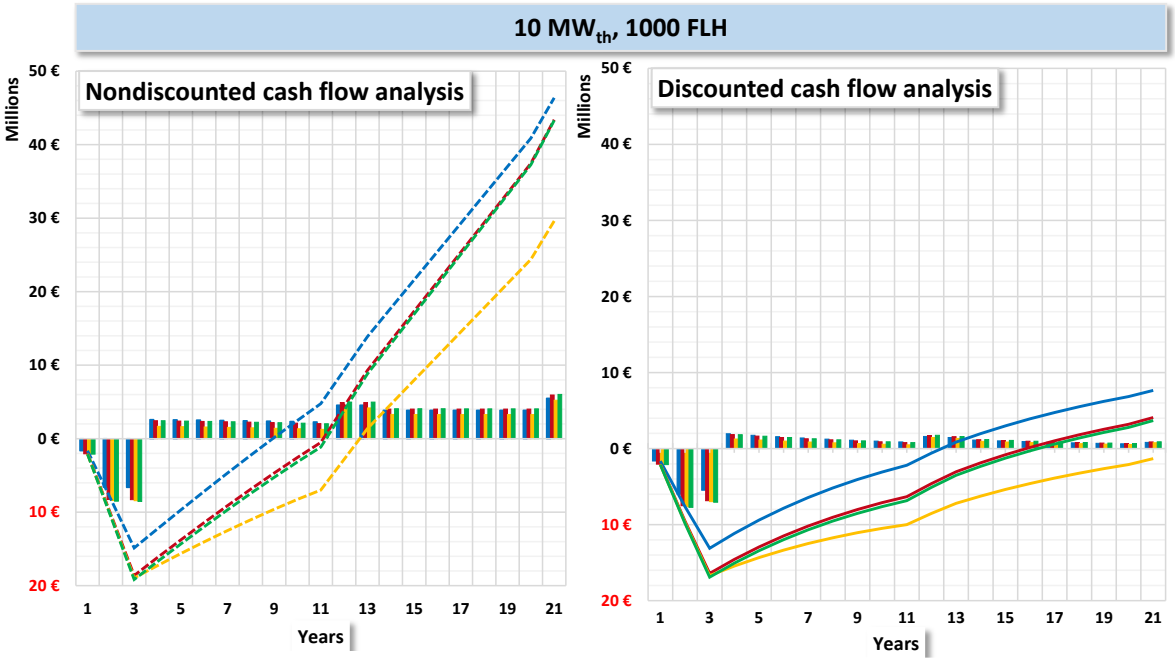

Figure 6.4 Nondiscounted (left) and discounted (right) cash flow

As can be seen, the nondiscounted cumulative cash flow, has a payback period of 9 years and a value at the end of investment of around 45 million Euros, while the discounted has a payback period of 13 years and final value of 7.5 million Euros. However, the reality is reflected only in the discounted cumulative cash flow, and the final value of the investment is none other than the NPV value of the investment. The reason is that the nondiscounted payback period fails to take into account the time value of money, which is constantly decreasing per year, and therefore produces incredibly profitable results. Thus, as expected, the nondiscounted methods are not suitable for investments of this magnitude and lifetime. Therefore only the discounted cash flow analysis will be taken into account.

The Discounted cash flow analysis, the NPV and the IRR are presented in Figure 6.5 for three cases of low, middle and high heat district demand.

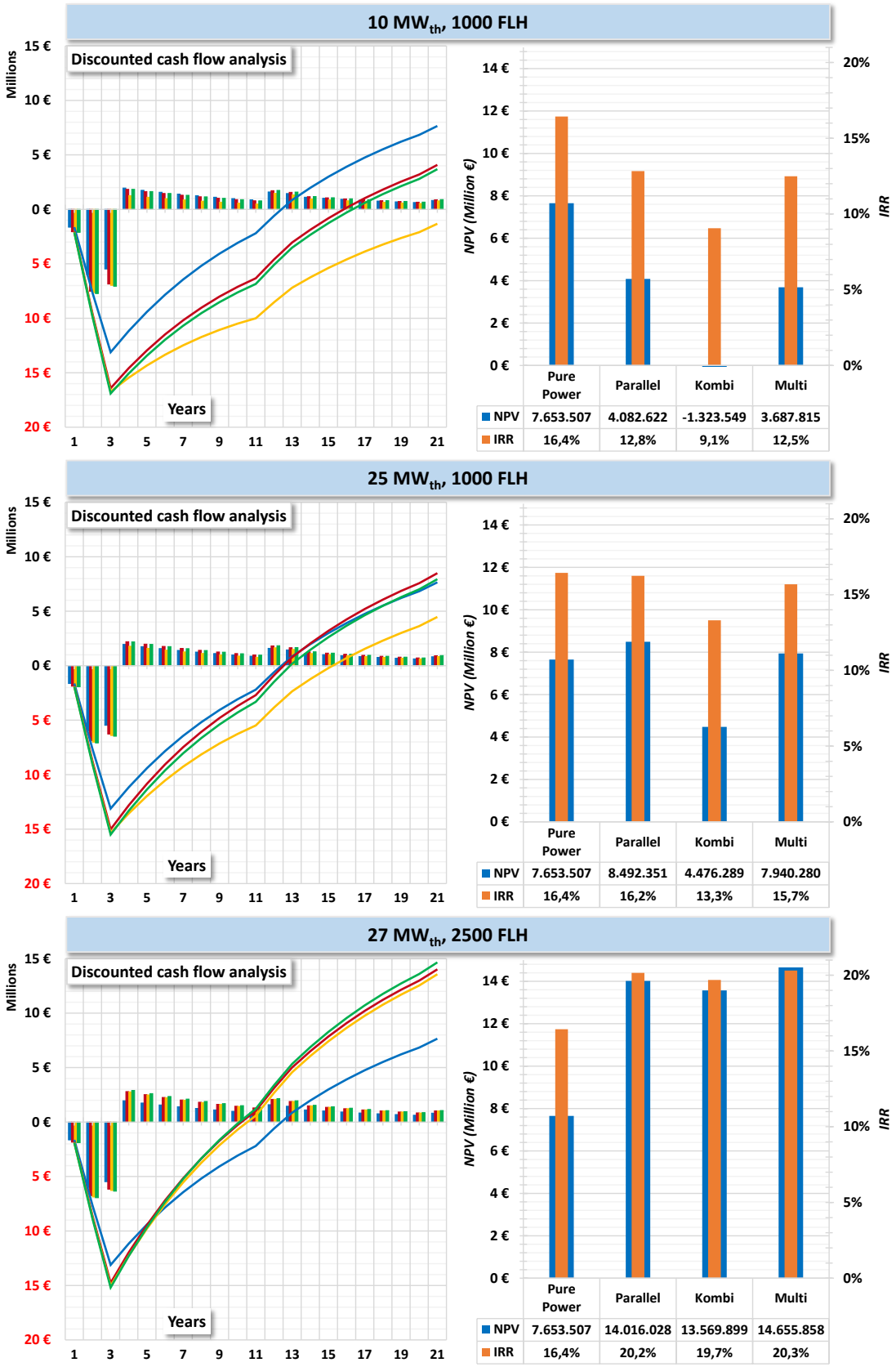

Figure 6.5 Discounted cash flow analysis (Left), NPV and IRR (Right)

According to the information shown in Figure 6.5, the following conclusions are drawn:

- In the third year of the investment, where the total investment costs have been paid, the pure power generation is considerable cheaper than the CHP concepts, which are more expensive because of the extra district heating costs.

- However with increasing heat demand, the difference is getting smaller, because the relative price of the CHP concept components is getting lower. This is due to the fact that in high heat demands, lower electric power is produced, and therefore the ORC components (evaporator, turbine etc.) are smaller and cheaper.

- The IRR increases at a slower rate than the NPV. Specifically, in the case of the 25 MW, 1000 FLH, the parallel concept has a higher NPV, but lower IRR than the pure generation. The reason is that, in this case, the profits of the parallel concept come later in the future (after 10 years) than the profits of the pure power generation. The profits earlier in time have a greater time value of money and less risk than profits in the far future. Exactly this risk is reflected in the IRR value.

- In this study, the discounted payback periods were in the range of 10-11 years in the case of CHP with high heat district demand, to 16-17 years with low demand. In the case of pure power generation it was estimated at 12-13 years.

Last but not least, more information can be extracted by Figure 6.6, on the next page. In this Figure, the sales of the investments (Revenue) are compared with the total produced energy. The total produced energy includes both electric and thermal GWh.

As shown in Figure 6.6, the Multi configuration (presented in Section 4.2.1, Figure 4.8) is producing the most energy, and therefore has the biggest revenues in every operational point, both in low and high heat demands. This is expected, since it was designed to function as a “hybrid” and have high gains in both low and high heat demands.

On the contrary, although the Multi configuration produces the most energy, it is not the most profitable investment for low heat demands. The reason is that although the Multi concept produces the most energy and has the highest revenue, it also has a higher component cost, for example a bigger turbine with intermediate steam extraction, second pump etc. Therefore only in higher heat demands is the extra cost justified and the higher power generation and revenue, lead to a more profitable investment.

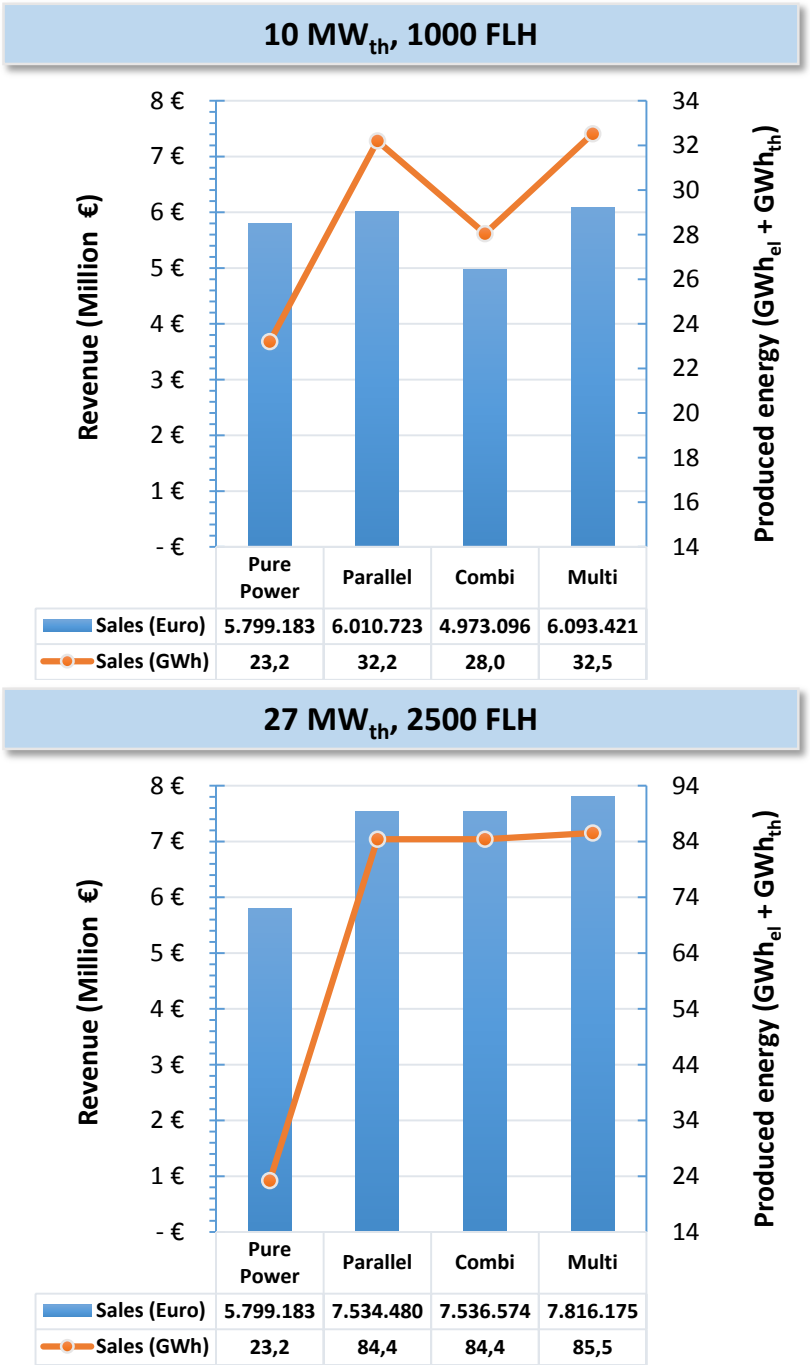

Figure 6.6 Revenue (Left), Produced electric and thermal energy (Right)

Finally, the most profitable configurations according to the heat district demand, are summarized in Figure 6.7.

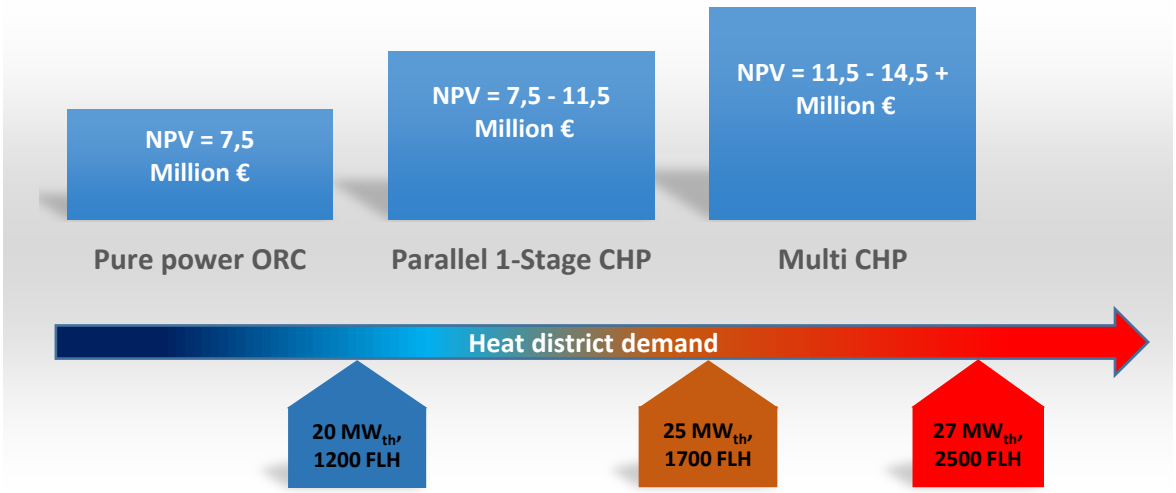

Figure 6.7 Most profitable configurations according to heat district demand

- For low heat demands, up to 20 MW_{th} and 1200 FLH, the pure power generation standard ORC is the most profitable investment, with a NPV value up to 7.5 million €. The gains from the heat sales of every Combined Heat and Power configuration, are not high enough to compensate for the increased equipment costs.

- For medium heat demands, between 20 MW_{th} - 1200 FLH and 25 MW_{th} - 1700 FLH, the parallel one-stage configuration is the most profitable investment, with NPV values ranging between 7.5 and 11.5 million €.

- For high heat demands, above 25 MW_{th} - 1700 FLH, the Multi configuration is the most profitable investment. The NPV values are above 11.5 million €. For example, for a high heat demand of 27 MW_{th} - 2500 FLH, the NPV equals 14.5 million €. The Multi configuration produces more electric and thermal power than every other configuration in all operation points, but has increased costs which make it more profitable in the high range of heat district demands.

6.2 Financial Mechanism sensitivity analysis

In this section a sensitivity analysis is carried out about the financial mechanism of the investment. All the financial data used in the previous section are from similar geothermal investments according to the sources in the corresponding chapter and therefore are considered the typical case.

However, the financial mechanism can still be highly variable because of the dependence on multiple factors. These include for example the economic power of the company which makes the investment, the bank which will supply the loan, the local revenue service, the type and nature of the economic agreement and many more. Therefore a sensitivity analysis is carried out in order to assess the results in the case where the most important variables of the financial mechanism tend to vary from the typical values.

In the figures below, the “typical” case refers to the boundary conditions assumed in the previous section. The main variables changed are the Debt to Capital ratio, Debt Term and interest rate. The results are presented in the charts below:

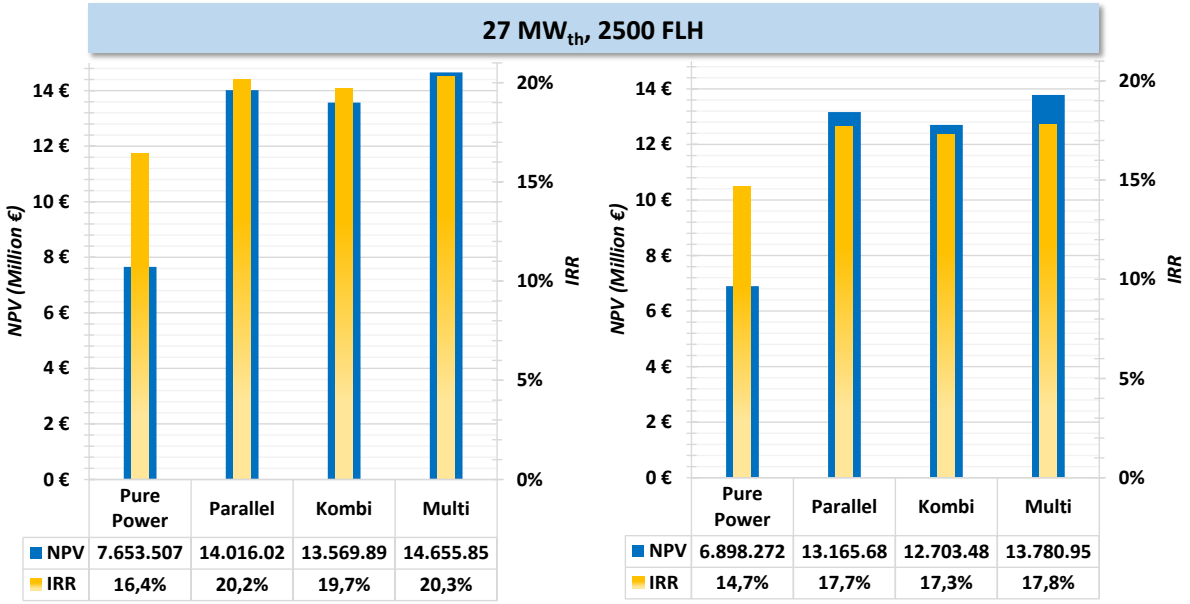

Figure 6.8 Left: Debt term 10 years (Typical)
Right: Debt term 5 years (50% decrease)

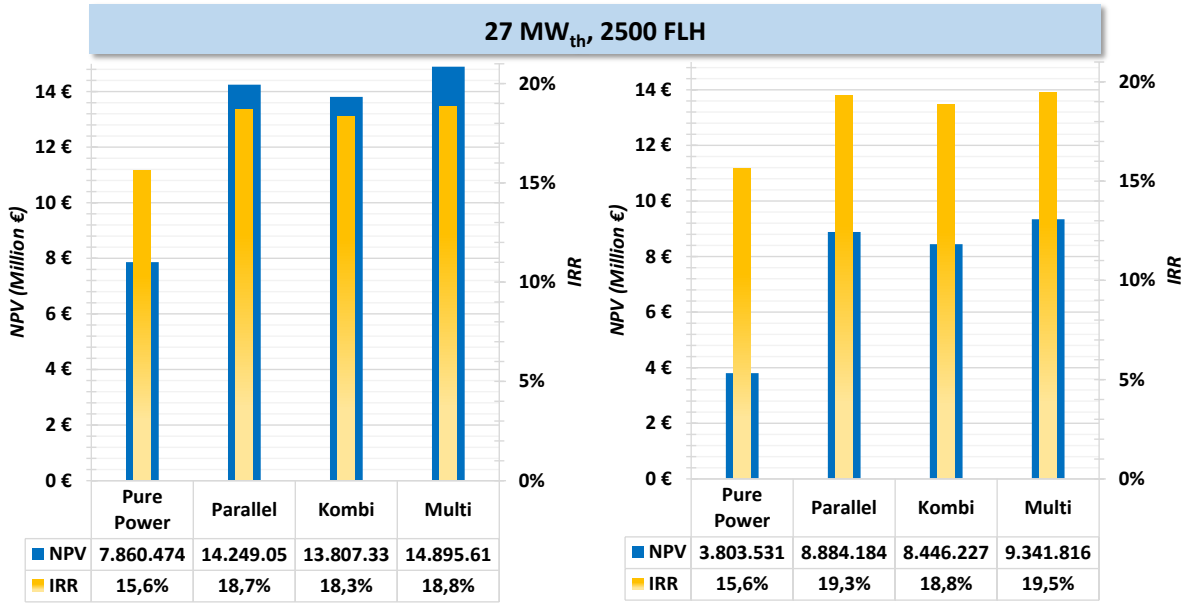

Figure 6.9 Left: Debt to Capital ratio 30% (50%decrease)
Right: Interest Rate 12% (+2% increase)

As is shown in Figures 6.8 and 6.9, reducing the Debt Term and Debt to Capital Ratio and increasing the Interest rate, affect negatively the investment each time in a different way. For example, for the Multi configuration, reducing the Debt term from 10 to 5 years decreases IRR by 2.5%, while the NPV decreases only by almost 1 million €.

Reducing the Debt to Capital ratio, decreases the IRR by 1.5% but increases the NPV by approximately 200,000 €. The reason for the increase of the NPV is that with a smaller loan, there less interest to pay the bank, but at the same time the IRR decreases since more capital has to be paid in the beginning of the investment. Capital in the beginning of the investment is more “expensive” than capital in later years, because of the time value of money.

Lastly, increase of the Interest rate, decreases the IRR only by 0.8%, but decreases the NPV by almost 5 million €. The interest rate is directly affecting the cost of borrowing money and the discount rate in the definitions of IRR and NPV. It generally represents the risk of the investment (for more information the reader may refer to paragraph 5.10)

The above analysis was done for a high district heating demand of 27 MWth and 2500 FLH. Although the profitability of the projects was reduced, the investments still remained largely profitable. The next figure depicts the same variable changes, but for a low heat demand of 10 MW_{th} with 1000 FLH.

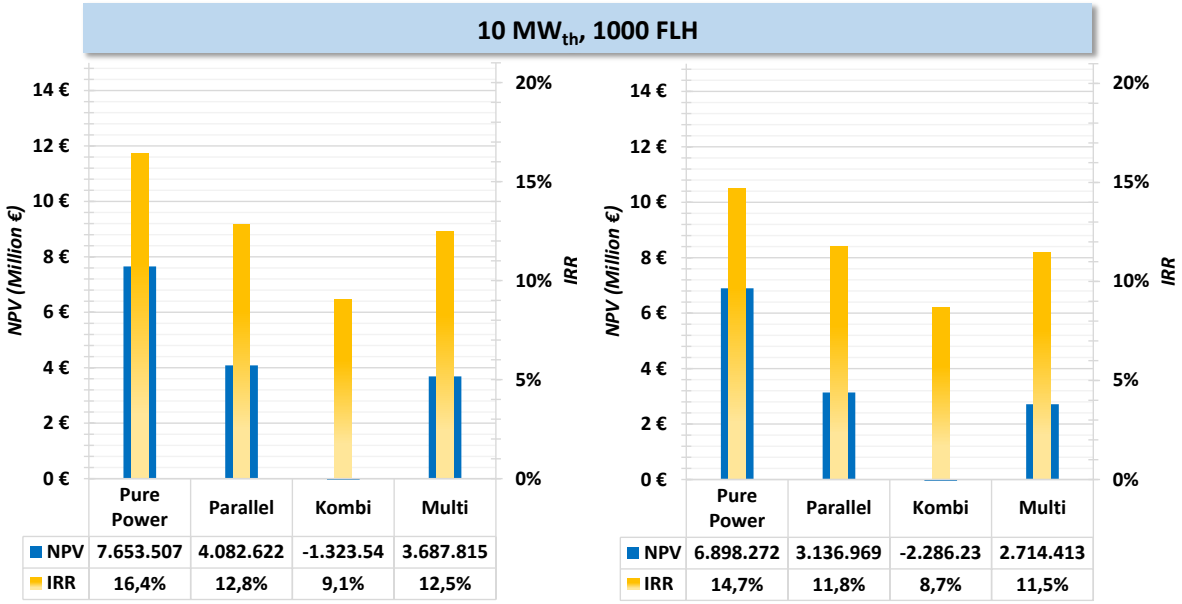

Figure 6.10 Left: Debt term 10 years (Typical)
Right: Debt term 5 years (50% decrease)

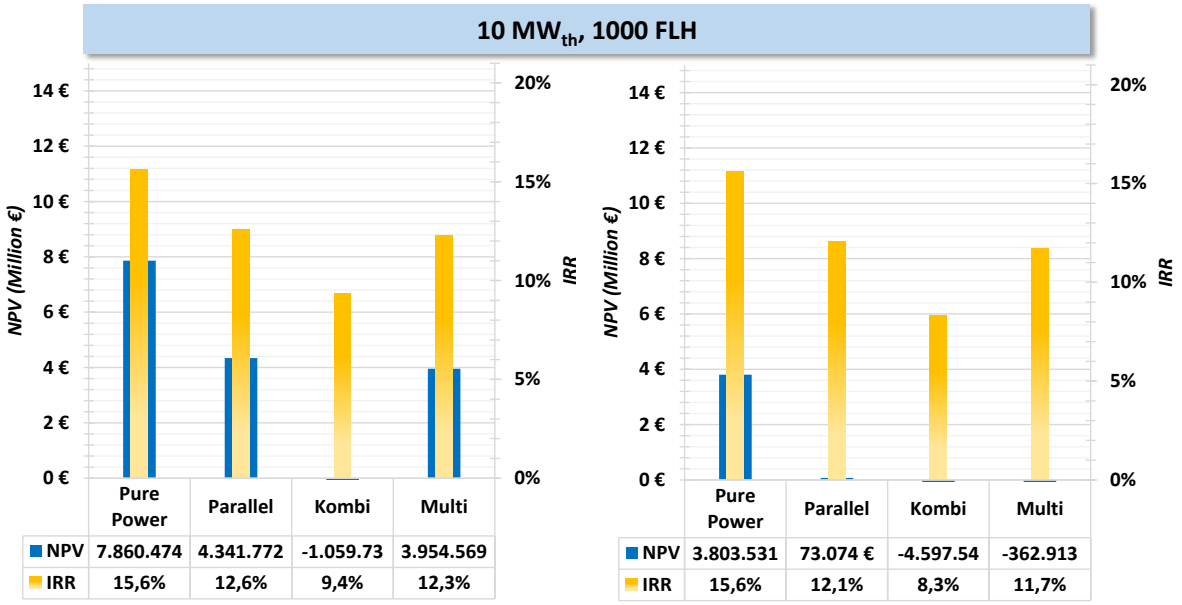

Figure 6.11 Left: Debt to Capital ratio 30% (50%decrease)
Right: Interest Rate 12% (+2% increase)

As can be seen in Figure 6.10 and 6.11, in the case of low heat district demands the consequences are the same, but more dire. For example, an increase in the interest rate of 2% renders all the CHP investments completely uneconomical, with negative NPV values. Therefore, the financial mechanism is extremely important in the economic analysis of the geothermal projects. A poor financial mechanism may not be able to support even the most technological and thermodynamical innovative concepts.

7 Conclusions

The objective of this study was to investigate and evaluate energetically and economically different Organic Rankine Cycle configurations for use with geothermal medium temperature sources for the generation of electricity and heat.

Nowadays, the world still relies heavily on fossil fuels to cover the energy demands, despite the increasing share of renewable energy that has been observed over the last years. The high share of fossil fuels creates a system that lacks diversity and security, threatens the health of the citizens, jeopardizes the stability of Earth's climate, and deprives the future generation of clean air, clean water and energy independence.

On the other hand, Geothermal Energy is the only renewable energy source which has the potential to provide a low-emission base-load power and heat by utilizing the natural hydrothermal resources of the planet. For low- to medium-temperature resources the Organic Rankine Cycle is the most promising and fastest-growing technology. Increased interest has been focused on CHP applications, since they make more efficient use of the geothermal resources by cascading the geothermal fluid to successively lower temperature applications, thereby have the potential to improve the economics of the entire system dramatically.

In this thesis, firstly the pure power generation applications for medium to low temperature geothermal source with HFOs as the working fluid were investigated. These were the R1234ze and R1234yf, the only two HFOs available in the REFPROP library. From the simulations it is established that:

- For a design temperature of 140 °C and above, the R1234ze is more suitable, while the R1234yf is better for the 120 -130 °C range. In low ranges, both HFOs are similar.

- The one-stage turbine ORC provides more power, while the two-stage ORC provides a higher outlet temperature for the geothermal fluid, making it more suitable for CHP applications.

- For the case of R1234ze, close to the supercritical conditions, the pinch point changes from the outlet of the preheater to the inlet. Therefore the pinch point location, depends on the fluid used, the evaporating pressure and the temperature of the geothermal fluid.

- The system and thermal efficiency are generally very low, ranging from 2% to 10%. On the other hand, the exergy efficiency takes into account the second thermodynamical law, and therefore has high values of 20-45%. All the efficiencies are depending on the fluid used, the evaporating pressure and the geothermal source temperature.

- For the two stage turbine model, increase in the intermediate temperature results in decrease of the power generation, system and exergy efficiency, and increase of the geothermal fluid at the ORC outlet, making it suitable for CHP applications. On the other hand, the thermal efficiency doesn't decrease, but attains certain maximum values for specific intermediate pressures. These intermediate pressures, are close to the geometric mean value of the evaporating and condensing pressure. A similar mechanism exists in the air conditioning and refrigeration applications, which states that for a perfect gas, the compression work is minimum if the intermediate pressures are the geometric mean values.

In the next section of the study, the CHP models were investigated. These included the parallel, serial/parallel, and an innovative combination configuration. All of these configurations were simulated with both one-stage turbine and two-stage turbine ORC modules. The results from this section are summarized below:

- The parallel configuration with one-stage turbine ORC module has a power generation which continually decreases with increasing heat district demand. It produces the most power and is the most efficient concept for low heat demands, up to 9 MW_{th} for 140C.

- The serial / parallel configuration with a two-stage turbine ORC module is the most efficient and with the greatest power output for middle to high district heating demands, namely 9-30 MW_{th} .

- The combination model, called for short "Multi", combines the most effective configurations into one concept, by a series of extra tubes and components. In low heat demands its operation equals the one of the parallel one-stage concept, while in higher heat demands it changes to the serial/parallel two-stage concept. Therefore, it produces the highest power and is most efficient in the entire region of 0-30MW_{th}.

- For very high heat demands, especially above 27 MW_{th}, all concepts approach and yield similar results.

In the next and final section, the economical evaluation for the profitability of the investments was carried out. The Total Capital Investment, the Revenue, the Financial Mechanism and different economic criteria were implemented using a very detailed scope of boundary conditions. Moreover, a sensitivity analysis was carried out for different heat district demands and financial mechanisms. The heat district demand was approximated by the Sochinsky curve and was based on existing district heating networks. The outcomes of this analysis are:

- The drilling costs of the geothermal plant investment, which include the exploration, confirmation and drilling phases, constitute the biggest share of total costs.

- For low heat demands, up to 20 MW_{th} and 1200 FLH, the pure power generation standard ORC is the most profitable investment, with a NPV value up to 7.5 million €. The gains from the heat sales of every Combined Heat and Power configuration, are not high enough to compensate for the increased equipment costs.

- For medium heat demands, between 20 MW_{th} - 1200 FLH and 25 MW_{th} - 1700 FLH, the parallel one-stage configuration is the most profitable investment, with NPV values ranging between 7.5 and 11.5 million €.

- For high heat demands, above 25 MW_{th} - 1700 FLH, the Multi configuration is the most profitable investment. The NPV values are above 11.5 million €. For example, for a high heat demand of 27 MW_{th} - 2500 FLH, the NPV equals 14.5 million €. The Multi configuration produces more electric and thermal power than every other configuration in all operation points, but has increased costs which make it more profitable in the high range of heat district demands.

- The IRR value is increasing at a slower rate than the NPV, for increasing heat district demands. The IRR, reflects the “risk” of the investment, while the NPV does not. Profits that come that earlier in the lifetime of a project are more valuable than profits towards the far future. This has to be taken into account for the geothermal power plants, since they have relative long payback periods.

- In this study, the discounted payback periods were in the range of 10 years in the case of CHP with high heat demand, to 16 years with low heat district demand. In the case of pure power generation it was estimated at 13 years.

- The financial mechanism of the investment is greatly affects the profitability of the investment. A poor financial mechanism may not be able to support even the most technological and thermodynamical innovative concepts.

Bibliography

US Energy Information Administration. 2013. *Levelized cost of new generation resources.* Annual Energy Outlook.

AACE, Standard. 2010. *Cost engineering terminology TCM Framework: General Reference.* Association for the Advancement of Cost Engineering International.

Alliance for Sustainable Energy, LLC. 2012. *Renewale Energy Finance Tracking Iniative (REFTI): Snapshot of Recent Geothermal Financing Terms.*

American Society of Heating, Refrigerating and Air-Conditioning Engineers. 2009. *2009 ASHRAE handbook: fundamentals.* Atlanta, GA: American Society of Heating, Refrigerating and Air-Conditioning Engineers.

2013. *Annual Report of Daldrup & Söhne AG, Geothermal power plants.*

Antics, Miklos, and Burkhard Sanner. 2007. *Status of Geothermal Energy Use and Resources in Europe.*

Automotive News. 2013. *German officials provide mixed ruling on Honeywell refrigerant.*

Bejan, Tsatsaronis., Moran. 1996. *Thermal design and optimization.* Inc. USA: John Wiley & Sons.

Bertani, R. 2010. "Geothermal Power Generation in the World 2005–2010 Update Report." *Proceedings at World Geothermal Congress 2010.* Bali, Indonesia.

Brown, J.S. 2009. "HFOs – new, low global warming potential refrigerants." *ASHRAE J* 22–29.

Chammas, Clodic D. 2005. "Combined cycle for hybrid vehicles." *SAE Technical Paper* 01-1171.

March 2014. *Chemical Engineering, VOL. 121, NO. 3.*

2014. *climatedata.eu.* http://www.climatedata.eu/climate.php?loc=gmxx0087&lang=en.

Domanski, Piotr A. 1995. *Minimizing throttling losses in the refrigeration cycle.* National Institute of Standards and Technology.

n.d. *EBSILON Professional 7.00.* http://www.sofbid.com.

EGEC. 2009. *Geothermal electricity and combined heat and power.* Brussels, Belgium: European Geothermal Energy Council.

Ehrig, R., C. Kristöfel, and C. Pointner. 2011. *Operating Figures and Investment Costs for District Heating.*

Emsley, John. 1991. *The Elements.* Oxford University Press.

Fridleifsson, Ingvar B., Ruggero Bertani, Ernst Huenges, John W. Lund, Arni Ragnarsson, and Ladislaus Rybach. 2008. *The possible role and contribution of geothermal energy to the mitigation of climate change.* Luebeck: IPCC Scoping Meeting on Renewable Energy Sources.

Gerber, Leda. 2012. *Environomic optimal configurations of geothermal energy conversion systems: Application to the future construction of Enhanced Geothermal Systems in Switzerland.* Lausanne, Switzerland: Industrial Energy Systems Laboratory, Ecole Polytechnique Fédérale de Lausanne.

August 2014. *Gesetz für den Ausbau erneuerbarer Energien, Erneuerbare-Energien-Gesetz.* Erneuerbare-Energien-Gesetz - EEG.

Gilliland. 1978. *Energy Analysis: A New Public Policy Tool.* Westview Press.

Grundfos. 2009. *Engineering Manual - Industrial Boilers.* GRUNDFOS Management A/S.

Guthrie, K. M. 1969. *Capital Cost Estimating.* Chem. Eng. 76, no. 3, p. 114.

—. 1974. *Process Plant Estimating, Evaluation and Control.* Solana: Solana Beach.

Guus J. M. Velders, David W. Fahey, John S. Daniel, Mack McFarland, and Stephen O. Andersen. 2009. *The large contribution of projected HFC emissions to future climate forcing.* Bilthoven: PNAS.

Heberle, Florian. 2014. *Thermoeconomic Analysis of Hybrid Power Plant Concepts for Geothermal Combined Heat and Power Generation.* Energies 2014, 7, 4482-4497.

Hettiarachchi, H.D.M., M. Golubovic, W.M. Worek, and Y. Ikegami. 2007. “Optimum design criteria for an Organic Rankine cycle using low-temperature geothermal heat sources.” *Energy.*

Hewitt, G. F. 1990. *Hemisphere handbook of heat exchanger design.* New York: Hemisphere Publishing Corporation .

Hohmeyer, Olav, and Tom Trittin. 2008. *IPCC scoping meeting on renewable energy sources.* Lübeck, Germany.

Holzheizwerke, Arbeitsgemeinschaft QM. 2004.

Ibrahim Dinçer, Mehmet Kanoglu. 2010. *Refrigeration Systems and Applications.* John Wiley & Sons.

International Energy Agency. 2010. *Renewable Energy Essentials: Geothermal.*

Investopedia. 2014. *Debt/Equity Ratio.* http://www.investopedia.com/terms/d/debtequityratio.asp.

Kakaç, Saldic, and Hongtan Liu. 1998. *Heat Exchangers: Selection, Rating and Thermal Design.* CRC Press LLC.

Knapek, E., and G Kittl. 2007. *Unterhaching Power Plant and Overall System.* Proceedings European Geothermal Congress .

Kuno Schallenberg, Dr.-Ing. Heiner Menzel. 1996. *Wärmebedarfsdeckung aus geothermischer Energie im Betriebsjahr 1996, Geothermie Report 99-1.* GeoForschungsZentrum Potsdam .

Kyoto Protocol Reference Manual. 2008. *Kyoto Protocol Reference Manual on Accounting of Emissions and Assigned Amounts.* Bohn: United Nations Framework Convention on Climate Change.

Lukawski, Majiec. 2009. *Design and Optimization of Standardized Organic Rankine Cycle Power Plant for European Conditions.* Akureyri: School for Renewable Energy Science in affiliation with University of Iceland.

Lund, John W. 2005. *Combined heat and power plant Neustadt-Glewe, Germany.* Germany.: GHC Bulletin.

Marc Jüdes, Stefan Vigerske, George Tsatsaronis. 2009. *Optimization of the Design and Partial-Load Operation of Power Plants Using Mixed-Integer Nonlinear Programming.* Berlin: Institute for Energy Engineering, Technische Universität Berlin.

Mercedes Ibarra, Antonio Rovira, Diego Padila, Julian Blanco. 2014. "Performance of a 5 kWe Organic Rankine Cycle at part-load operation." *Applied Energy* 147-158.

Navarrete, P. F. 1995. *Planning, Estimating, and Control of Chemical Construction Projects.* New York: Marcel Dekker, Inc.

2012. "Ormat Technologies Long-Term Debt Financing." *http://www.ormat.com/news/latest-items/ormat-technologies-signs-long-term-debt-financing-310-million-olkaria-iii-geotherm.* August 27.

Prasad, Manohar. 2003. *Refrigeration and Air Conditioning.* New Age International.

Qiu, Guoquan. 2012. "Selection of working fluids for micro-CHP systems with ORC." *Renewable Energy 48* 565-570.

R. K. Shah, D. P. Sekulic. 2003. *Fundamentals of heat exchanger design.* ohn Wiley and Sons, Inc.

Rybach, Ladislaus. 2007. *Geothermal Sustainability.* Zurich: Geo-Heat Centre Quarterly Bulletin.

S. Karellas, A.-D. Leontaritis, G. Panousis, E. Bellos, E. Kakaras. 2013. "Energetic and exergetic analysis of waste heat recovery systems in the cement industry." *Energy 58* 147-156.

Schulz, R. 2005. *Assessment of Probability of Success for Hydrothermal Wells.* Proceedings World Geothermal Congress .

Spliethoff, H., Wieland, C. 2012. *8. Internationale Geothermiekonferenz.* Freiburg.

Sylvain Quoilin, Martijn Van Den Broek, Sebastien Declaye , Pierre Dewallef, Vincent Lemort. 2013. "Techno-economic survey of Organic Rankine Cycle (ORC) systems." *Renewable and Sustainable Energy Reviews 22* 168–186.

Tchanche BF, Lambrinos G, Frangoudakis A, Papadakis G. 2011. "Low-grade heat conversion into power using organic Rankine cycles—a review of various applications. ." *Renewable and Sustainable Energy Reviews* 15:3963–79.

2011. *Technology Roadmap: Geothermal Heat and Power.* Paris: IEA Sustainable Energy Policy and Technology directorate.

Thome, John R. 2010. *Wolverine Tube, Inc. : Engineering Data Book.*

Turcotte, D. L. Schubert, G. 2002. *Geodynamics 2 ed.* Cambridge: Cambridge University Press.

Turton, Richard. 2012. *Analysis, Synthesis and Design of Chemical Processes.* Ann Arbor, Michigan: Pearson Education, Inc.

Ulrich, G. D. 1984. *Guide to Chemical Engineering Process Design and Economics.* New York: John Wiley and Sons.

VEA Bundesverband der Energieabnehmer e.V. 2013. *VEA-Fernwärme-Preisvergleich.*

Velez F, Segovia J, Martın MC, Antolın G, Chejne F, Quijano A. 2012. "A technical, economical and market review of Organic Rankine Cycles for the conversion of low-grade heat for power generation." *Renewable and Sustainable Energy Reviews* 6:4175–89.

Vera-Garcia, F. 2010. *A simplified model for shell-and-tubes heat exchangers: Practical application.* Applied Thermal Engineering 30 1231-1241.

Wei Liu, Dominik Meinel, Christoph Wieland, Hartmut Spliethoff. 2014. "Investigation of hydrofluoroolefins as potential working fluids in organic Rankine cycle for geothermal power generation." *Energy 67* 106-116.

Zervos, Arthouros. 2009. *Renewable Energy Sources Notes.* National Technical University of Athens.

Appendix

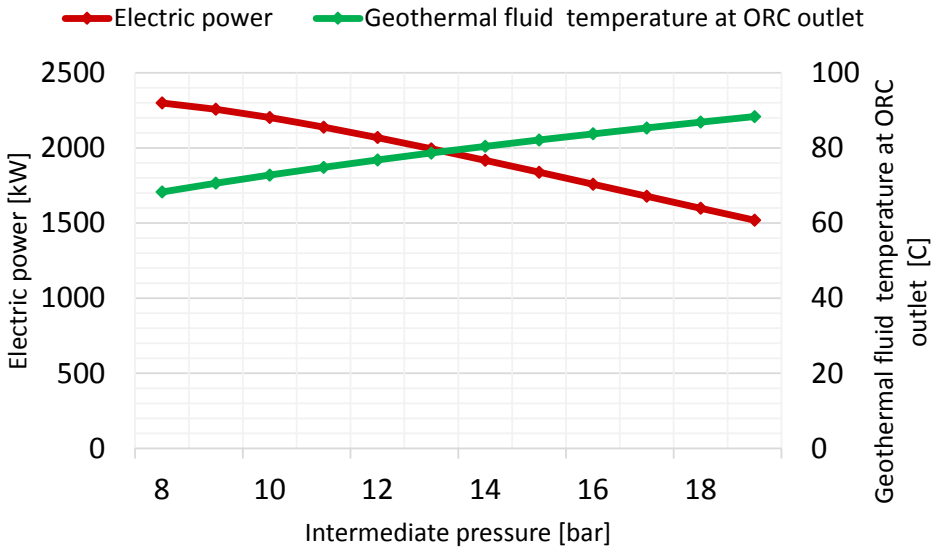

Figure A.1 Power generation and geothermal fluid outlet temperature for variable intermediate pressure (Geothermal source at 120 C°)

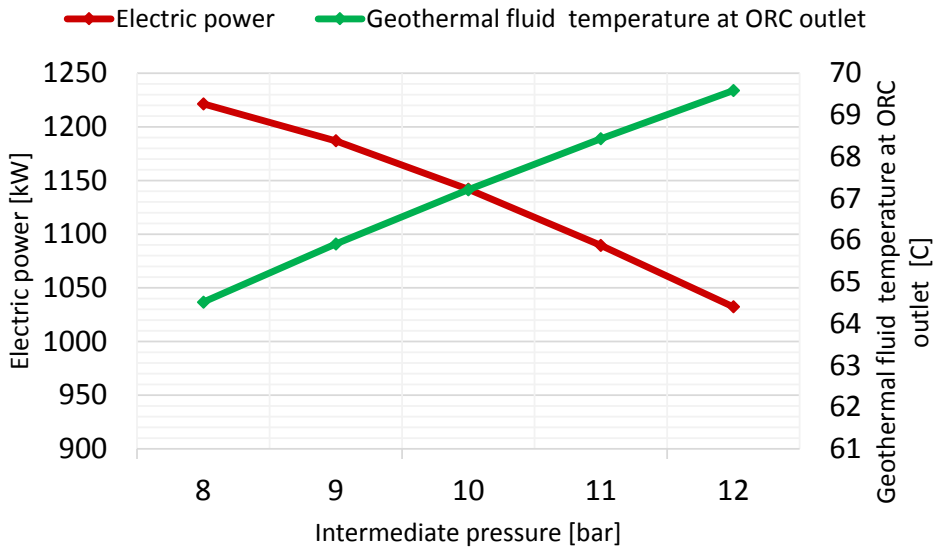

Figure A.2 Power generation and geothermal fluid outlet temperature for variable intermediate pressure (Geothermal source at 100 C°)

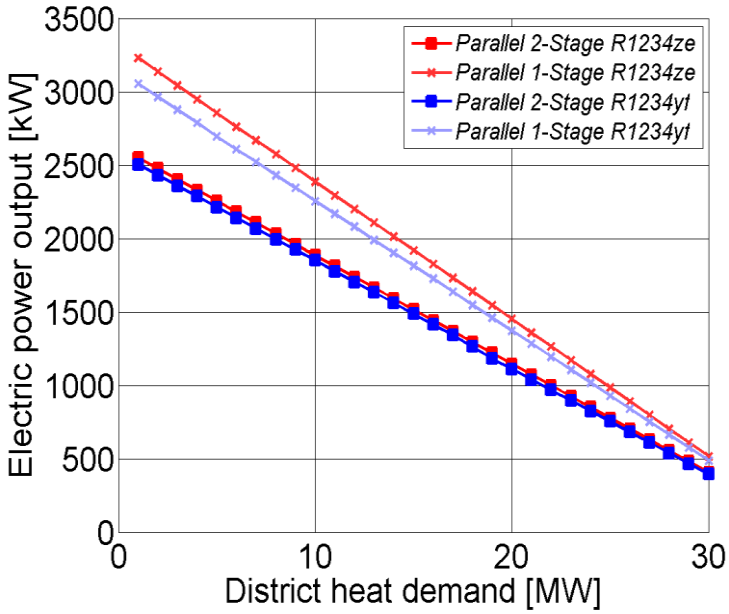

Figure A.3 Power generation – Parallel concepts

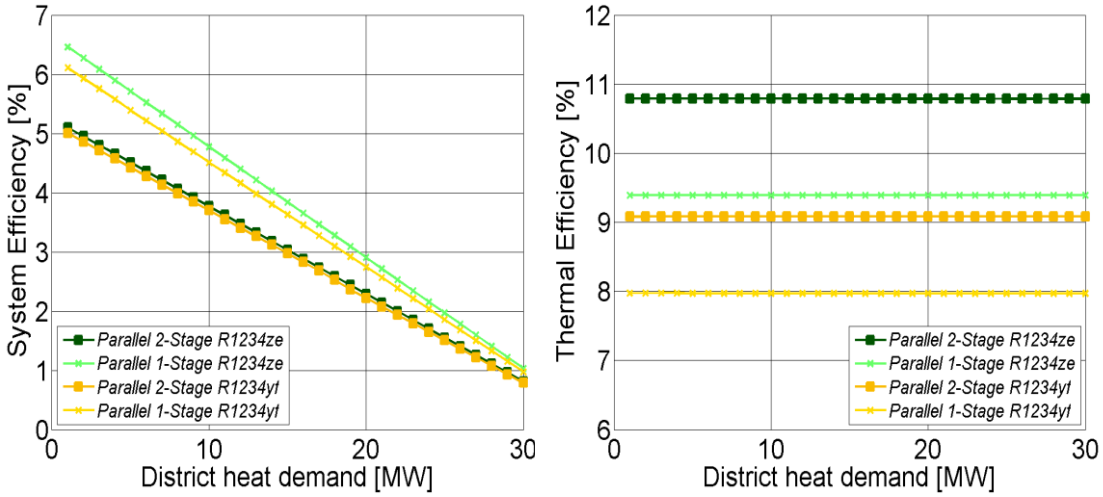

Figure A.4 Thermal and system efficiencies – Parallel concepts

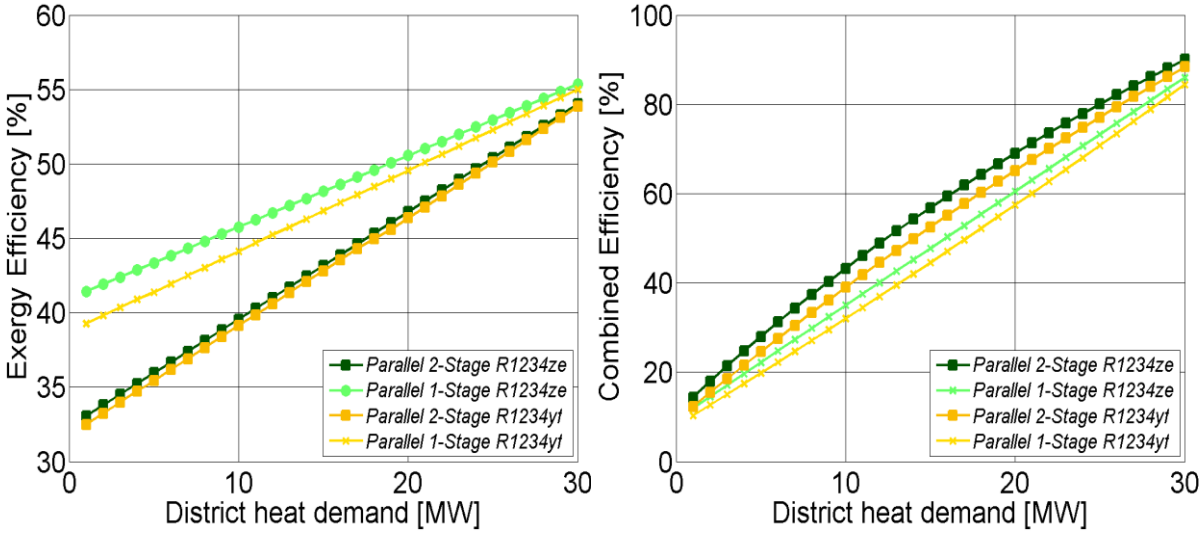

Figure A.5 Exergy and combined efficiencies – Parallel concepts

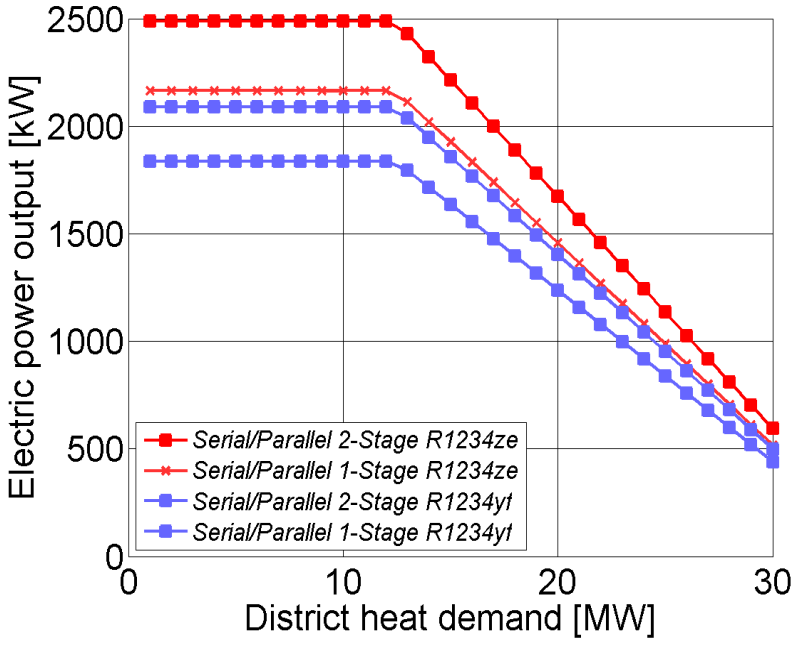

Figure A.6 Power generation – Serial/Parallel concepts

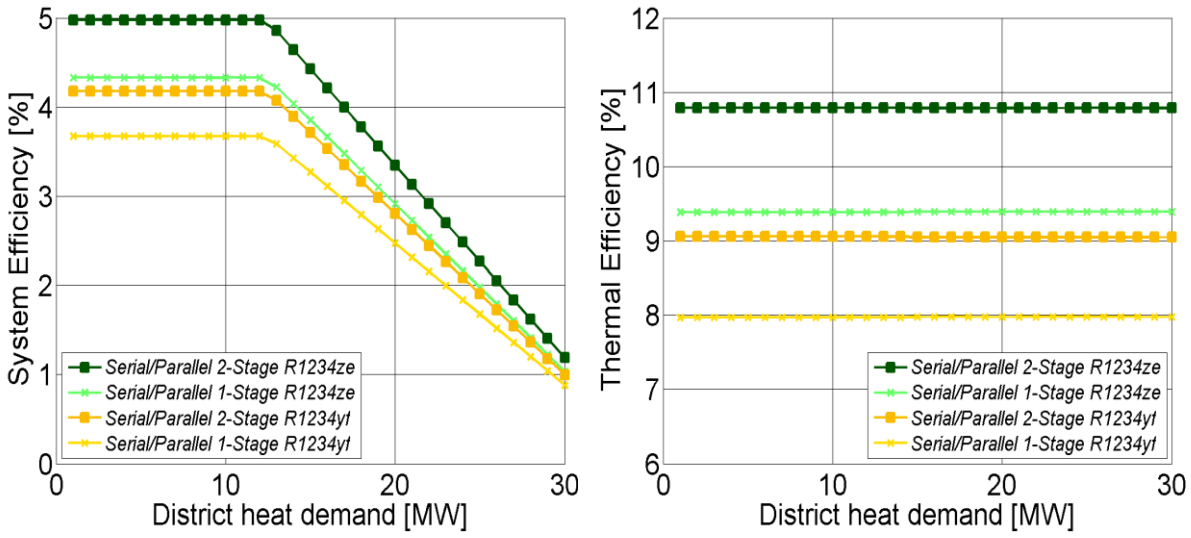

Figure A.7 Thermal and system efficiencies Serial/Parallel concepts

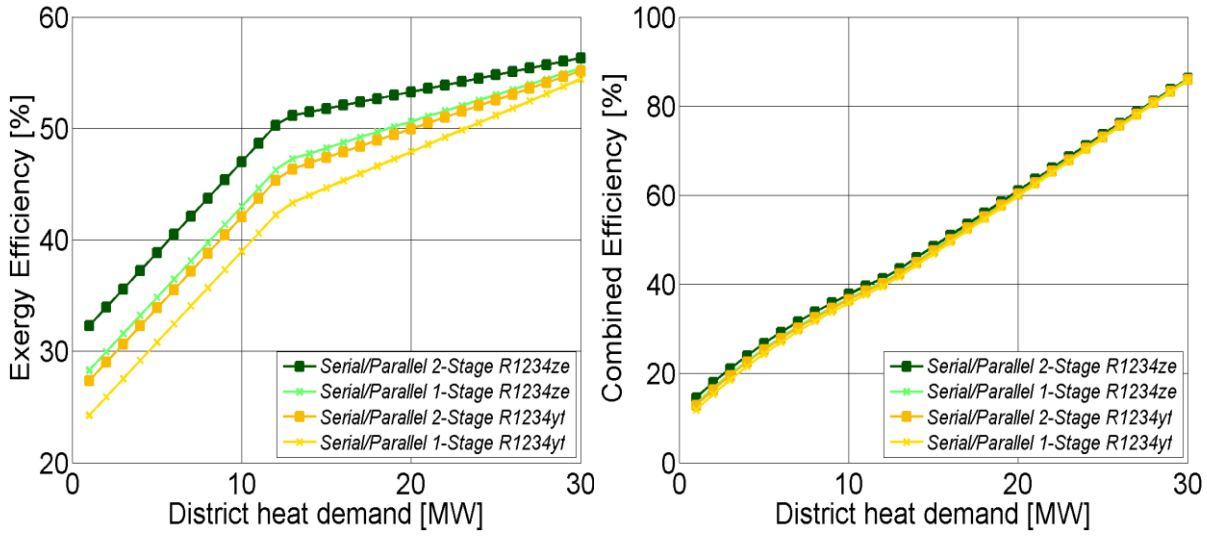

Figure A.8 Exergy and combined efficiencies – Serial/Parallel concepts

Table A-1 Profitability criteria for project evaluation

Nondiscounted Profitability Criteria		
Time Criterion	**Cash Criterion**	**Interest Rate Criterion**
Payback period (PBP)	Cumulative cash position (CCP)	Rate of return on investment (ROROI)
	Cumulative cash ratio (CCR)	
Discounted Profitability Criteria		
Time Criterion	**Cash Criterion**	**Interest Rate Criterion**
Discounted payback period (PBP)	Net present value (NPV)	Discounted cash flow rate of return (DCFROR)
	Present value ratio (PVR)	